國 立 交 通 大 學

電信工程學系碩士班

碩 士 論 文

多傳送多接收位元交錯調變碼系統之

低複雜度迭代訊號偵測設計

On the Design of Low Complexity Iterative Signal Detection for MIMO BICM Systems

研 究 生：曾鼎哲

指導教授：沈文和 博士

中 華 民 國 九 十 四 年 七 月

多傳送多接收位元交錯調變碼系統之

低複雜度迭代訊號偵測設計

On the Design of Low Complexity Iterative Signal Detection for MIMO BICM Systems

研 究 生：曾鼎哲 Student：Ting-Che Tseng

指導教授：沈文和 博士 Advisor：Dr. Wern-Ho Sheen

國 立 交 通 大 學

電 信 工 程 學 系 碩 士 班

碩 士 論 文

A Thesis

Submitted to Institute of Communication Engineering

College of Electrical Engineering and Computer Science

National Chiao Tung University

in Partial Fulfillment of the Requirements

for the Degree of

Master of Science

in

Communication Engineering

July 2005

Hsinchu, Taiwan, Republic of China

中華民國九十四年七月

多傳送多接收位元交錯調變碼系統之

低複雜度迭代訊號偵測設計

研究生：曾鼎哲　　　　　　　　指導教授：沈文和 博士

國立交通大學

電信工程學系碩士班

摘要

隨著數位多媒體時代的來臨，用戶對於資料的需求急速增加。下一代的無線通訊系統，如無線區域網路(802.11n)、第四代行動通訊系統，將可能採用多根天線傳送及接收(MIMO)技術以提高資料傳輸率。然而，要如何在現有的通訊系統中實現此新的技術是近年來熱門的研究。現行的通訊系統使用正交分頻多工(OFDM)技術和位元交錯調變碼(BICM)來克服多重路徑、瑞雷(Rayleigh)衰落通道，以提升系統效能。因此，此篇論文主要是在下一代通訊系統中，設計低複雜度迭代訊號偵測。在低複雜度零強制(ZF)和最小均值平方差(MMSE)訊號偵測器中，利用近似方法推導位元度規(bit metrics)的計算。另外，藉由渦輪(Turbo)原理，設計低複雜度迭代 MMSE 偵測器，並提出幾個近似的方法減少偵測器的運算。最後，採用下一代無線區域網路 802.11n 提案的系統架構，作為系統模擬環境。利用電腦模擬方式，印證使用近似的位元規度計算，能有效地提高系統效能。此外，在迭代 MMSE 偵測器中，從模擬結果顯示，利用這些近似的方法能降低計算的複雜度，但不會減弱系統效能。

On the Design of Low Complexity Iterative Signal Detection for MIMO BICM Systems

Student: Ting-Che Tseng Advisor: Dr. Wern-Ho Sheen

Department of Communication Engineering

National Chiao Tung University

Abstract

With the advent of digital multimedia communications era, the amount of the demand for data stream of subscribes is increasing rapidly. The next generation of wireless communications, such as 802.11n wireless local area networks (WLAN), 4G mobile communications, may utilize multiple input multiple output (MIMO) approach to enhance data rate. Existing communications use orthogonal frequency division multiplexing (OFDM) and bit-interleaved coded modulation (BICM) techniques to overcome multipath Rayleigh fading channels. Hence, the theme of my thesis is to design low complexity iterative signal detection for next generation of wireless communications. We derive the bit metrics based on zero-forcing (ZF) and minimum mean squared error (MMSE) detector by approximation. Besides, we design low complexity iterative MMSE detector with turbo principle and propose some methods of approximation to reduce computation complexity. Finally, we apply them to the system model of 802.11n Proposal. From simulation results, it proves that using approximated bit metrics can improve the performance, and employing the approximation of iterative MMSE detector can reduce the computation complexity without performance deterioration.

誌　謝

本篇論文得以順利完成，首先要特別感謝我的指導教授 沈文和博士，在兩年研究過程中給予非常多的指導與建議，並教導我進行研究的方法與態度，尤其沈文和教授做研究謹慎小心的態度，讓我印象深刻，對我這兩年在研究所以及未來做研究有影響很大。在本篇論文中，有許多的觀念及推導方式都學習沈教授做研究的方法和教導，才使得研究工作能夠順利進行。另外，要感謝口試委員 祁忠勇教授和李大嵩教授的指正與建議，使我的碩士論文更加完善。

除此之外，我要感謝無線寬頻接取系統實驗室的學長許正欣博士、郭志成、傅宜康、蕭昌龍，以及同學蔡政龍與林愷昕，另外，還有其他已畢業的學長姐們，學長曾俊傑博士、何建興博士、李育瑋、黃亮維、陳長新、方凱易和學姐楊雁雯等，以及許多曾經幫助過我的人。此外，要特別感謝徐進發同學，和我頻繁的討論，共同架設以及驗證模擬平台，並給我許多建議。在這兩年研究生活中，感謝大家所給予的鼓勵與幫忙，讓我克服種種困難，論文得以順利完成。

最後，感謝我的家人，尤其是我的父母和阿姨，在求學的過程中，給我無憂無慮的生活，讓我能專心致力讀書與研究。還有感謝姐姐為我禱告，使我能順利完成學業。另外，要感謝我最親愛的雙胞胎弟弟，聖哲，是和我相處最久的人，一起讀書討論，在生活上也互相照應。無論遭遇任何挫折你們總是給我最大的支持並陪伴我渡過難關，謝謝你們。

民國九十四年七月

研究生曾鼎哲謹識於交通大學

Contents

List of Tables

List of Figures

Chapter 1:

Introduction

With the advent of digital multimedia communication era, such as wireless local area networks (WLAN), digital audio broadcasting (DAB), digital video broadcasting television (DVB-T), mobile communications, and video conference, the amount of the demand for data stream of subscribers is increasing rapidly. The existing wireless communication systems may not satisfy the users. Increasing the transmission bandwidth is a method to enhance data rate. However, the available spectrum is limited and precious so the mean of increasing the transmission bandwidth to raise data rate is inefficiency. Recently, advances in coding, for example turbo code [7] and low density parity check (LDPC) code [8], are used to approach the Shannon bound [9] and then to enhance the capacity of channel. Nevertheless, those advances need a high-complexity receiver. Multiple-input multiple-output (MIMO) technique can enhance the data rate without increasing transmission bandwidth.

The MIMO techniques use multiple antennas to transmit and receive signals. The utility of multiple antennas offers extended range, improved reliability, or higher throughputs. Two main functions of multiple antennas are diversity and multiplexing. If all transmitter antennas send identical data simultaneously with the same bandwidth, such as smart antenna based systems or space-time code (STC) based systems, the systems can provide antenna gain, interference suppression and diversity gain in a fading channel. Smart antenna based systems may have array of multiple antennas only at one end of communication link, such as multiple-input single-output (MISO) and single-input multiple-output (SIMO). STC based systems, such as Alamouti code based systems, can provide diversity for MIMO channels. In my thesis, we focus on the other function of MIMO techniques－multiplexing. In spatial multiplexing-based MIMO systems, each transmit antenna can broadcast an independent signal sub-stream at the same time and in the same bandwidth. Using MIMO techniques with *n* transmitter antennas and *n* receiver antennas can increase *n* times data rate than those in systems with single-antenna. This technique is going to be implemented in the growing demand for future high data rate WLAN, WAN, PAN and 4G systems

In order to overcome fading channel, our system design is based on the orthogonal frequency division multiplexing (OFDM) and bit-interleaved coded modulation (BICM) [13] techniques. The two techniques are widely used in existing wireless communications, such as DAB, DVB, WLAN and wireless metropolitan area networks (Wireless MAN). OFDM technique was proposed in 1967 [12]. Due to the difficult and expansive hardware implementation of orthogonal multiple carriers and the lack of digital signal processing (DSP), this technique was not popular at that time. Until the discrete Fourier transform (DFT) was proposed by Weistein and Ebert in 1971, people paid more attention to OFDM technique again. Zehavi used bit-interleaver between encoder and modulator in 1992 [23]. Then the diversity order of coding could be increased by the minimum number of distinct coded bits. This technique was called as BICM in 1998 [13]. It has better performance than symbol interleaver over fading channels with the same coding and decoding architecture.

Since 1998, there have been more and more papers and documents to discuss and analyze MIMO techniques. Telatar and Foschini discuss the fundamental capacity limits for MIMO channels in [10] and [11], respectively. For MIMO multiplexing systems, all spatial streams would interfere with one another and be mixed at the receiver. All signals are not separated easily, especially in correlated channels. How to separate and detect data from blended received signals is a critical issue. There are many kinds of detector, such as a maximum likelihood (ML) detector, a minimum mean square errors (MMSE) detector, and a zero-forcing (ZF) detector. The main goal in my thesis is to design a low complexity detector. A MMSE detector is used popularly in MIMO systems. It has higher performance than the other linear detectors and lower complexity compared to the ML detector. Hence, we design a detector based on the MMSE criterion for MIMO-BICM systems.

In the paper [14], author expanded the BICM technique to multiple antenna transmission to obtain its merits in fading channels and derived the optimal bit metrics computations for MIMO-OFDM BICM systems. It is based on a ML detector and has more complex computation. In the paper [15], Butler presented the weight of bit metrics calculation based on a ZF detector. However, the performance of the ZF detector is poor. Hence, we derive the approximation of bit metrics for MIMO-OFDM-BICM systems based on popular MMSE detector by Gaussian approximation. We are going to discuss and analyze the improvement of performance of MMSE detector with the approximated bit metrics. The second topic in my thesis is to design a low complexity iterative MMSE detector based on the turbo principle to improve performance. We derive the bit metrics and coefficients of a iterative MMSE detector. We propose some methods of approximation to reduce computation of a iterative MMSE detector. Those methods of approximation can decrease much computation without deteriorating performance for many iterations and long packets.

The reset of this thesis is organized as follows: in chapter 2, we depict our simulation scenario, channel models, and system architectures. Moreover, we give the notations for MIMO-OFDM systems and definition of the signal-to-noise ratio (SNR). In chapter 3, we present the approximation of bit metric calculation based on a ZF detector and a MMSE detector for MIMO-OFDM BICM systems. In chapter 4, we design a low-complexity iterative MMSE detector and use some methods of approximation to reduce the computation complexity of the detector. Finally, we give some conclusions and future works in chapter 5.

Chapter 2:

System Model

The next generation of wireless local area networks (WLAN), IEEE802.11n, is based on multiple input multiple output (MIMO) and orthogonal frequency division multiplexing (OFDM) techniques to provide a point-to-point high throughput transmission. The working group of IEEE802.11n holds a conference on the odd months. There are four complete proposals proposed last year by four different groups, TGn Sync, WWiSE, MitMot, and Qualcomm. In the beginning of this year, the Qualcomm gave up their proposal and joined the TGn Sync group which is composed of Agere Systems Inc., Intel Corporation, Marvell Semiconductor Inc., and etc. Mitsubish and Motorola gave up their proposal (MitMot) and joined the TGn Sync and the WWiSE groups, respectively. Hence, there are tow major groups, the TGn Sync and the WWiSE to compete in order to make their own proposal to become the standard of IEEE802.11n.

The physical layer of two proposals of TGn Sync and WWiSE are based on the same MIMO-OFDM systems, but whole system design are different, especially the preamble format and transmission mode. Here, our simulation platform is based on version 3 of the TGn Sync proposal to IEEE 802.11n.

Equation Section 2

2.1 Introduction to TGn Sync Proposal

The block diagram of transmitter in TGn Sync Proposal for throughput enhancement is shown in Fig. 2-1.

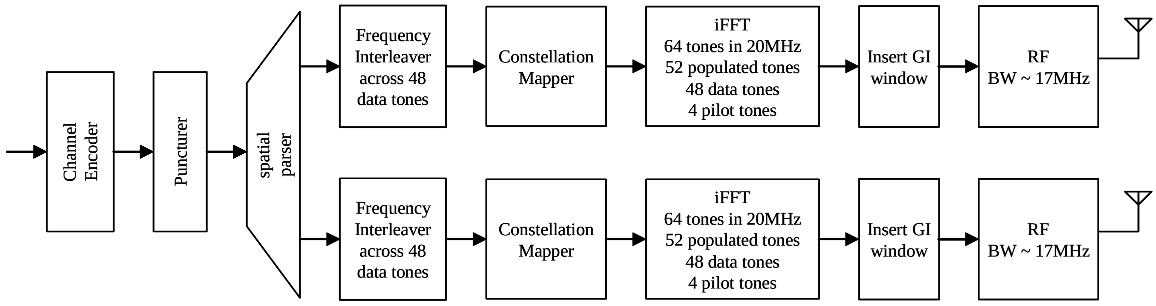

Fig. 2-1: Transmitter diagram of TGn Sync proposal for MIMO-OFDM systems in 20MHz

The basic configuration of this proposal delivers a maximum mandatory rate of 243 Mbps with only two antennas. This rate is 5 times the rate of 802.11a/g (54Mbps). The proposal also includes options for higher rates beyond 600 Mbps. In order to achieve the higher data rates, the PHY techniques use MIMO techniques with spatial division multiplexing of spatial streams and evolution of 802.11 OFDM PHY. The proposal uses wider bandwidth options, 40MHz channelization, to increase data rate. Timing related parameters is shown in Table 2-1.

2.1.1 Preamble Format

The PPDU format for transmission with 2 antennas in a 20MHz channelization is shown in Fig. 2-2.

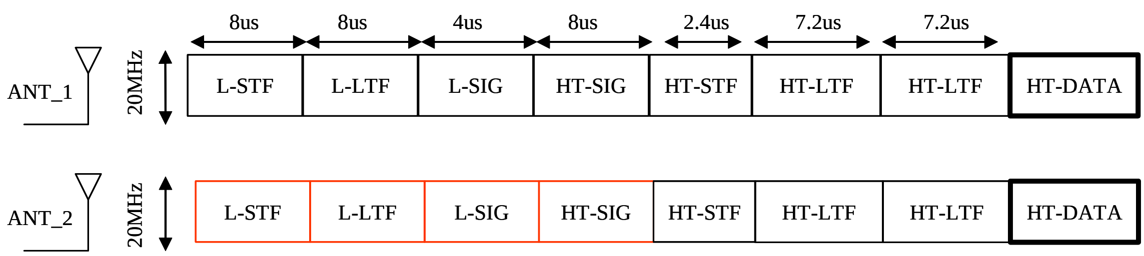

Fig. 2-2: PPDU format for 2x20 mandatory basic MIMO transmission

The high through (HT) preamble of TGn Sync proposal is a concatenation of the legacy preamble (802.11.a) and a HT-specific preamble. The functions performed by the preamble include start of packet detection, auto-gain-control (AGC), coarse frequency offset estimation, coarse timing offset estimation, fine frequency offset estimation, fine frequency offset estimation, and channel estimation.

Parameter	Value for 20 MHz Channel	Value for 40 MHz Channel
N_{SD} : Number of data subcarriers	48	108
N_{SP} : Number of pilot subcarriers	4	6
N_{SN} : Number of center null subcarriers	1 (tone = 0)	3 (tones = -1,0,+1)
N_{SR} : Subcarrier range (index range)	26 (-26 … +26)	58 (-58 … +58)
Δ_F : Subcarrier frequency spacing	0.3125 MHz (= 20 MHz / 64)	0.3125 MHz (= 40 MHz / 128)
T_{FFT} : IFFT/FFT period	3.2 μsec	3.2 μsec
T_{GI} : GI duration	0.8 μsec	0.8 μsec
$T_{ShortGI}$: Short GI duration	0.4 μsec	0.4 μsec
T_{GI2} : Legacy LongTraining symbol GI duration	1.6 μsec	1.6 μsec
T_{SYM} : Symbol interval	4 μsec	4 μsec
T_{LONG} : Long training field duration	8 μsec	8 μsec
$T_{HT-LONG}$:HT Long training field duration	7.2 μsec	7.2 μsec
T_{SHORT} : Short training field duration	8 μsec	8 μsec
$T_{HT-SHORT}$: HT Short training field duration	2.4 μsec	2.4 μsec
T_S : Nyquist sampling interval	50 nsec	25 nsec

Table 2-1: Timing related parameters

2.1.2 Encoder and Puncturing

A mandatory encoder is a convolutional encoder and a optional encoder is a low-density-parity-check (LDPC) encoder. In our simulation platform, the transmitter is implemented by the mandatory encoder. The convolutional encoder should work by the industry-standard generator polynomials, $g_0 = 133_8$ and $g_1 = 171_8$, with the constraint length 7 of the code rate $R_c = \frac{1}{2}$, as shown in Fig. 2-3.

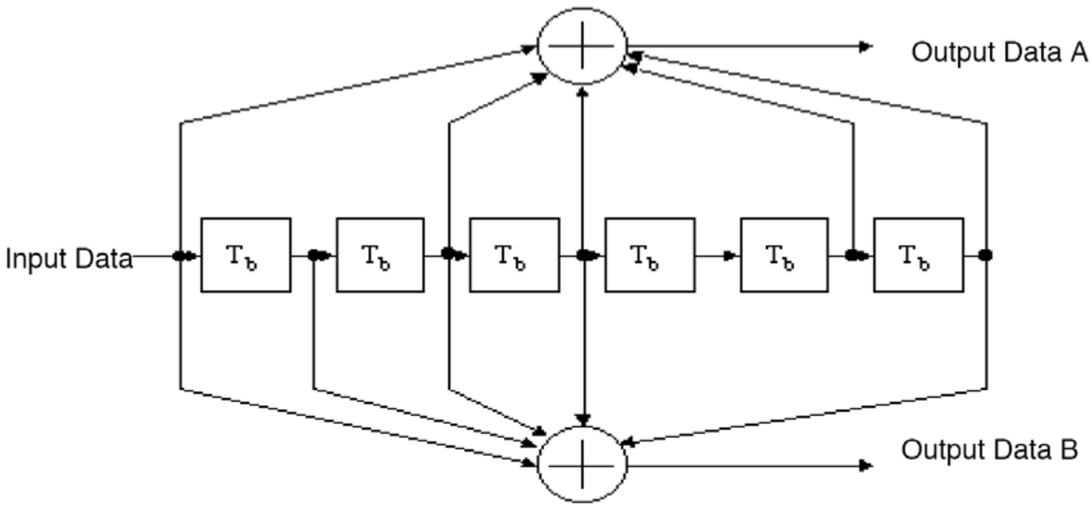

Fig. 2-3: The convolutional encoder (K=7, R=1/2)

In order to achieve high data rate and different coding rate R_c with the same the industry-standard convolutional encoder, the transmitter would employ a puncturing method. Puncturing the coded bits is shown in Fig. 2-4 and Fig. 2-5 to reach coding rate $R_c = 2/3$ and $R_c = 3/4$, respectively. In our receiver design, we choose the soft Viterbi decoding to decode information bits. However, we use a MAP decoder to design an iterative receiver.

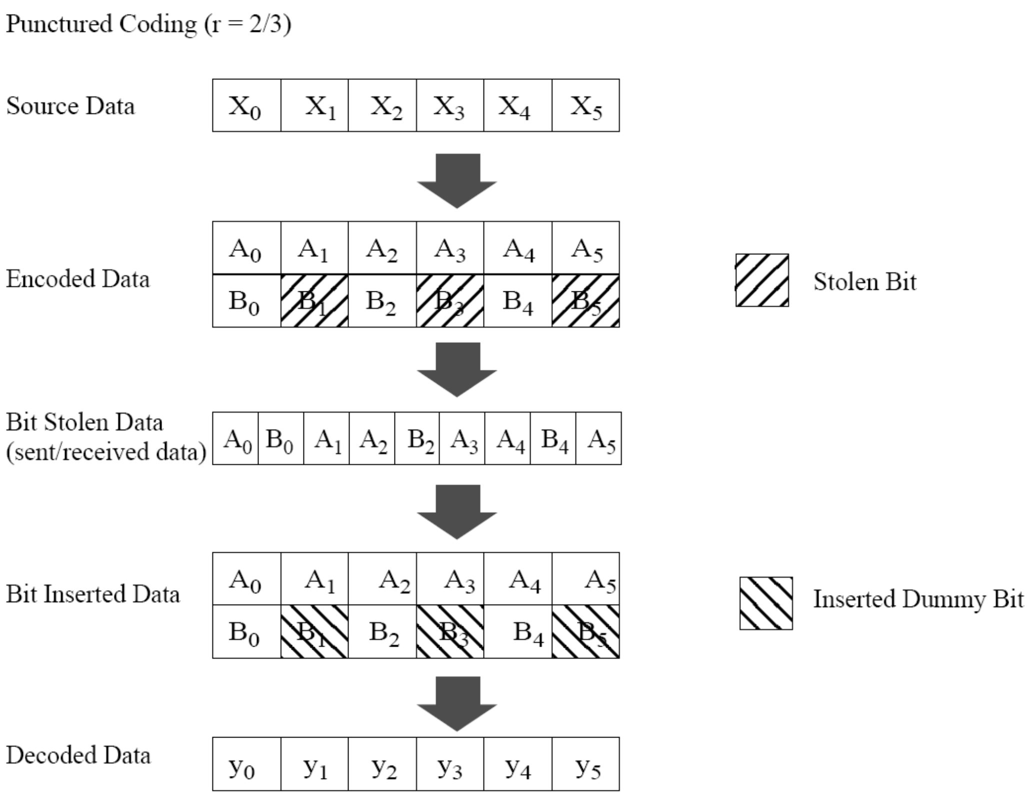

Fig. 2-4: The bit-stealing and bit-insertion procedure for code rate R_c=2/3

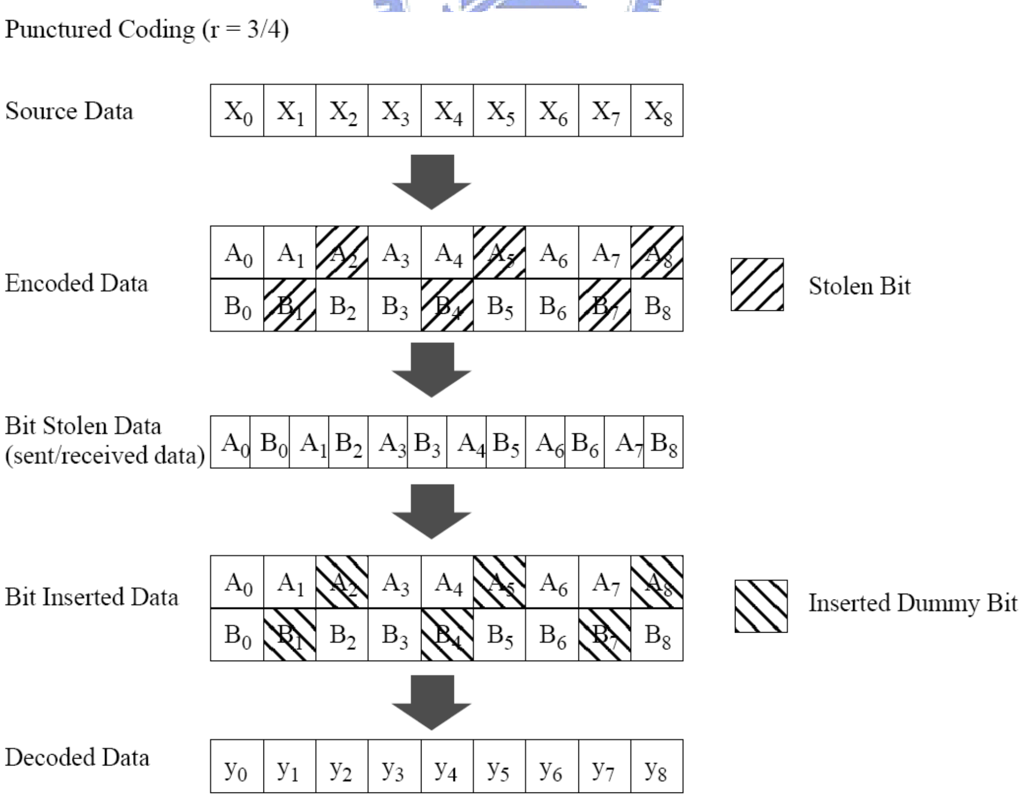

Fig. 2-5: The bit-stealing and bit-insertion procedure for code rate R_c=3/4

2.1.3 Bit Interleaving

In order to overcome the Rayleigh fading channel and avoid any transmitter antenna fade, this proposal utilizes a space-frequency bit interleaving shown in Fig. 2-6. Coded and punctured bits are interleaved across spatial streams and frequency tones by two steps— spatial stream parsing and frequency interleaving.

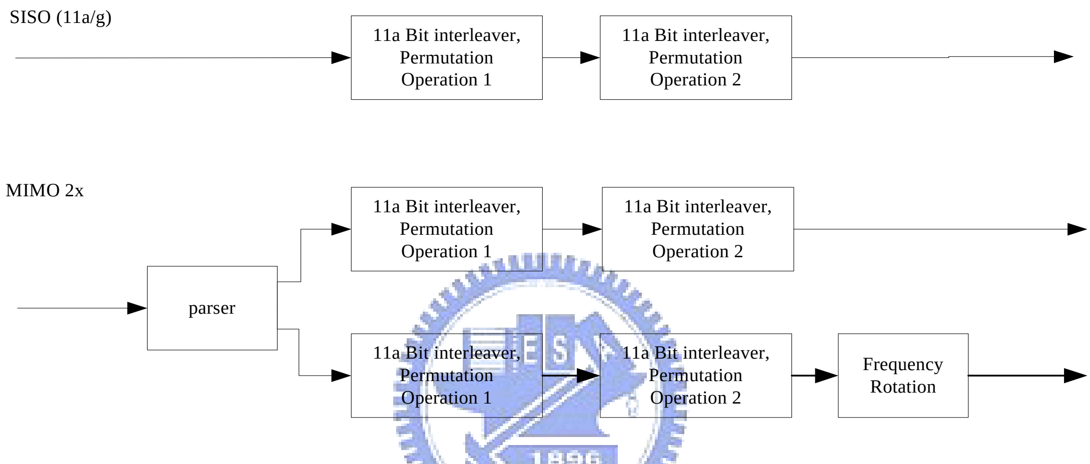

Fig. 2-6: Bit interleaver for MIMO systems in TGn Sync proposal

Spatial stream parsing uses a round-robin parser to parse coded and punctured bits to multiple spatial streams, defined by

$$s = \max\left\{N_{BPSC}/2,1\right\} \qquad (2.1)$$

where N_{BPSC} is the number of bits per subcarrier and s is the number of QAM bit order values. The parser sends consecutive blocks of s bits to different spatial streams.

The second step is frequency interleaver based on the 802.11a interleaver with certain modifications. It can be divided to three permutations.

The first permutation is defined by the rule

$$i = N_{row} \times \left(k \bmod N_{column}\right) + \text{floor}\left(k / N_{column}\right), \;\; k = 0,1,\ldots,N_{CBPS} - 1 \tag{2.2}$$

where N_{CBPS} is the number of coded bits per OFDM symbol.

The second permutation is defined by the rule

$$\begin{aligned} j = s \times \text{floor}\left(i / s\right) + \left(i + N_{CBPS} - \text{floor}\left(N_{column} \times i / N_{CBPS}\right)\right) \bmod s, \\ i = 0,1,\ldots,N_{CBPS} - 1 \end{aligned} \tag{2.3}$$

where s is determined by $s = \max\left(N_{BPSC} / 2, 1\right)$

The third permutation is defined by the rule

$$\begin{aligned} r = \left(j - \left(\left(2 \times i_{ss}\right) \bmod 3 + 3 \times \text{floor}(i_{ss} / 3)\right) \times N_{rot} \times N_{BPSC}\right) \bmod N_{CBPS} \\ j = 0,1,\ldots,N_{CBPS} - 1 \end{aligned} \tag{2.4}$$

where $i_{SS} = 0,1,\ldots,N_{SS} - 1$ is the index of the spatial stream on which this interleaver is operating.

Channelization		20MHz				40MHz			
Total # of Streams		1	2	3	4	1	2	3	4
Frequency Rotation	1st stream	0	0	0	0	0	0	0	0
	2nd stream		22	22	22		58	58	58
	3rd stream			11	11			29	29
	4th stream				33				87

Table 2-2: Frequency rotation

2.1.4 Signal Mapping

The signal of OFDM subcarriers should be modulated by BPSK, QPSK, 16-QAM, or 64-QAM with the gray labeling. It is the same as the modulation scheme of the standard of IEEE802.11a. The constellations of BPSK, QPSK, and 16-QAM are shown in Fig. 2-7. The constellations of 64-QAM is shown in Fig. 2-8.

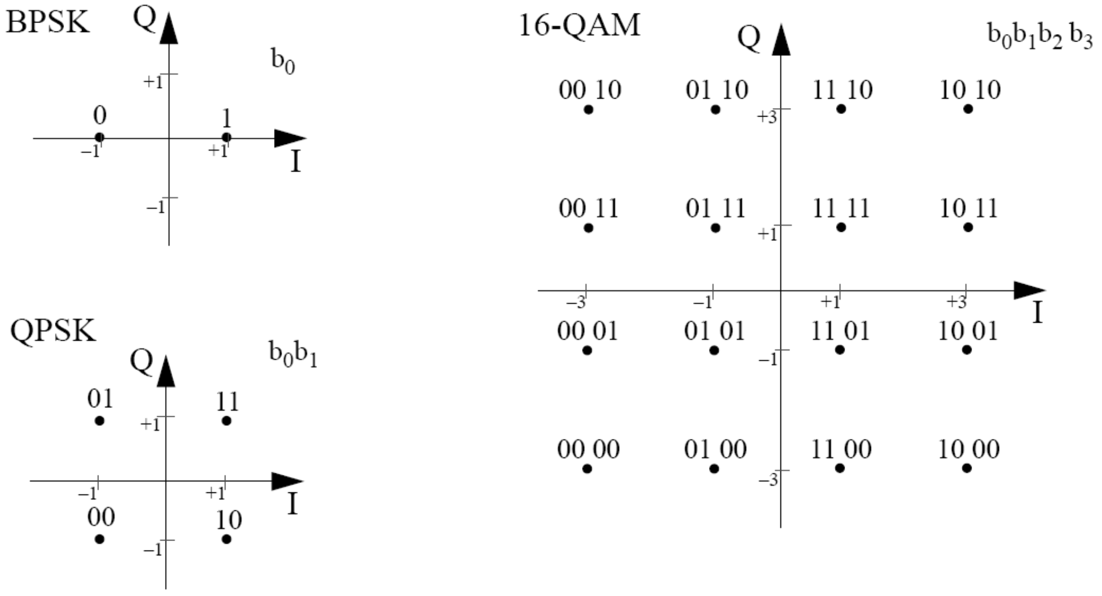

Fig. 2-7: BPSK, QPSK, and 16-QAM constellation bit encoding

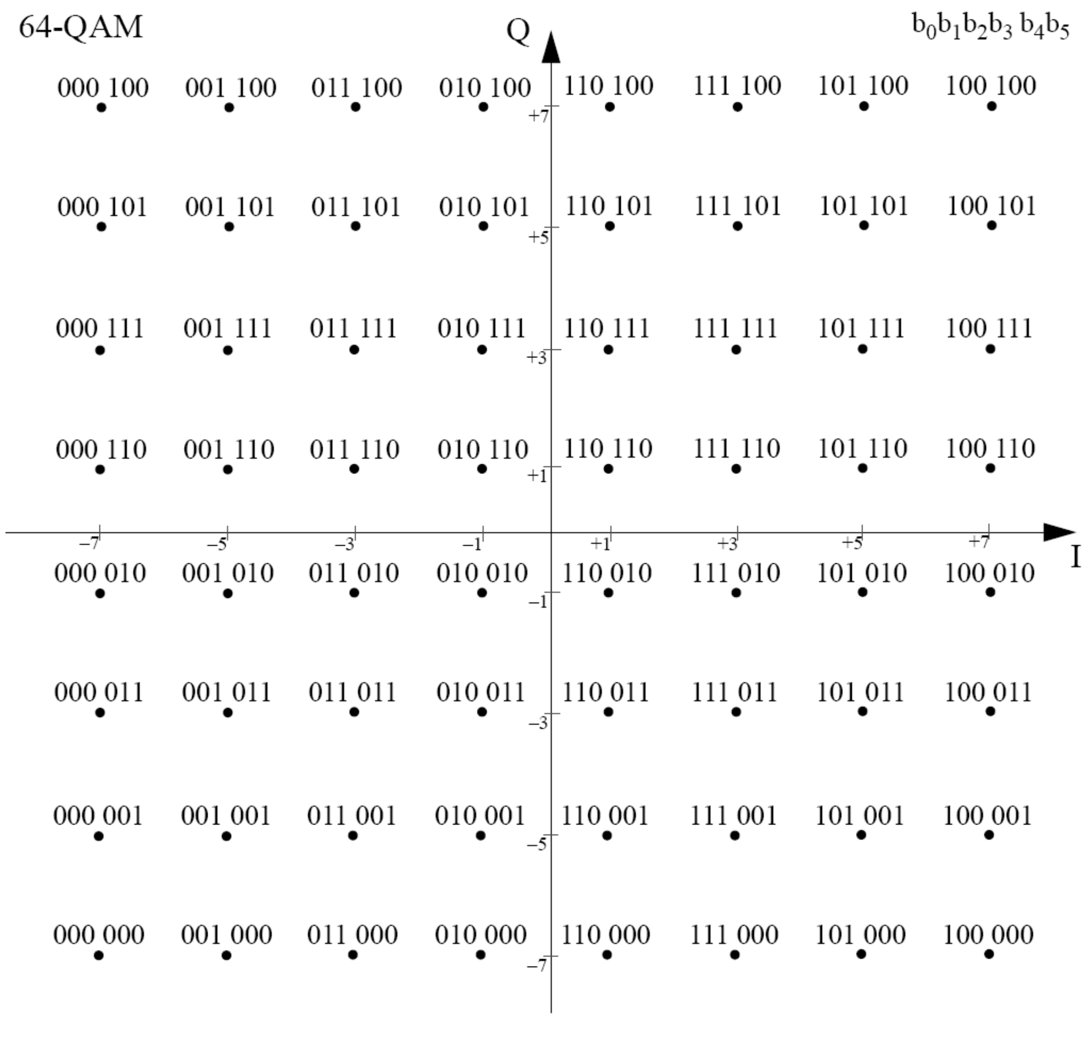

Fig. 2-8: 64-QAM constellation bit encoding

2.2 MIMO Channel Model

The block diagram of the MIMO indoor channel model proposed by IEEE802.11 TGn is shown in Fig. 2-9.

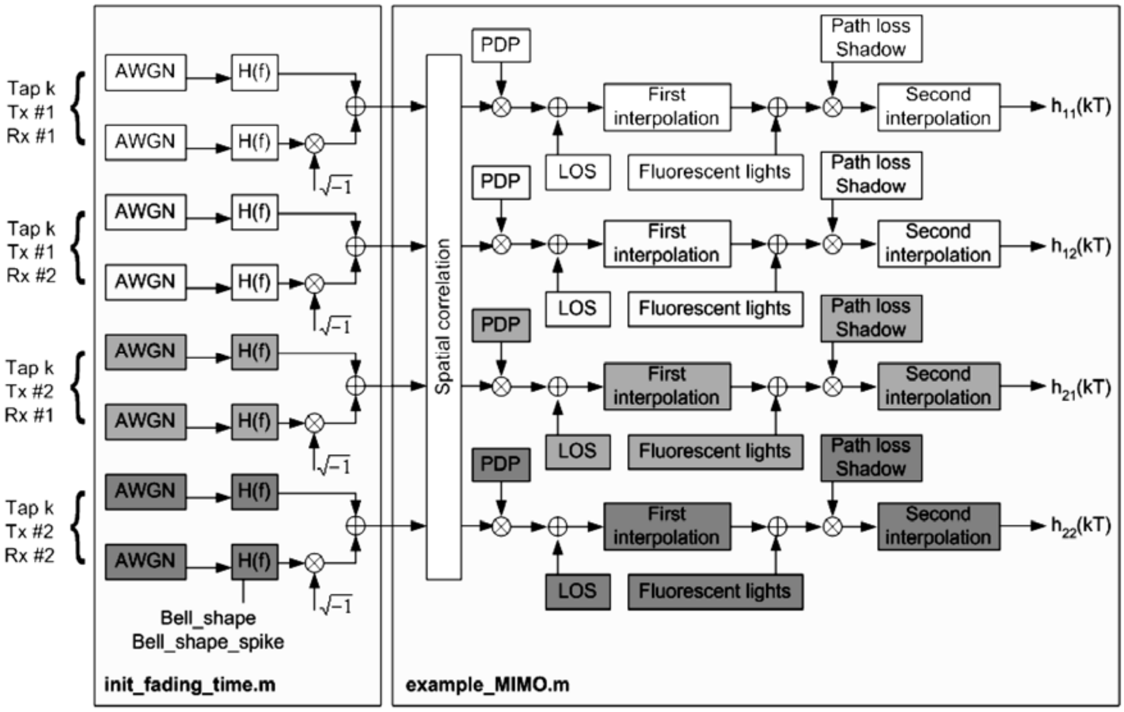

Fig. 2-9: The block diagram of the MIMO channel model

There are six channel models defined in IEEE 802.11n document [29] for next generation of WLAN. The properties of these channel models are shown in Table 2-3 and Table 2-4. *K*-factor for LOS conditions applies only to the first tap, for all other taps $K = -\infty$ dB.

Model	Conditions	K-factor (dB)	RMS delay spread (ns)	# of clusters
A (optional)	LOS/NLOS	0/ -∞	0	1 tap
B	LOS/NLOS	0 / -∞	15	2
C	LOS/NLOS	0 / -∞	30	2
D	LOS/NLOS	3 / -∞	50	3
E	LOS/NLOS	6 / -∞	100	4
F	LOS/NLOS	6 / -∞	150	6

Table 2-3: Summary of model parameters for LOS/NLOS conditions.

New Model	d_{BP} (m)	Slope before d_{BP}	Slope after d_{BP}	Shadow fading std. dev. (dB) before d_{BP} (LOS)	Shadow fading std. dev. (dB) after d_{BP} (NLOS)
A (optional)	5	2	3.5	3	4
B	5	2	3.5	3	4
C	5	2	3.5	3	5
D	10	2	3.5	3	5
E	20	2	3.5	3	6
F	30	2	3.5	3	6

Table 2-4: Path loss model parameters

We choose channel model B for our simulation environment. There are 2 clusters shown in Fig. 2-10 and 9 multipaths in channel model B. The power delay profile of channel model B is shown in Fig. 2-11. The cumulative distribution function (CDF) of channel model is shown in Fig. 2-12. The channel model B is a multipath Rayleigh fading channel with the speed of pedestrian v=1.2 km/hr .

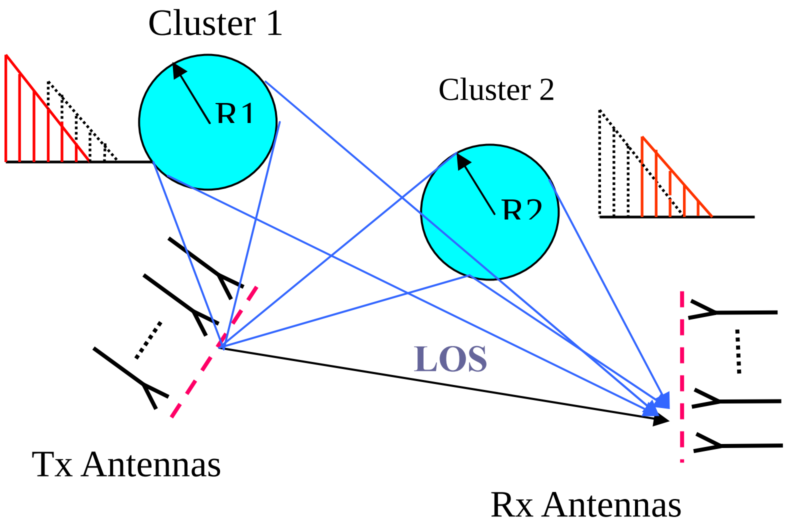

Fig. 2-10: Multipath MIMO channels with two clusters

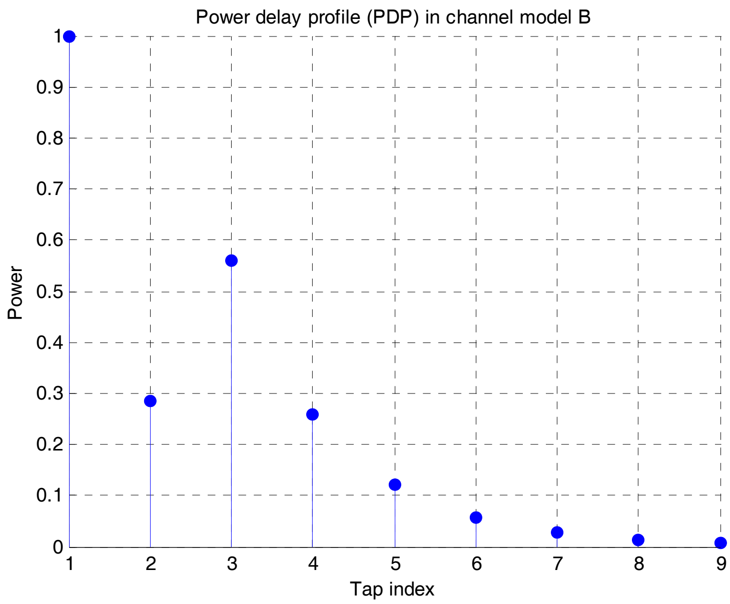

Fig. 2-11: Power delay profile (PDP) in channel model B

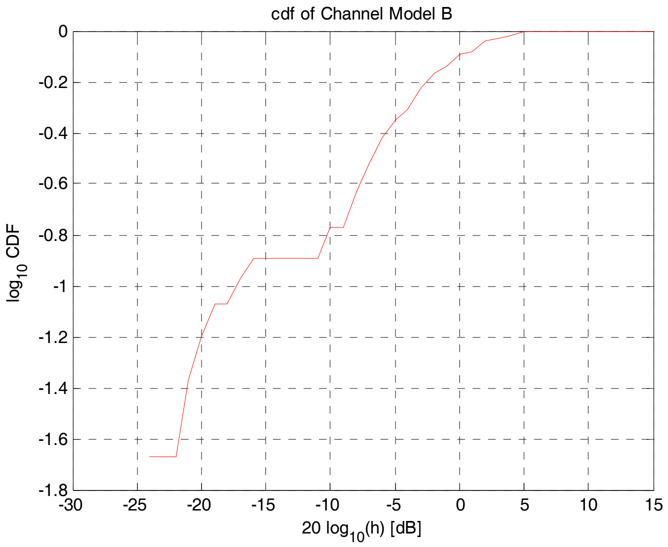

Fig. 2-12: CDF of channel model B

The fading characteristics of the indoor wireless channels are very different from the mobile case. Transmitter and receiver are stationary and people are moving between them in indoor wireless systems, but the user terminals are often moving through an environment in outdoor mobile systems. Therefore, a new function $S(f)$ can be defined as (2.5) for indoor scenario to fit the Doppler power spectrum measurements. (in linear values, not dB values):

$$S(f) = \left[1 + A\left(f / f_d\right)^2\right]^{-1} \tag{2.5}$$

where A is a constant, used to define the $0.1\,S(f)$, at a given frequency f_d, being the Doppler Spread.

$$\left(S(f)\right)\Big|_{f=f_d} = 0.1 \tag{2.6}$$

where

- $f_d = \dfrac{v_o}{\lambda}$: the Doppler spread
- v_o is the environmental speed (default value is 1.2 km/hr)
- $\lambda = \dfrac{c}{f_c}$: the wavelength

• c: the light speed • f_c: the carrier frequency

$S(f)$ is similar to the "Bell" shape spectrum, as shown in

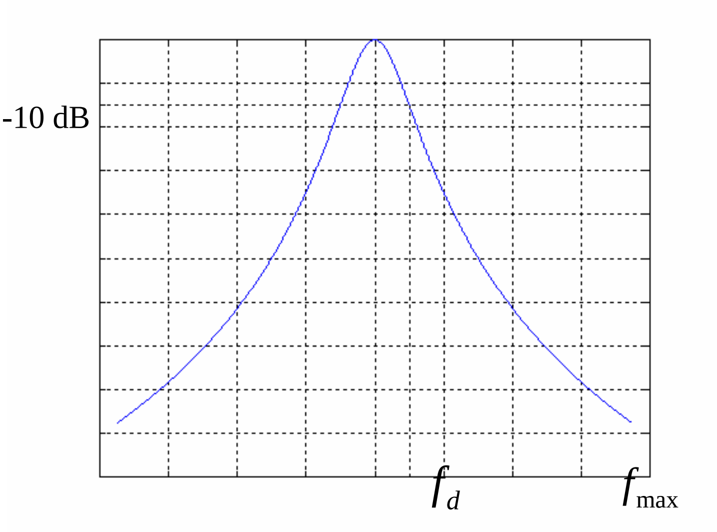

Fig. 2-13: "Bell" shape Doppler power spectrum

$f_{\max}$ is the maximum frequency component of the Doppler power spectrum.

2.3 Signal-to-Noise Ratio (SNR) Definition

The signal to noise ratio is defined as the ratio of the signal power in the aggregate of the -10dB signal bandwidths divided by the noise power in the aggregate of the -10dB signal power bandwidths. In addition, the signal power at the receiver is the sum of signal powers from all the transmitter antennas for MIMO systems.

$$\text{Channel Gain} = \mathrm{E}\left\{ \frac{\left(\sum_{j=1}^{N_R} P_r(j)\right) / N_R}{\sum_{j=1}^{N_T} P_t(j)} \right\} \tag{2.7}$$

where

• $P_r(j)$ is the received signal power at j^{th} receiver antenna

• $P_t(j)$ is the transmitted signal power at j^{th} transmitter antenna

2.4 Notation of MIMO-OFDM Systems

The notations of MIMO-OFDM transmitter is shown in Fig. 2-14.

where

- b_n: the n^{th} information bit
- c_n: the n^{th} coded bit
- $\tilde{c}_n^p$: the n^{th} interleaved bit at the p^{th} transmitter antenna
- $\tilde{s}_{\ell,k}^p$: the modulated signal at the k^{th} subcarrier and the ℓ^{th} OFDM symbol at the p^{th} transmitter antenna
- $s'_p(t)$: the transmitted signal at time t at the p^{th} transmitter antenna
- $p \in \{1, \cdots, N_T\}$: the index of transmitter antenna
- n : the index of bit sequence
- ℓ : the index of modulated symbol sequence
- t : time index
- N_T: the number of transmitter antennas
- L_b : the number of information bits b_n
- $L_c = L_b / \mathrm{R_c}$: the number of coded bits c_n, where $\mathrm{R_c} = \frac{k_0}{n_0}$ is code rate
- $L_{\tilde{c}} = \lceil \frac{L_c}{N_T} \rceil$: the number of interleaved bits $\tilde{c}_n^p$ per tx antenna
- K=52 : the number of OFDM subcarriers
- $L_{\tilde{s}} = \lceil \frac{L_{\tilde{c}}}{K \cdot log_2 M} \rceil$: the number of OFDM symbols per tx antenna for M-QAM

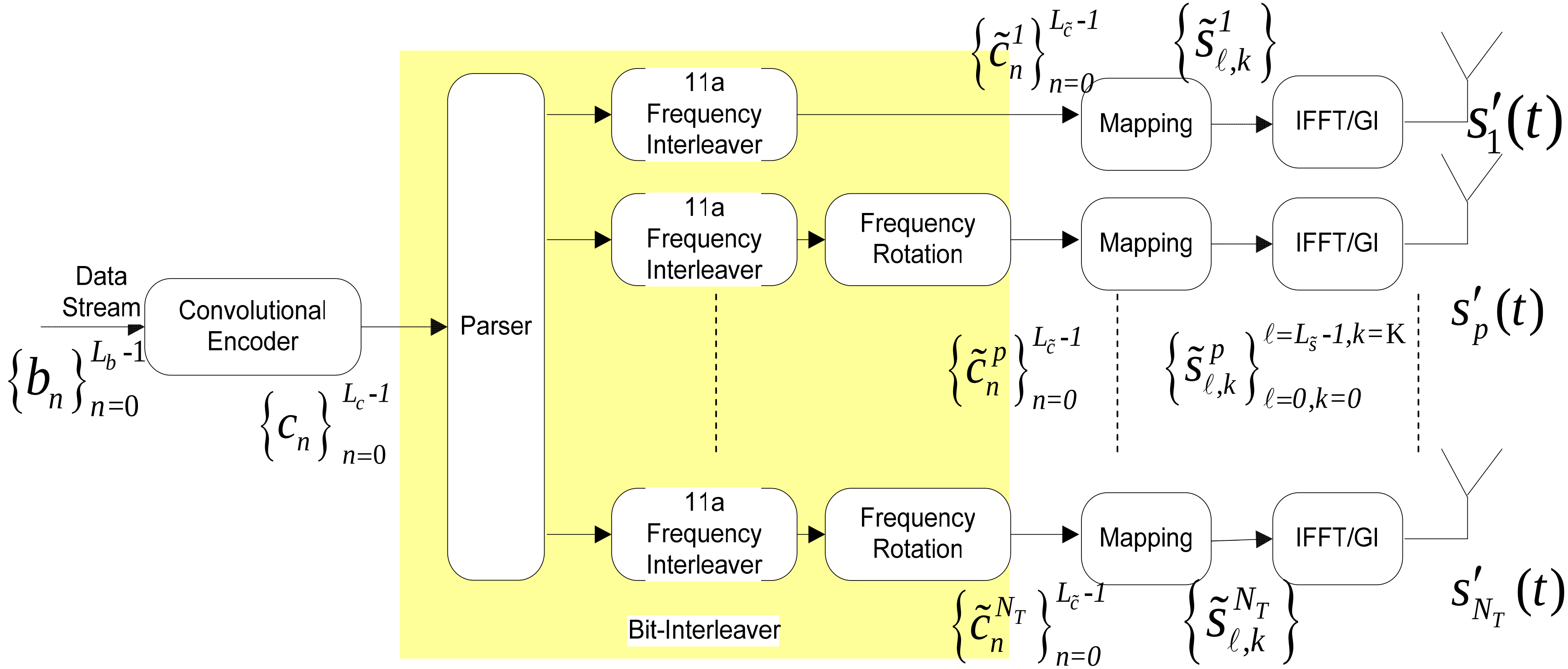

Fig. 2-14: Notations of a MIMO-OFDM transmitter

The notations of MIMO-OFDM receiver is shown in.Fig. 2-15

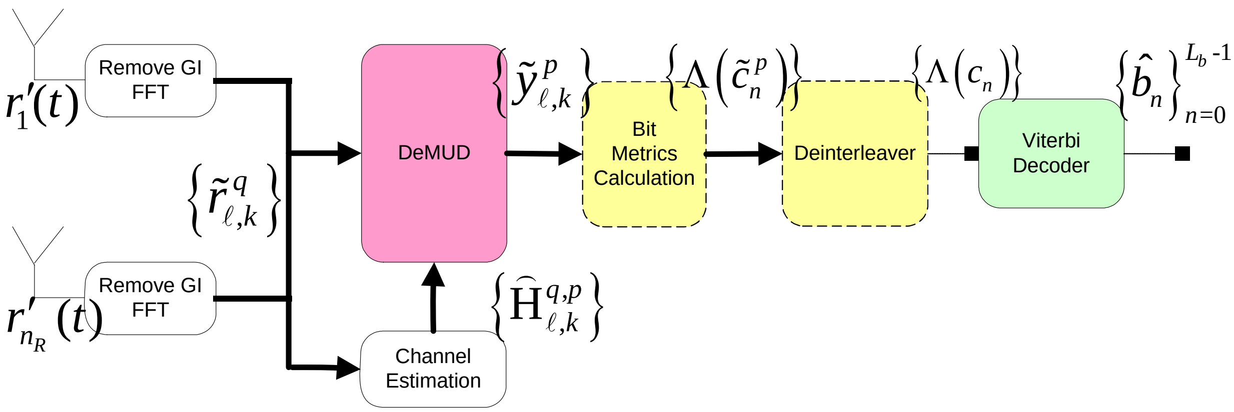

Fig. 2-15: Notations of a MIMO-OFDM receiver

where

- $r'_q(t)$: the received signal at time t at the q^{th} transmitter antenna
- $\tilde{r}^q_{\ell,k}$: the modulated signal at the k^{th} subcarrier and the ℓ^{th} OFDM symbol at the q^{th} transmitter antenna
- $\tilde{y}^p_{\ell,k}$: the detected signal at the k^{th} subcarrier and the ℓ^{th} OFDM symbol from the p^{th} transmitter antenna
- $\Lambda\left(\tilde{c}^p_n\right)$: the a posteriori log likelihood ratio of $\tilde{c}^p_n$
- $\Lambda\left(c_n\right)$: the a posteriori log likelihood ratio of deinterleaved bit c_n
- $\hat{b}_n$: the n^{th} estimated information bit
- $q \in \{1, \cdots, N_R\}$: the index of receiver antenna
- N_R: the number of transmitter antennas

Chapter 3:

Linear Multi-Stage Detection

This chapter considers MIMO-OFDM systems with bit-interleaved coded modulation (BICM) [7]. The maximum likelihood (ML) receiver has higher computation complexity. Therefore, we design a low-complexity receiver with a linear detector based on zero-forcing (ZF) and minimum mean squared errors (MMSE) algorithms. Here, we propose how to calculate the bit metrics for BICM on a ZF receiver and an MMSE receiver.

Equation Section 3

3.1 Bit Metrics for BICM

BICM technique is suited to multipath fast-fading channels, then the sub-channels of OFDM systems with bit-interleaver can be approximated as independently fast-fading. For better performance, the decoder is implemented by soft Viterbi decoding. Because bit interleaving is applied to the encoded bit before the M-QAM modulator, maximum likelihood decoding of BICM signals would require joint decoding and demodulation. According to the MAP criterion, estimate the coded bit sequence $\left\{\tilde{c}_n^p\right\}_{n=0}^{L_{\tilde{c}}-1}$ at the p^{th} sub-stream by

$$\left\{\hat{\tilde{c}}_n^p\right\}_{n=0}^{L_{\tilde{c}}-1} = \arg \max_{\left\{\tilde{c}_n^p\right\}_{n=0}^{L_{\tilde{c}}-1}} \left\{ \mathrm{p}\left[\left\{\tilde{c}_n^p\right\}_{n=0}^{L_{\tilde{c}}-1} \middle| \left\{\tilde{y}_{\ell,k}^p\right\}_{\ell=0,k=0}^{\ell=L_{\tilde{s}}-1,k=K-1} \right] \right\} \tag{3.1}$$

Thus, all possible coded and interleaved bit sequences would be calculate in (3.1). Zehavi proposed a decoding scheme in [23] to compute sub-optimal simplified bit metrics to be used inside a Viterbi decoder for path metric computation.

Define the bit metrics of coded and interleaved bit $\tilde{c}^{p}_{\ell,k,m}$ for BICM system by ignoring the noise color, i.e., assuming the real part and the image part of noise are independent.

$$\Lambda\left(\tilde{c}^{p}_{\ell,k,m}\right) \triangleq ln\left(\frac{p\left[\tilde{c}^{p}_{\ell,k,m}=1\middle|\tilde{y}^{p}_{\ell,k}\right]}{p\left[\tilde{c}^{p}_{\ell,k,m}=0\middle|\tilde{y}^{p}_{\ell,k}\right]}\right) \tag{3.2}$$

We redefine coded and interleaved bit $\tilde{c}^{p}_{n}$ to be $\tilde{c}^{p}_{\ell,k,m}$,

$$\tilde{c}^{p}_{\ell,k,m}=\tilde{c}^{p}_{n}, \tag{3.3}$$

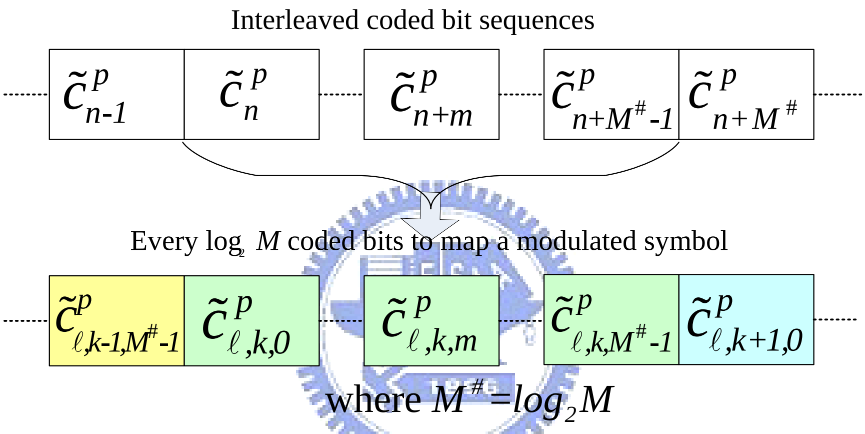

Fig. 3-1: To group *M* interleaved-coded bits to map a modulated symbol for MIMO-OFDM systems

where

- $n = \ell \cdot K + k \cdot log_2 M + m,$
- $m \in \left(0,\cdots,log_2 M - 1\right)$, the bit index of constellation
- $\ell \in \left(0,\cdots,L_{\tilde{s}} - 1\right)$, the OFDM symbol index
- $k \in \left(0,\cdots,K - 1\right)$, the subcarrier index

$\tilde{c}^{p}_{\ell,k,m}$ is the coded bit in the m^{th} bit mapped onto a M-QAM symbol ψ ,at the k^{th} subcarrier, at the ℓ^{th} OFDM symbol, and at the p^{th} sub-stream. Because the computation of bit metrics of coded bit $\tilde{c}^{p}_{\ell,k,m}$ depends only on detected signal $\tilde{y}^{p}_{\ell,k}$ at the k^{th} subcarrier, at the ℓ^{th} OFDM symbol, and at the p^{th} sub-stream, we can ignore the subcarrier index k and the OFDM symbol index ℓ.

Let $\tilde{c}^{p}_{m}=\tilde{c}^{p}_{\ell,k,m}$, $\tilde{y}^{p}=\tilde{y}^{p}_{\ell,k}$ and the bit metrics of $\tilde{c}^{p}_{m}$ is

$$\Lambda\left(\tilde{c}^{p}_{m}\right)\triangleq ln\left(\frac{p\left[\tilde{c}^{p}_{m}=1\middle|\tilde{y}^{p}\right]}{p\left[\tilde{c}^{p}_{m}=0\middle|\tilde{y}^{p}\right]}\right) \tag{3.4}$$

A posteriori probability log likelihood ratio (LLR) can be shown as

$$ln\left(\frac{p\left[\tilde{c}^{p}_{m}=1\middle|\tilde{y}^{p}\right]}{p\left[\tilde{c}^{p}_{m}=0\middle|\tilde{y}^{p}\right]}\right)=ln\left(\frac{\sum\limits_{\psi=\Psi^{(1)}_{m}}p\left[\tilde{s}^{p}=\psi\middle|\tilde{y}^{p}\right]}{\sum\limits_{\psi=\Psi^{(0)}_{m}}p\left[\tilde{s}^{p}=\psi\middle|\tilde{y}^{p}\right]}\right) \tag{3.5}$$

where

- $\Psi^{(1)}_{m}$: the subset of all symbols with $\tilde{c}^{p}_{m}=1$
- $\Psi^{(0)}_{m}$: the subset of all symbols with $\tilde{c}^{p}_{m}=0$

By the Bayes rules,

$$ln\left(\frac{\sum\limits_{\psi=\Psi^{(1)}_{m}}p\left[\tilde{s}^{p}=\psi\middle|\tilde{y}^{p}\right]}{\sum\limits_{\psi=\Psi^{(0)}_{m}}p\left[\tilde{s}^{p}=\psi\middle|\tilde{y}^{p}\right]}\right)=ln\left(\frac{\sum\limits_{\psi=\Psi^{(1)}_{m}}p\left[\tilde{y}^{p}\middle|\tilde{s}^{p}=\psi\right]p\left[\tilde{s}^{p}=\psi\right]}{\sum\limits_{\psi=\Psi^{(0)}_{m}}p\left[\tilde{y}^{p}\middle|\tilde{s}^{p}=\psi\right]p\left[\tilde{s}^{p}=\psi\right]}\right) \tag{3.6}$$

Because all symbols on the constellation are transmitted with equal probability, then equation (3.6) can be modified to

$$ln\left(\frac{\sum\limits_{\psi=\Psi^{(1)}_{m}}p\left[\tilde{s}^{p}=\psi\middle|\tilde{y}^{p}\right]}{\sum\limits_{\psi=\Psi^{(0)}_{m}}p\left[\tilde{s}^{p}=\psi\middle|\tilde{y}^{p}\right]}\right)=ln\left(\frac{\sum\limits_{\psi=\Psi^{(1)}_{m}}p\left[\tilde{y}^{p}\middle|\tilde{s}^{p}=\psi\right]}{\sum\limits_{\psi=\Psi^{(0)}_{m}}p\left[\tilde{y}^{p}\middle|\tilde{s}^{p}=\psi\right]}\right) \tag{3.7}$$

By equations (3.5) and (3.7), the bit metrics is equal to

$$\Lambda\left(\tilde{c}_m^p\right)=ln\left(\frac{\sum\limits_{\psi=\Psi_m^{(1)}} p\left[\tilde{y}^p\left|\tilde{s}^p=\psi\right.\right]}{\sum\limits_{\psi=\Psi_m^{(0)}} p\left[\tilde{y}^p\left|\tilde{s}^p=\psi\right.\right]}\right) \tag{3.8}$$

Sub-optimal simplified LLR can be reduced by the log-sum approximation

$$ln\left(\sum_i x_i\right)\approx \max_i\left(ln\left(x_i\right)\right) \tag{3.9}$$

The log-sum approximation is a good approximation if the summation in the left-hand side of equation (3.9) is dominated by the largest term. Then, at high signal-to-noise ratio (SNR), the bit metrics can be approximated by the log-sum approximation, see

$$\Lambda\left(\tilde{c}_m^p\right)\approx ln\left(\frac{\max\limits_{\psi=\Psi_m^{(1)}} p\left[\tilde{y}^p\left|\tilde{s}^p=\psi\right.\right]}{\max\limits_{\psi=\Psi_m^{(0)}} p\left[\tilde{y}^p\left|\tilde{s}^p=\psi\right.\right]}\right) \tag{3.10}$$

3.2 ZF Criterion

In this section, use ZF approach to detect signal. Because the MIMO-OFDM systems is used in the indoor WLAN scenario, we can assume the MIMO channel is multipath quasi-static Rayleigh fading channel. The frequency response $\mathbf{H}_k$ of MIMO channel in the k^{th} subchannel of OFDM systems is defined as.

$$\mathbf{H}_k=\begin{bmatrix} H_k^{1,1} & \cdots & H_k^{1,N_T} \\ \vdots & H_k^{q,p} & \vdots \\ H_k^{N_R,1} & \cdots & H_k^{N_R,N_T} \end{bmatrix} \tag{3.11}$$

The transmitted signal vector before IFFT/GI is defined as $\tilde{\mathbf{s}}_{\ell.k}$

$$\tilde{\mathbf{s}}_{\ell.k}=\left[\tilde{s}_{\ell.k}^{1},\cdots,\tilde{s}_{\ell.k}^{N_T}\right]^{\mathrm{T}} \tag{3.12}$$

The received signal vector after FFT/remove-GI is defined as $\tilde{\mathbf{r}}_{\ell.k}$

$$\tilde{\mathbf{r}}_{\ell.k} = \left[\tilde{r}_{\ell.k}^{1}, \cdots, \tilde{r}_{\ell.k}^{N_R} \right]^{\mathrm{T}} \tag{3.13}$$

And the received signal vector after FFT/remove-GI can be represented as

$$\tilde{\mathbf{r}}_{\ell.k} = \mathbf{H}_k \tilde{\mathbf{s}}_{\ell.k} + \tilde{\mathbf{n}}_{\ell.k} \tag{3.14}$$

where $\tilde{\mathbf{n}}_{\ell.k} = [\tilde{n}_{\ell.k}^{1}, \cdots, \tilde{n}_{\ell.k}^{N_R}]$ is the received noise vector.

Define the coefficient of the linear detector in the k^{th} subchannel is

$$\mathbf{G}_k^{\mathrm{ZF}} = \begin{bmatrix} g_k^{1,1} & \cdots & g_k^{1,N_R} \\ \vdots & g_k^{p,q} & \vdots \\ g_k^{N_T,1} & \cdots & g_k^{N_T,N_R} \end{bmatrix} \text{ and } \mathbf{g}_k^{p} = \left[g_k^{p,1}, \cdots, g_k^{p,N_R} \right]^{\mathrm{H}} \tag{3.15}$$

To detect signal at the p^{th} sub-stream based on the zero-forcing criterion.

$$\text{ZF criterion: } \mathbf{G}_k^{\mathrm{ZF}} \hat{\mathbf{H}}_k = 1 \tag{3.16}$$

So,

$$\mathbf{G}_k^{\mathrm{ZF}} = \left[\left(\hat{\mathbf{H}}_k \right)^{\mathrm{H}} \hat{\mathbf{H}}_k \right]^{-1} \hat{\mathbf{H}}_k \tag{3.17}$$

Then, the output signal of the ZF receiver is

$$\tilde{\mathbf{y}}_{\ell.k} = \mathbf{G}_k^{\mathrm{ZF}} \tilde{\mathbf{r}}_{\ell.k} = \mathbf{G}_k^{\mathrm{ZF}} \mathbf{H}_k \tilde{\mathbf{s}}_{\ell.k} + \mathbf{G}_k^{\mathrm{ZF}} \tilde{\mathbf{n}}_{\ell.k} \tag{3.18}$$

Assume there is perfect channel estimation. Then the detected signal vector is

$$\tilde{\mathbf{y}}_{\ell.k} = \tilde{\mathbf{s}}_{\ell.k} + \mathbf{G}_k^{\mathrm{ZF}} \tilde{\mathbf{n}}_{\ell.k} \tag{3.19}$$

where

$$\tilde{\mathbf{y}}_{\ell.k} = \left[\tilde{y}_{\ell.k}^{1}, \cdots, \tilde{y}_{\ell.k}^{N_R} \right]^{\mathrm{T}}$$

3.2.1 Approximation of Bit Metrics

Observe the p^{th} sub-stream detected signal $\tilde{y}_{\ell.k}^{p}$,

$$\tilde{y}_{\ell.k}^{p} = \tilde{s}_{\ell.k}^{p} + \left(\mathbf{g}_k^{p}\right)^{\mathrm{H}} \tilde{\mathbf{n}}_{\ell.k} \tag{3.20}$$

The received noises $\tilde{n}_{\ell.k}^{1}, \cdots, \tilde{n}_{\ell.k}^{N_R}$ are statistically independent and identically distributed complex Gaussian random variables with zero mean and variance $\sigma_{\tilde{n}}^2$.

Define over all noise term in the equation (3.20) is

$$\tilde{z}_{\ell.k}^{p} = \left(\mathbf{g}_k^{p}\right)^{\mathrm{H}} \tilde{\mathbf{n}}_{\ell.k} = g_k^{p,1} \tilde{n}_{\ell.k}^{1} + \cdots + g_k^{p,N_R} \tilde{n}_{\ell.k}^{N_R} \tag{3.21}$$

Then $\tilde{z}_{\ell.k}^{p}$ is still a complex Gaussian random variable with zero mean and variance $\sigma_{\tilde{z}_{\ell.k}^{p}}^2$.

$$\sigma_{\tilde{z}_{\ell.k}^{p}}^2 = \left(g_k^{p,1}\right)^2 \sigma_{\tilde{n}_{\ell.k}^{1}}^2 + \cdots + \left(g_k^{p,N_R}\right)^2 \sigma_{\tilde{n}_{\ell.k}^{N_R}}^2 = \sigma_{\tilde{n}}^2 \cdot \sum_{q=1}^{N_R} \left| g_k^{p,q} \right|^2 \tag{3.22}$$

where

$$\sigma_{\tilde{n}_{\ell.k}^{1}}^2 = \cdots = \sigma_{\tilde{n}_{\ell.k}^{N_R}}^2 = \sigma_{\tilde{n}}^2$$

Then the detect signal is shown as

$$\tilde{y}_{\ell.k}^{p} = \tilde{s}_{\ell.k}^{p} + \tilde{z}_{\ell.k}^{p} \tag{3.23}$$

The conditional pdf of $\tilde{y}_{\ell.k}^{p}$ is a complex Gaussian distribution,

$$p\left(\tilde{y}_{\ell.k}^{p} \,\middle|\, \tilde{s}_{\ell.k}^{p} = \psi\right) = \frac{1}{\pi \left|\sigma_{\tilde{z}_{\ell.k}^{p}}\right|} \exp\left\{ \frac{-1}{\sigma_{\tilde{z}_{\ell.k}^{p}}^2} \left(\tilde{y}_{\ell.k}^{p} - \psi\right)^2 \right\} \tag{3.24}$$

By the equation (3.10) and (3.24), the bit metrics $\tilde{c}_{\ell.k,m}^{p}$ is equal to

$$\begin{aligned} \Lambda\left(\tilde{c}_{\ell.k,m}^{p}\right) &= ln\left(\frac{\max\limits_{\psi=\Psi_m^{(1)}} \exp\left\{ \frac{-1}{\sigma_{\tilde{z}_{\ell.k}^{p}}^2} \left(\tilde{y}_{\ell.k}^{p} - \psi\right)^2 \right\}}{\max\limits_{\psi=\Psi_m^{(0)}} \exp\left\{ \frac{-1}{\sigma_{\tilde{z}_{\ell.k}^{p}}^2} \left(\tilde{y}_{\ell.k}^{p} - \psi\right)^2 \right\}} \right) \\ &= \frac{1}{\sigma_{\tilde{z}_{\ell.k}^{p}}^2} \left\{ -\min_{\psi=\Psi_m^{(1)}} \left(\tilde{y}_{\ell.k}^{p} - \psi\right)^2 + \min_{\psi=\Psi_m^{(0)}} \left(\tilde{y}_{\ell.k}^{p} - \psi\right)^2 \right\} \end{aligned} \tag{3.25}$$

Then, define the coefficients of bit metrics $\tilde{c}^{p}_{\ell.k,m}$ for BICM

$$W^{p}_{\ell.k} = \frac{1}{\sigma^2_{\tilde{z}^{p}_{\ell.k}}} = \left[\sigma^2_{\tilde{n}} \cdot \sum_{q=1}^{N_R} \left| g_k^{p,q} \right|^2 \right]^{-1} \tag{3.26}$$

By the way, the signal-to-noise ratio of $\tilde{y}^{p}_{\ell.k}$ is

$$\text{SNR}=\frac{\mathrm{E}\left\{ \left| \tilde{s}^{p}_{\ell.k} \right|^2 \right\}}{\mathrm{E}\left\{ \left| \tilde{z}^{p}_{\ell.k}{}^2 \right| \right\}} = \frac{\sigma^2_{\tilde{s}}}{\sigma^2_{\tilde{n}} \cdot \sum_{q=1}^{N_R} \left| g_k^{p,q} \right|^2} \tag{3.27}$$

So the coefficient of bit metrics $\tilde{c}^{p}_{\ell.k,m}$ for BICM is directly proportional to the signal-to-noise ratio of detected signal $\tilde{y}^{p}_{\ell.k}$.

3.2.2 Simulation Results

Our simulation platform is based on the proposal of TGn Sync. The signal bandwidth (BW) is 20MHz. The transmitter and receiver use 128-points IFFT and FFT, respectively. The antenna spacing in the transmitter and receiver are equal to 0.5 wavelength. The decoder uses soft Viterbi algorithm to decide information bits with trace back length of 128. Assume there are perfect synchronization in the receiver, i.e. without frequency offset, clock offset, and phase rotation. The channel is well-kwon in the receiver. There are 8000 information bits per packet. There are at least 500 packet errors down to 1% packet error rate (PER) or a total of 10,000 packets in our simulation. The detector design in this section is based on the ZF criterion. Compare the equal weight $W^{p}_{\ell.k} = 1$ and weighted $W^{p}_{\ell.k} = \left[\sigma^2_{\tilde{z}^{p}_{\ell.k}} \right]^{-1}$ of bit metrics calculation.

Case1: Channel B of IEEE802.11n, 2x2

From the simulation results Fig. 3-2 and Fig. 3-3, we can discover that the performance of weighted coefficients for bit metrics computation is much better than those of equal gain. There are about 4~5 dB improvement under the PER=0.1.

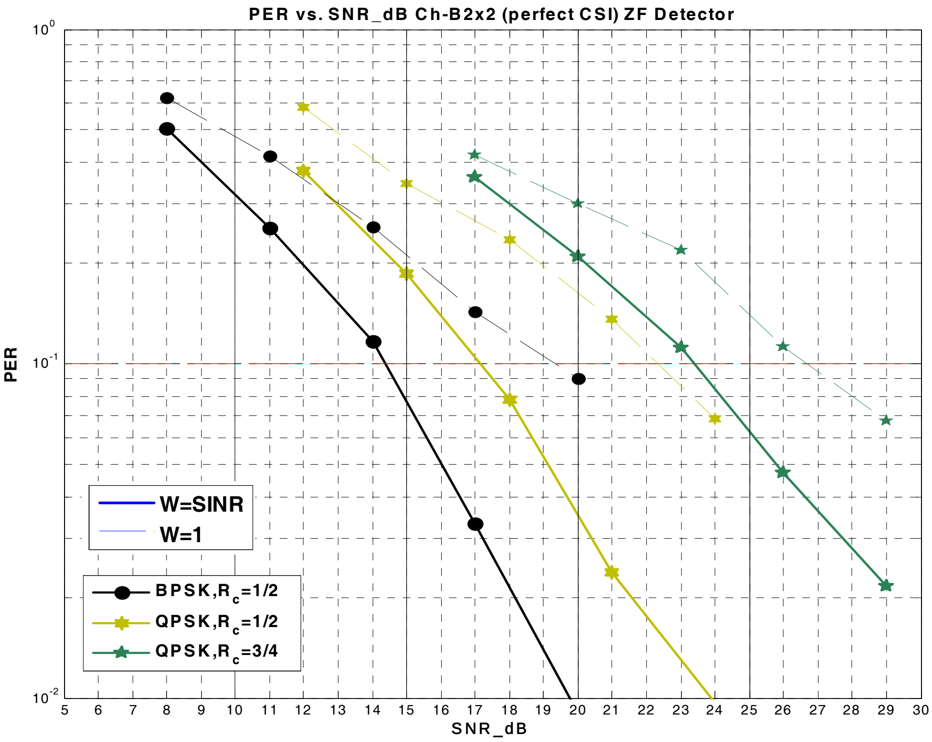

Fig. 3-2: PER of bit metrics calculation with equal and weighted coefficients by ZF detector for BPSK and QPSK in channel B, 2x2

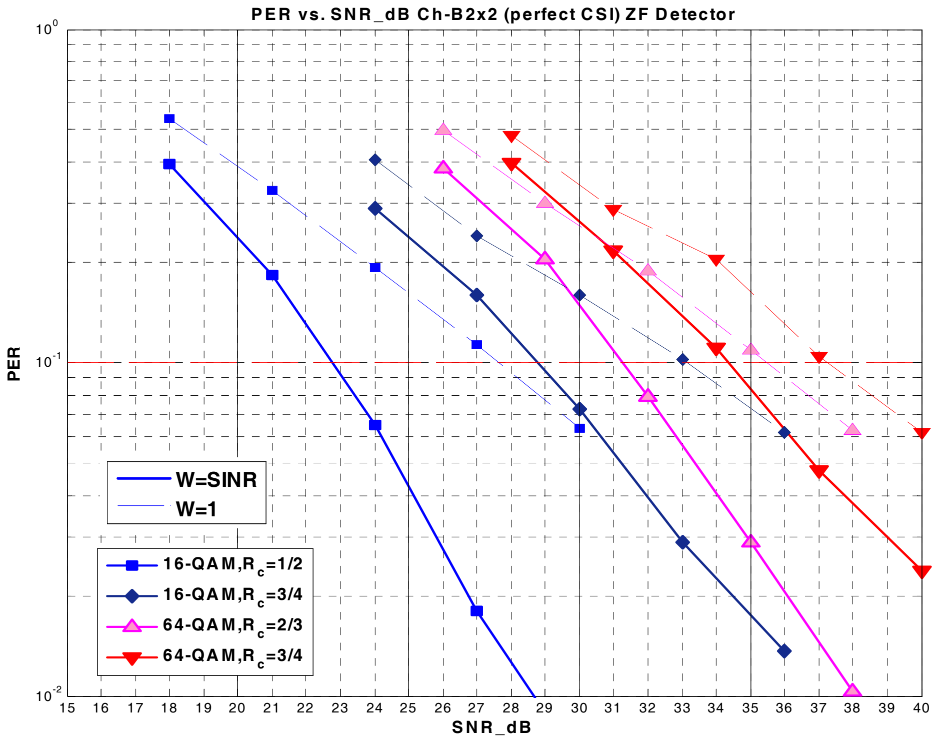

Fig. 3-3: PER of bit metrics calculation with equal and weighted coefficients by ZF detector for 16-QAM and 64-QAM in channel B, 2x2

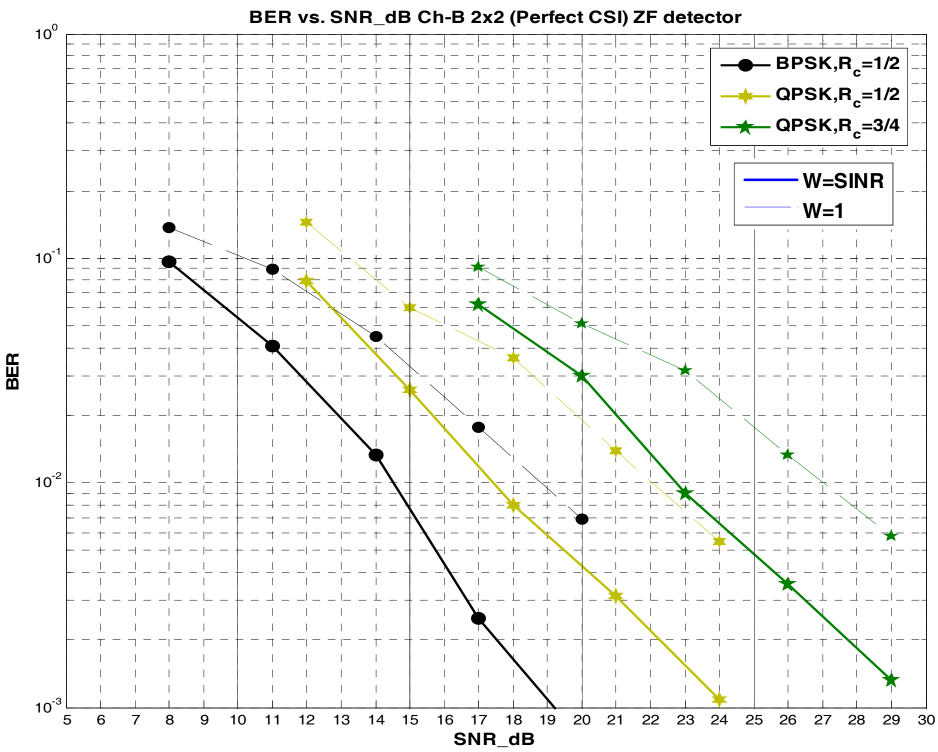

Fig. 3-4: BER of bit metrics calculation with equal and weighted coefficients by ZF detector for BPSK and QPSK in channel B, 2x2

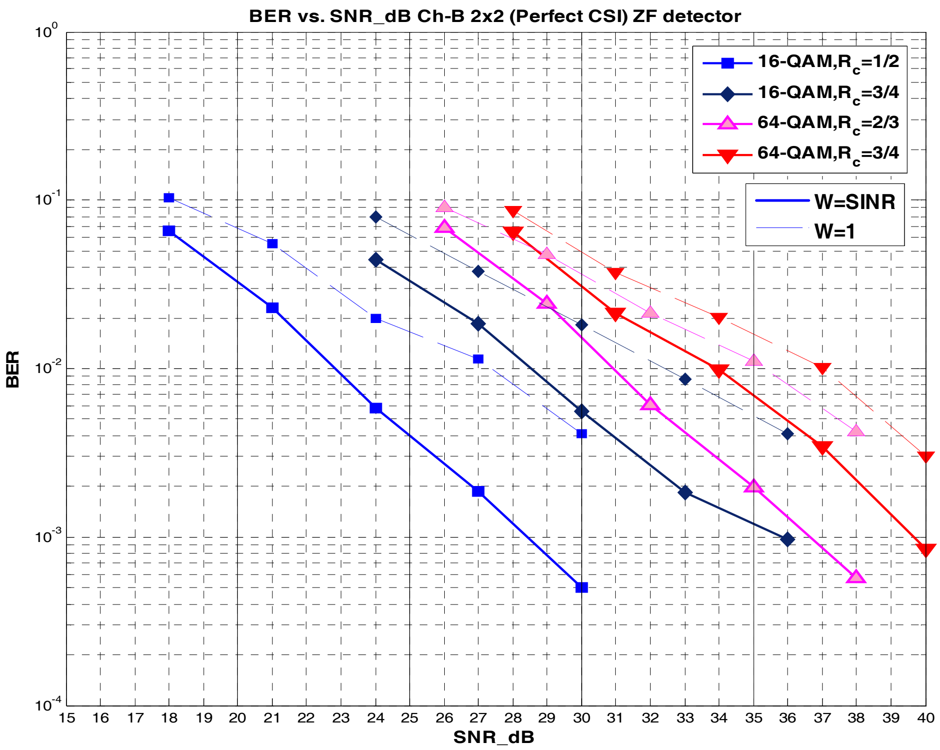

Fig. 3-5: BER of bit metrics calculation with equal and weighted coefficients by ZF detector for 16-QAM and 64-QAM in channel B, 2x2

3.3 MMSE Criterion

In this section, use MMSE approach to detect signal. It is similar to a ZF receiver. Assume the MIMO channel is multipath quasi-static Rayleigh fading channel. The received signal vector after FFT/remove-GI is defined in (3.14) and the output signal vector $\tilde{\mathbf{y}}_{\ell.k}$ of MMSE detector is defined as

$$\tilde{\mathbf{y}}_{\ell.k} = \mathbf{G}_k^{\mathrm{MMSE}} \tilde{\mathbf{r}}_{\ell.k} \tag{3.28}$$

Now, base on the MMSE criterion to minimize the error of the detected signal vector $\tilde{\mathbf{y}}_{\ell.k}$ and a transmitter signal vector $\tilde{\mathbf{s}}_{\ell.k}$

$$\mathbf{G}_k^{\mathrm{MMSE}} = \arg \min_{\mathbf{G}_k^{\mathrm{MMSE}}} \mathrm{E}\left\{ \left| \tilde{\mathbf{y}}_{\ell.k} - \tilde{\mathbf{s}}_{\ell.k} \right|^2 \right\} = \arg \min_{\mathbf{G}_k^{\mathrm{MMSE}}} \mathrm{E}\left\{ \left| \mathbf{G}_k^{\mathrm{MMSE}} \tilde{\mathbf{r}}_{\ell.k} - \tilde{\mathbf{s}}_{\ell.k} \right|^2 \right\} \tag{3.29}$$

See Appendix A, assume the energy of signal is equal to 1.

Then, the coefficients of an MMSE detector is

$$\mathbf{G}_k^{\mathrm{MMSE}} = \left(\mathbf{H}_k\right)^{\mathrm{H}} \left[\mathbf{H}_k \left(\mathbf{H}_k\right)^{\mathrm{H}} + \sigma_{\tilde{n}}^2 \mathbf{I}_{N_R}\right]^{-1} \tag{3.30}$$

3.3.1 Approximation of Bit Metrics

Observe the p^{th} sub-stream detected signal $\tilde{y}^p_{\ell.k}$,

$$\tilde{y}^p_{\ell.k} = \left(\mathbf{g}_k^p\right)^{\mathrm{H}} \mathbf{h}_k^p \tilde{s}^p_{\ell.k} + \left(\mathbf{g}_k^p\right)^{\mathrm{H}} \left(\sum_{j \neq p} \mathbf{h}_k^j \tilde{s}^j_{\ell.k}\right) + \left(\mathbf{g}_k^p\right)^{\mathrm{H}} \tilde{\mathbf{n}}_{\ell.k} \tag{3.31}$$

where we define $\mathbf{h}_k^j$ is the j^{th} column vector of $\mathbf{H}_k$

$$\mathbf{h}_k^j = \left[H_k^{1,j}, \cdots, H_k^{N_R,j}\right]^{\mathrm{T}} \tag{3.32}$$

Because $\left(\mathbf{g}_k^p\right)^{\mathrm{H}} \mathbf{h}_k^j \neq 0$, for any j, there are co-antenna interference $\tilde{\mu}^p_{\ell.k}$

$$\tilde{\mu}^p_{\ell.k} = \left(\mathbf{g}_k^p\right)^{\mathrm{H}} \left(\sum_{j \neq p} \mathbf{h}_k^j \tilde{s}^j_{\ell.k}\right) \tag{3.33}$$

In [21], H.V. Poor and S.Verdu show that the MMSE estimate approximates a Gaussian distribution. Hence, the co-antenna interference and noise are considered together as complex Gaussian noise $\tilde{z}^p_{\ell.k}$ with Gaussian approximation.

$$\tilde{z}^p_{\ell.k} = \left(\mathbf{g}_k^p\right)^{\mathrm{H}} \left(\sum_{j \neq p} \mathbf{h}_k^j \tilde{s}^j_{\ell.k}\right) + \left(\mathbf{g}_k^p\right)^{\mathrm{H}} \tilde{\mathbf{n}}_{\ell.k} \tag{3.34}$$

The variance of complex Gaussian noise $\tilde{z}^p_{\ell.k}$ is

$$\sigma^2_{\tilde{z}^p_{\ell.k}} = \mathrm{E}\left\{\left|\tilde{z}^p_{\ell.k}\right|^2\right\} = \mathrm{E}\left\{\left|\left(\mathbf{g}_k^p\right)^{\mathrm{H}} \left(\sum_{j \neq p} \mathbf{h}_k^j \tilde{s}^j_{\ell.k}\right) + \left(\mathbf{g}_k^p\right)^{\mathrm{H}} \tilde{\mathbf{n}}_{\ell.k}\right|^2\right\} \tag{3.35}$$

Due to $\tilde{s}^1_{\ell.k}, \cdots, \tilde{s}^{N_T}_{\ell.k}$ and $\tilde{n}^1_{\ell.k}, \cdots, \tilde{n}^{N_R}_{\ell.k}$ are statistically independent,

$$\sigma^2_{\tilde{z}^p_{\ell.k}} = \sigma^2_{\tilde{s}} \sum_{j \neq p} \left| \left(\mathbf{g}^p_k \right)^{\mathrm{H}} \mathbf{h}^j_k \right|^2 + \sigma^2_{\tilde{n}} \cdot \sum_{q=1}^{N_R} \left| g^{p,q}_k \right|^2 \tag{3.36}$$

Then the detect signal is shown as

$$\tilde{y}^p_{\ell.k} = \left(\mathbf{g}^p_k \right)^{\mathrm{H}} \mathbf{h}^p_k \tilde{s}^p_{\ell.k} + \tilde{z}^p_{\ell.k} \tag{3.37}$$

The conditional pdf of $\tilde{y}^p_{\ell.k}$ is a complex Gaussian distribution,

$$p\left(\tilde{y}^p_{\ell.k} \middle| \tilde{s}^p_{\ell.k} = \psi \right) = \frac{1}{\pi \left| \sigma_{\tilde{z}^p_{\ell.k}} \right|} \exp\left\{ \frac{-1}{\sigma^2_{\tilde{z}^p_{\ell.k}}} \left(\tilde{y}^p_{\ell.k} - \left(\mathbf{g}^p_k \right)^{\mathrm{H}} \mathbf{h}^p_k \psi \right)^2 \right\} \tag{3.38}$$

By the equation (3.10) and (3.38), the bit metrics $\tilde{c}^p_{\ell.k,m}$ is equal to

$$\begin{aligned} \Lambda\left(\tilde{c}^p_{\ell.k,m} \right) &= ln \left(\frac{\max\limits_{\psi = \Psi^{(1)}_m} \exp\left\{ \frac{-1}{\sigma^2_{\tilde{z}^p_{\ell.k}}} \left(\tilde{y}^p_{\ell.k} - \left(\mathbf{g}^p_k \right)^{\mathrm{H}} \mathbf{h}^p_k \psi \right)^2 \right\}}{\max\limits_{\psi = \Psi^{(0)}_m} \exp\left\{ \frac{-1}{\sigma^2_{\tilde{z}^p_{\ell.k}}} \left(\tilde{y}^p_{\ell.k} - \left(\mathbf{g}^p_k \right)^{\mathrm{H}} \mathbf{h}^p_k \psi \right)^2 \right\}} \right) \\ &= \frac{1}{\sigma^2_{\tilde{z}^p_{\ell.k}}} \left\{ - \min_{\psi = \Psi^{(1)}_m} \left(\tilde{y}^p_{\ell.k} - \left(\mathbf{g}^p_k \right)^{\mathrm{H}} \mathbf{h}^p_k \psi \right)^2 + \min_{\psi = \Psi^{(0)}_m} \left(\tilde{y}^p_{\ell.k} - \left(\mathbf{g}^p_k \right)^{\mathrm{H}} \mathbf{h}^p_k \psi \right)^2 \right\} \end{aligned} \tag{3.39}$$

To normalize $\tilde{y}^p_{\ell.k}$ by dividing $\left(\mathbf{g}^p_k \right)^{\mathrm{H}} \mathbf{h}^p_k$,

$$\tilde{\zeta}^p_{\ell.k} = \tilde{y}^p_{\ell.k} \cdot \left[\left(\mathbf{g}^p_k \right)^{\mathrm{H}} \mathbf{h}^p_k \right]^{-1} = \tilde{s}^p_{\ell.k} + \tilde{z}^p_{\ell.k} \cdot \left[\left(\mathbf{g}^p_k \right)^{\mathrm{H}} \mathbf{h}^p_k \right]^{-1} \tag{3.40}$$

Then, the bit metrics is

$$\Lambda\left(\tilde{c}^p_{\ell.k,m} \right) = \frac{\left| \left(\mathbf{g}^p_k \right)^{\mathrm{H}} \mathbf{h}^p_k \right|^2}{\sigma^2_{\tilde{z}^p_{\ell.k}}} \left\{ - \min_{\psi = \Psi^{(1)}_m} \left(\tilde{\zeta}^p_{\ell.k} - \psi \right)^2 + \min_{\psi = \Psi^{(0)}_m} \left(\tilde{\zeta}^p_{\ell.k} - \psi \right)^2 \right\} \tag{3.41}$$

The coefficient of bit metrics $\tilde{c}^p_{\ell.k,m}$ for BICM in MMSE detector is

$$W^p_{\ell.k} = \frac{\left| \left(\mathbf{g}^p_k \right)^{\mathrm{H}} \mathbf{h}^p_k \right|^2}{\sigma^2_{\tilde{z}^p_{\ell.k}}} = \left| \left(\mathbf{g}^p_k \right)^{\mathrm{H}} \mathbf{h}^p_k \right|^2 \left[\sigma^2_{\tilde{s}} \sum_{j \neq p} \left| \left(\mathbf{g}^p_k \right)^{\mathrm{H}} \mathbf{h}^p_j \right|^2 + \sigma^2_{\tilde{n}} \cdot \sum_{q=1}^{N_R} \left| g^{p,q}_k \right|^2 \right]^{-1} \tag{3.42}$$

By the way, the signal-to-interference-and-noise ratio of $\tilde{y}^p_{\ell.k}$ is

$$\mathrm{SNR}=\frac{\mathrm{E}\left\{\left|\tilde{s}_{\ell.k}^{p}\right|^{2}\right\}}{\mathrm{E}\left\{\left|\tilde{z}_{\ell.k}^{p}{}^{2}\right|\right\}}=\frac{\left|\left(\mathbf{g}_{k}^{p}\right)^{\mathrm{H}}\mathbf{h}_{k}^{p}\right|^{2}\sigma_{\tilde{s}}^{2}}{\sigma_{\tilde{s}}^{2}\sum_{j\neq p}\left|\left(\mathbf{g}_{k}^{p}\right)^{\mathrm{H}}\mathbf{h}_{k}^{j}\right|^{2}+\sigma_{\tilde{n}}^{2}\cdot\sum_{q=1}^{N_R}\left|g_{k}^{p,q}\right|^{2}} \tag{3.43}$$

So the coefficient of bit metrics $\tilde{c}_{\ell.k,m}^{p}$ for BICM is directly proportional to the signal-to-interference-and-noise ratio of detected signal $\tilde{y}_{\ell.k}^{p}$.

3.3.2 Simulation Results

Our simulation platform is based on the proposal of TGn Sync. The signal bandwidth (BW) is 20MHz. The transmitter and receiver use 128-points IFFT and FFT, respectively. The antenna spacing in the transmitter and receiver are equal to 0.5 wavelength. The decoder uses soft Viterbi algorithm to decide information bits with trace back length of 128. Assume there are perfect synchronization in the receiver, i.e. without frequency offset, clock offset, and phase rotation. The channel is well-kwon in the receiver. There are 8000 information bits per packet. There are at least 500 packet errors down to 1% packet error rate (PER) or a total of 10,000 packets in our simulation. The detector design in this section is based on the MMSE criterion. Compare the performance of equal and weighted coefficients of bit metrics calculation. The SNR is defined in chapter 2.

Case1: Orthogonal AWGN channel, 2x2

The signal is transmitted through the AWGN channel with orthogonal MIMO channel.

$$\mathbf{H}=\frac{1}{\sqrt{2}}\begin{bmatrix}1 & 1\\ 1 & -1\end{bmatrix} \tag{3.44}$$

From Fig. 3-6, we can find that the performances of bit metrics calculation with equal and weighted coefficients are almost the same. That’s because the frequency response of all subchannel are equal.

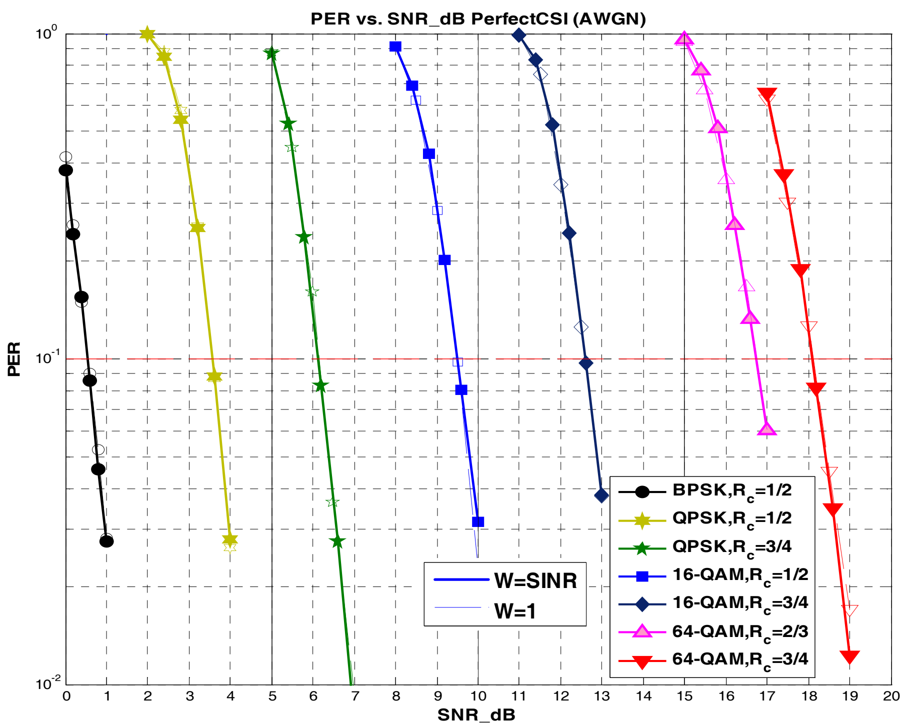

Fig. 3-6: PER of bit metrics calculation with equal and weighted coefficients by MMSE detector in AWGN channel, 2x2

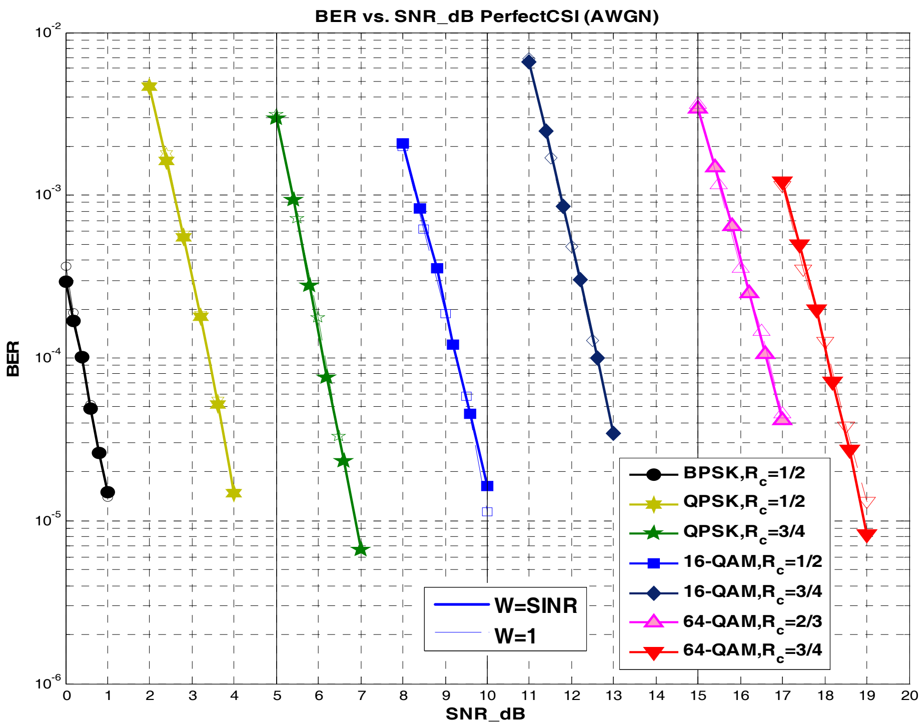

Fig. 3-7: BER of bit metrics calculation with equal and weighted coefficients by MMSE detector in AWGN channel, 2x2

Case2: Channel B of IEEE802.11n, 2x2

From Fig. 3-8 and Fig. 3-9, we can find that the performance of weighted gain for bit metrics computation is better than those of equal gain. There are about 1dB improvement for BPSK and QPSK, about 3dB improvement for 16-QAM and about 4dB improvement for 64-QAM under the PER=0.1. Compare to ZF detectors, the improvement of MMSE detects is smaller than those of ZF detector, especially for lower modulation. That is because we use the Gaussian approximation in MMSE detector. Then in the low modulation scheme and fewer sub-streams, the Gaussian approximation of interference is loose.

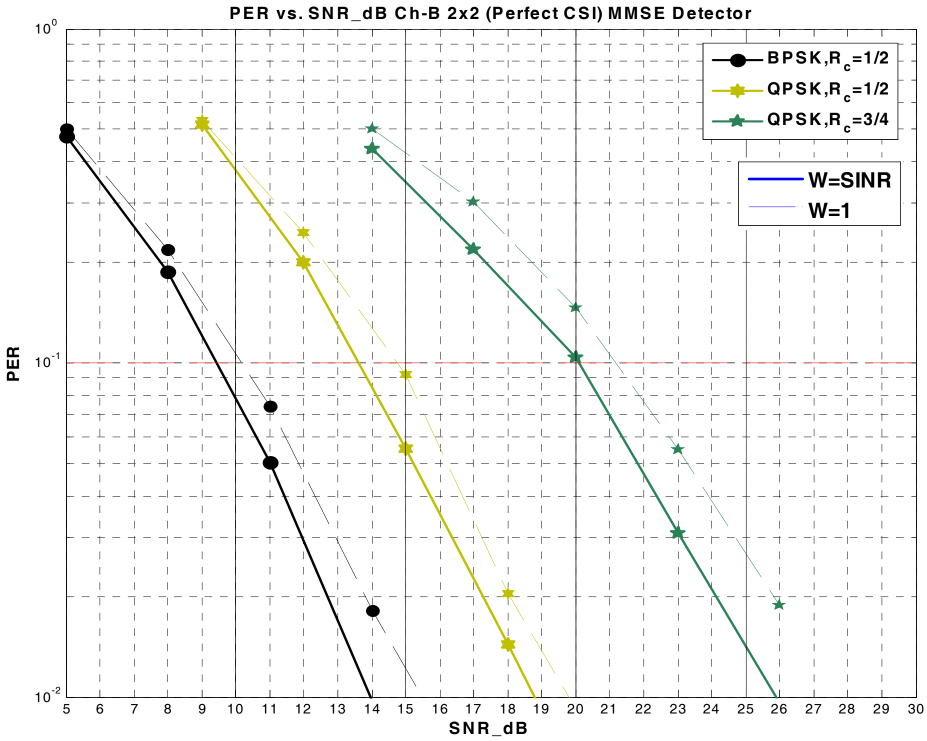

Fig. 3-8: PER of bit metrics calculation with equal and weighted coefficients by MMSE detector for BPSK and QPSK in channel B, 2x2

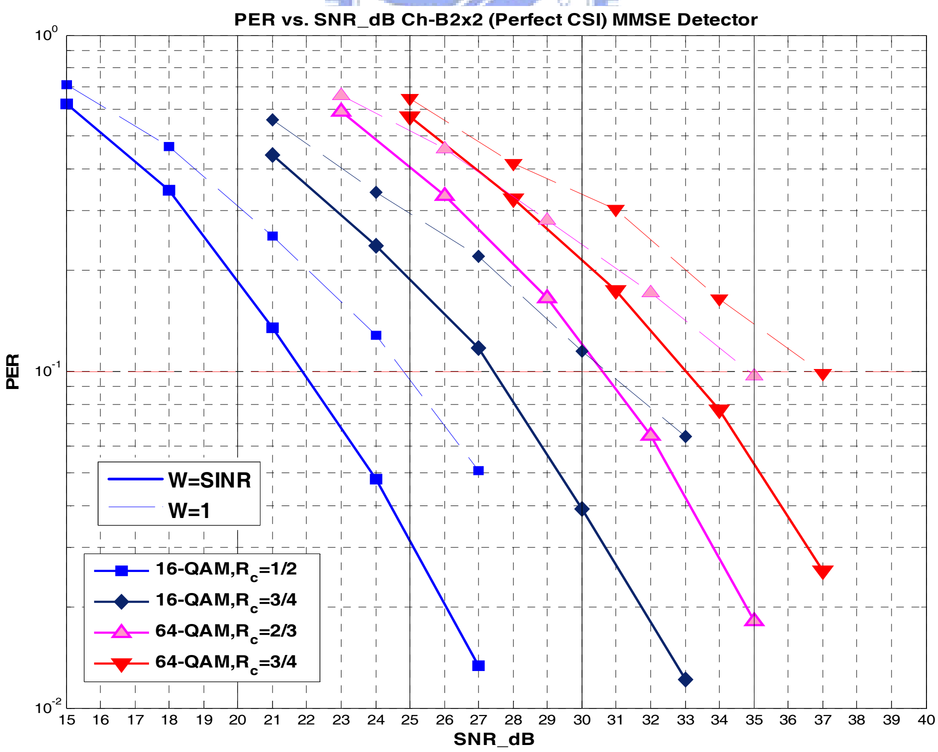

Fig. 3-9: PER of bit metrics calculation with equal and weighted coefficients by MMSE detector for 16-QAM and 64-QAM in channel B, 2x2

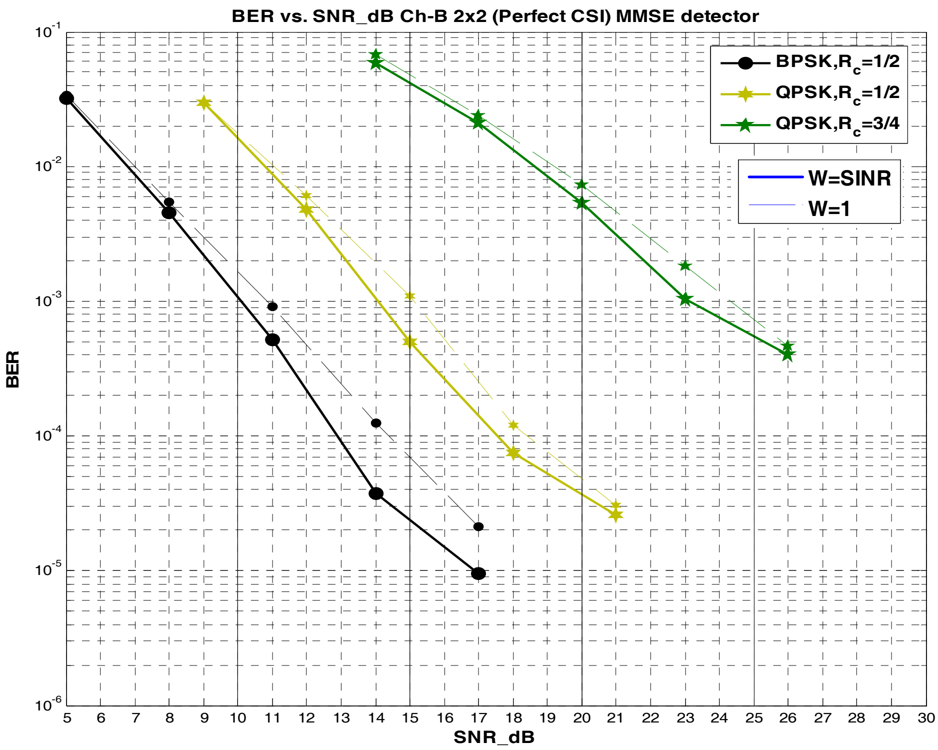

Fig. 3-10: BER of bit metrics calculation with equal and weighted coefficients by MMSE detector for BPSK and QPSK in channel B, 2x2

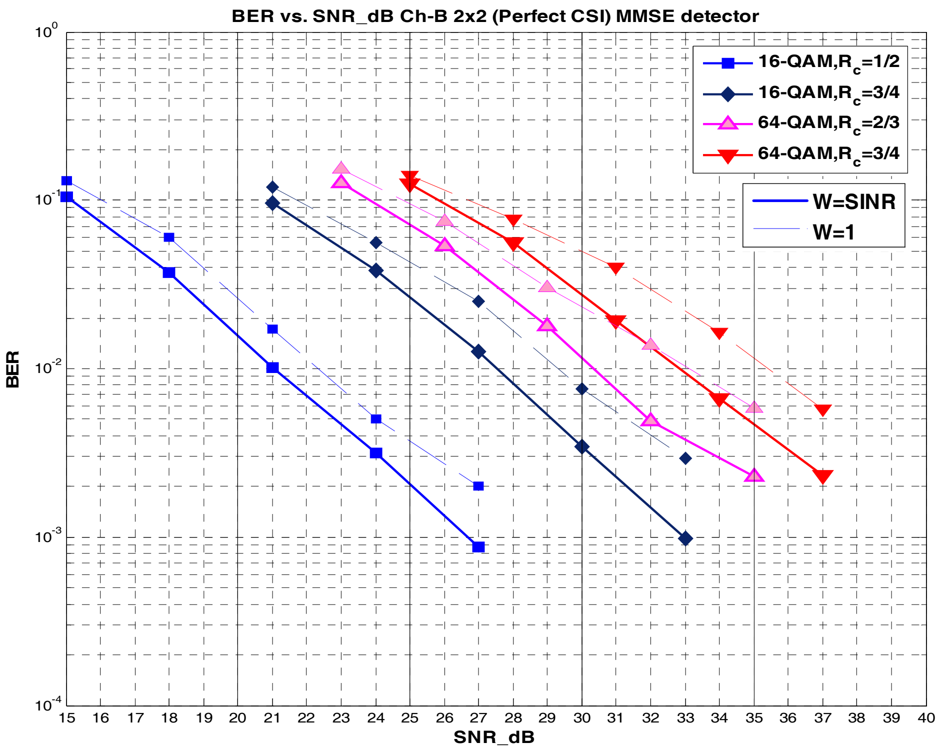

Fig. 3-11: BER of bit metrics calculation with equal and weighted coefficients by MMSE detector for 16-QAM and 64-QAM in channel B, 2x2

Case3: Channel B of IEEE802.11n, 2x3

In this case, the receiver uses three antennas to receive signal. From Fig. 3-12 and Fig. 3-13, we can find that the performance of weighted gain for bit metrics computation is better than those of equal gain. There are smaller than 0.5dB improvement for BPSK and QPSK, about 1dB improvement for 16-QAM and about 1.5dB improvement for 64-QAM under the PER=0.1. Compare to case2, the receiver in the case3 uses more receiver antenna than those in case2, and then the receiver has more diversity gain. Therefore, the weight for bit metrics is close to equal.

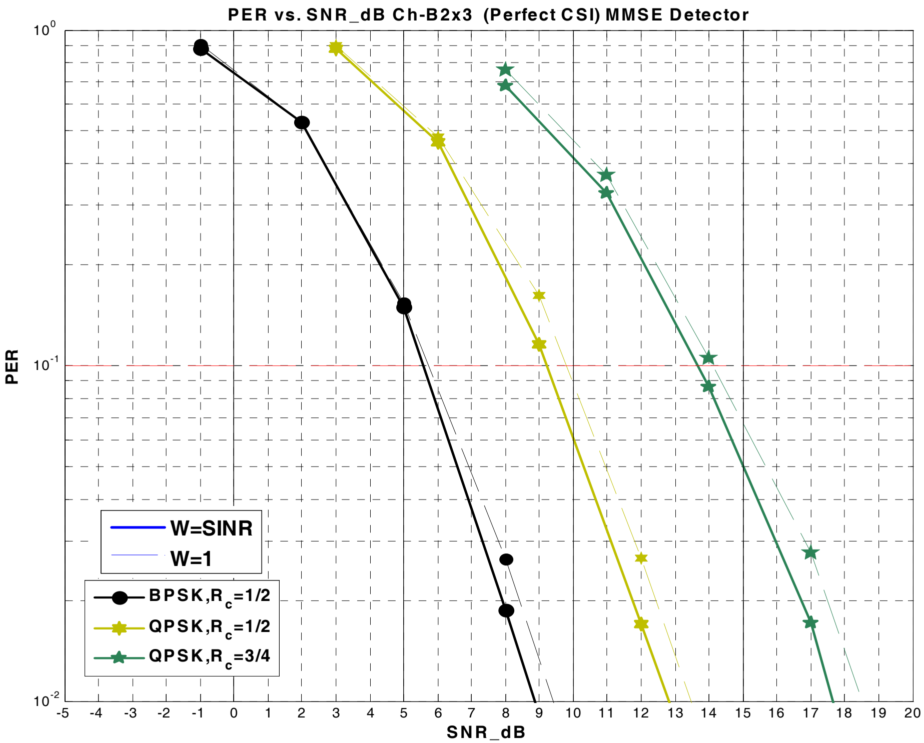

Fig. 3-12: PER of bit metrics calculation with equal and weighted coefficients by MMSE detector for BPSK and QPSK in channel B, 2x3

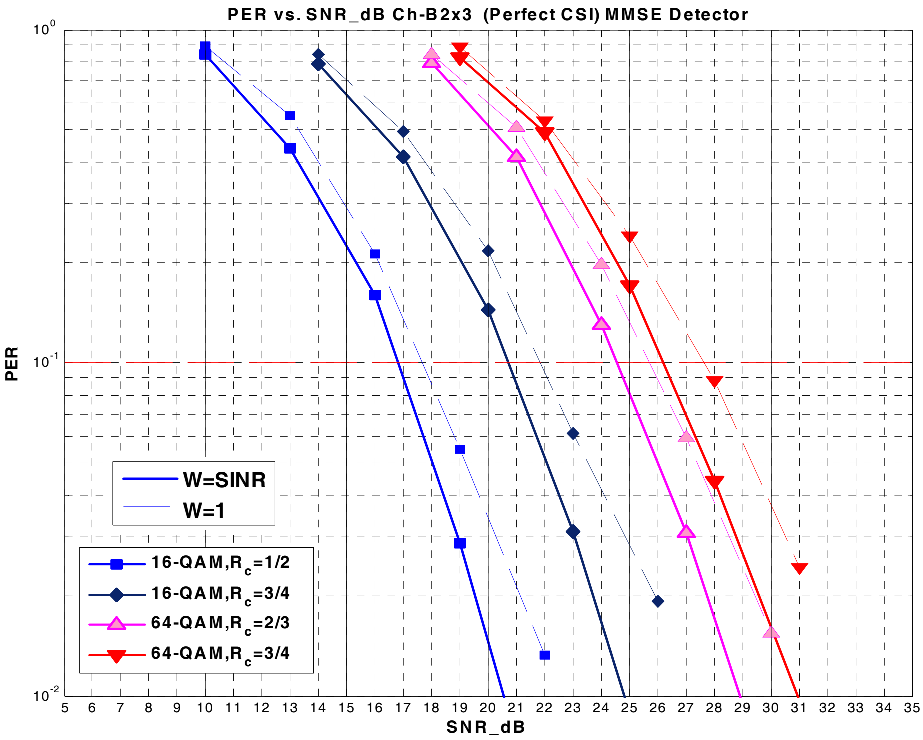

Fig. 3-13: PER of bit metrics calculation with equal and weighted coefficients by MMSE detector for 16-QAM and 64-QAM in channel B, 2x3

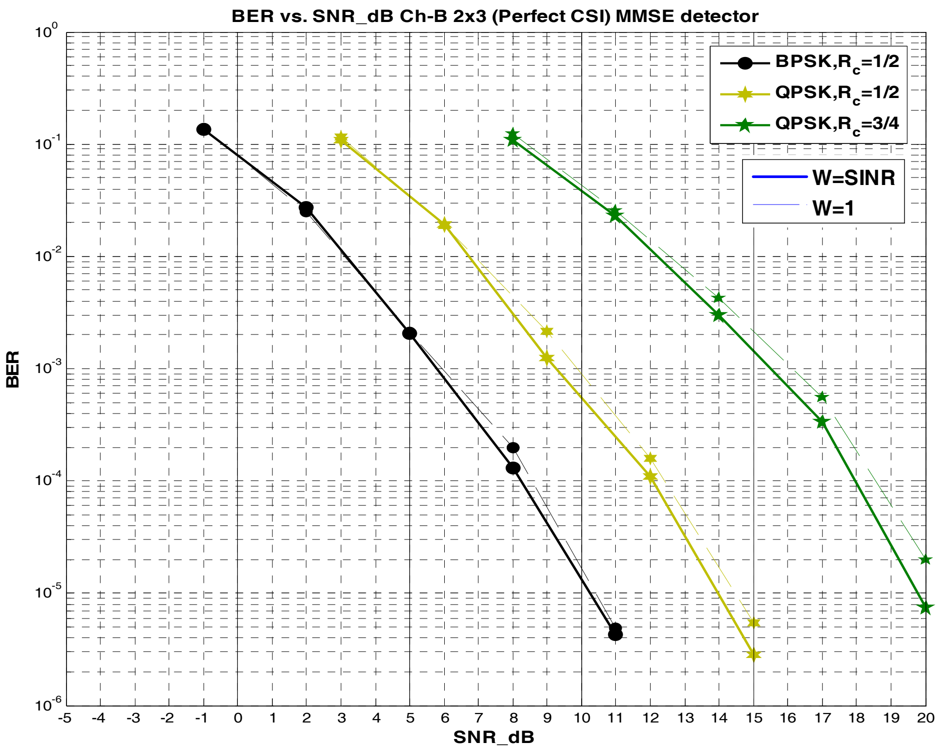

Fig. 3-14: BER of bit metrics calculation with equal and weighted coefficients by MMSE detector for BPSK and QPSK in channel B, 2x3

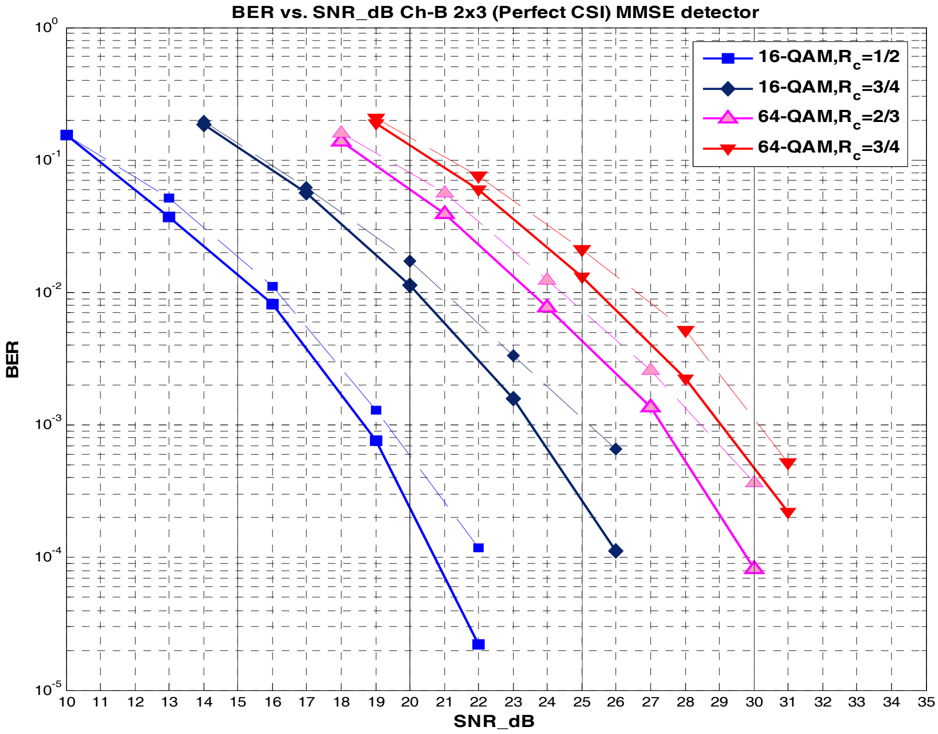

Fig. 3-15: PER of bit metrics calculation with equal and weighted coefficients by MMSE detector for 16-QAM and 64-QAM in channel B, 2x3

Case4: Channel B of IEEE802.11n, 3x3

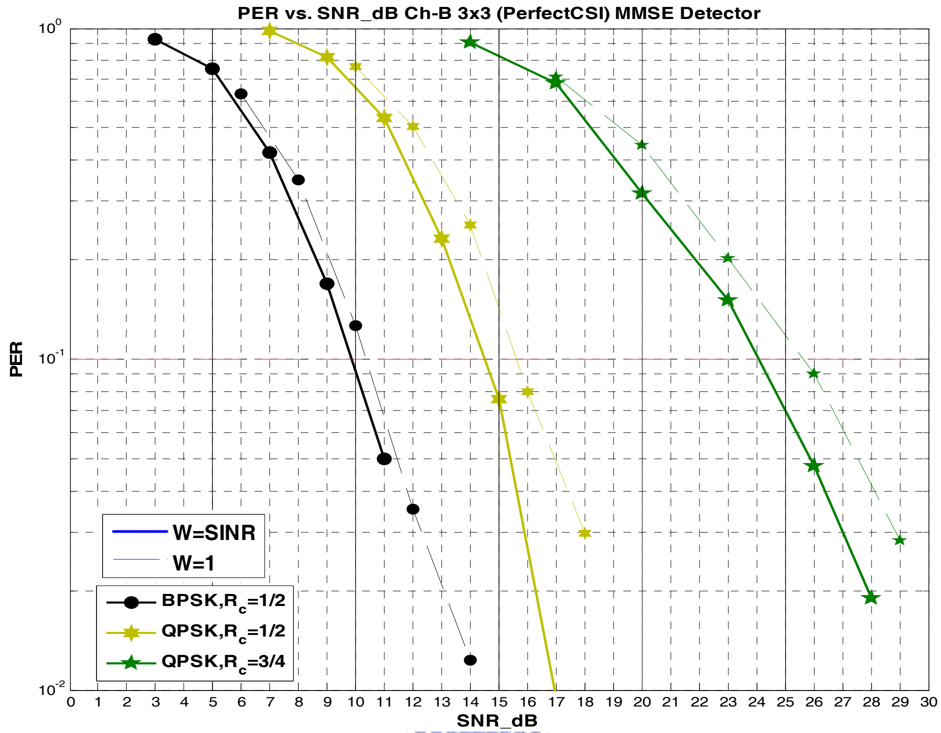

Fig. 3-16: PER of bit metrics calculation with equal and weighted coefficients by MMSE detector for BPSK and QPSK in channel B, 3x3

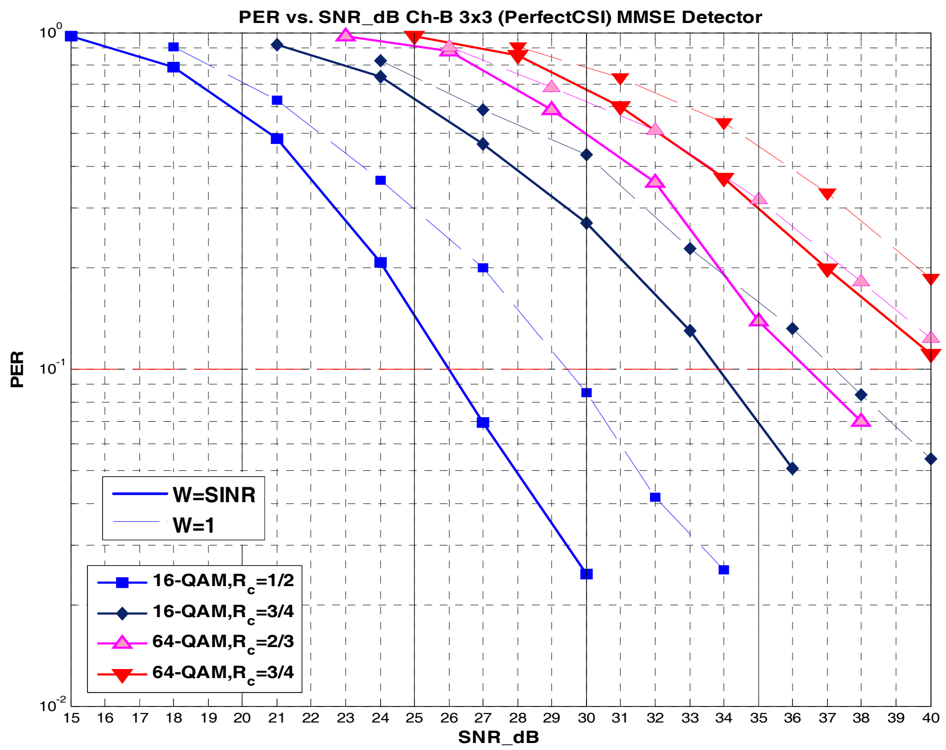

Fig. 3-17: PER of bit metrics calculation with equal and weighted coefficients by MMSE detector for 16-QAM and 64-QAM in channel B, 3x3

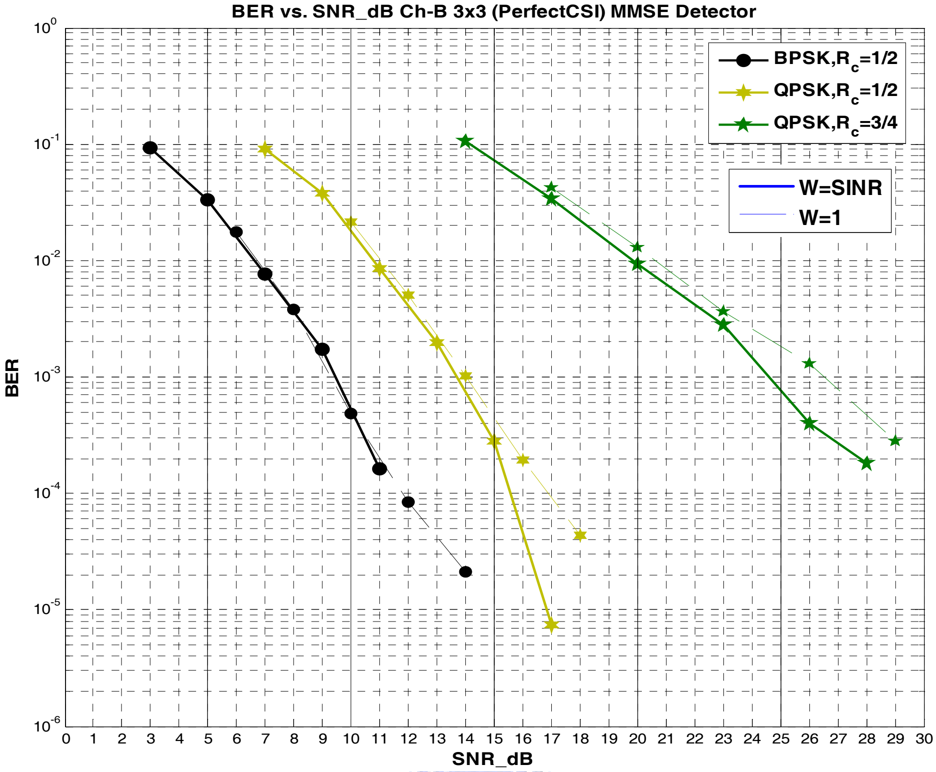

Fig. 3-18: BER of bit metrics calculation with equal and weighted coefficients by MMSE detector for BPSK and QPSK in channel B, 3x3

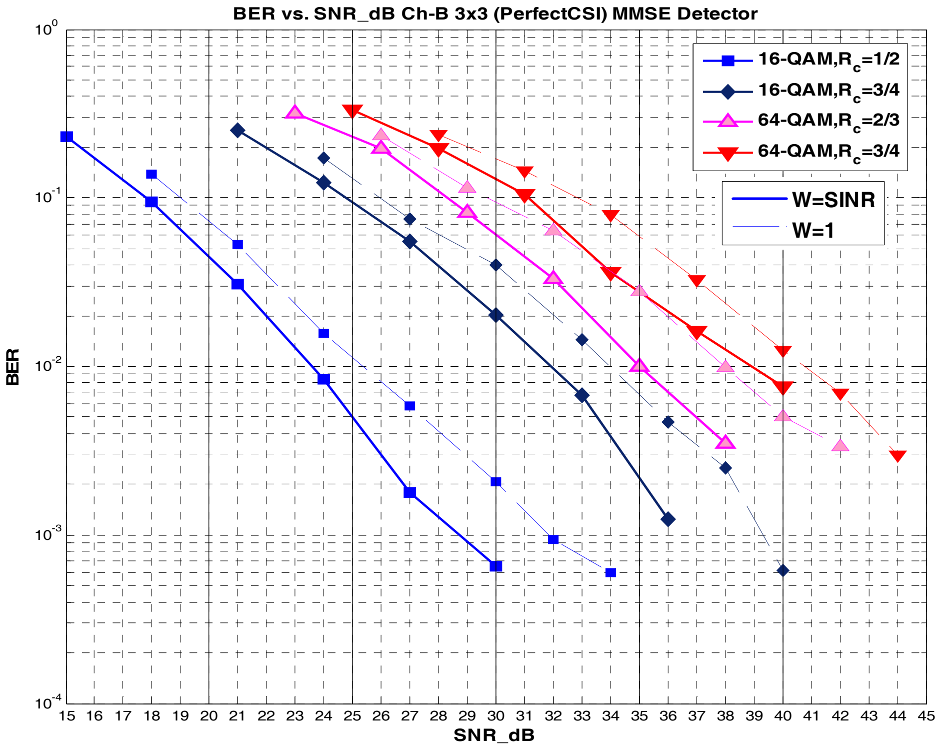

Fig. 3-19: BER of bit metrics calculation with equal and weighted coefficients by MMSE detector for 16-QAM and 64-QAM in channel B, 3x3

Case5: Compare MMSE and ZF detector in channel B of IEEE802.11n, 2x2

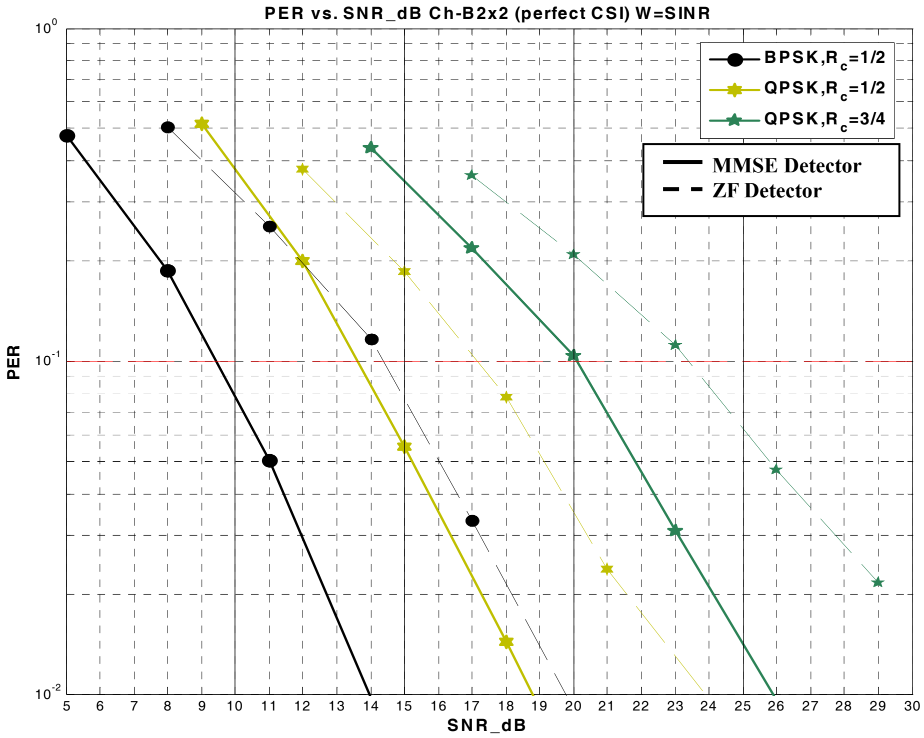

Fig. 3-20: PER of bit metrics calculation with weighted coefficients by MMSE detector and ZF detector for BPSK and QPSK in channel B, 2x2

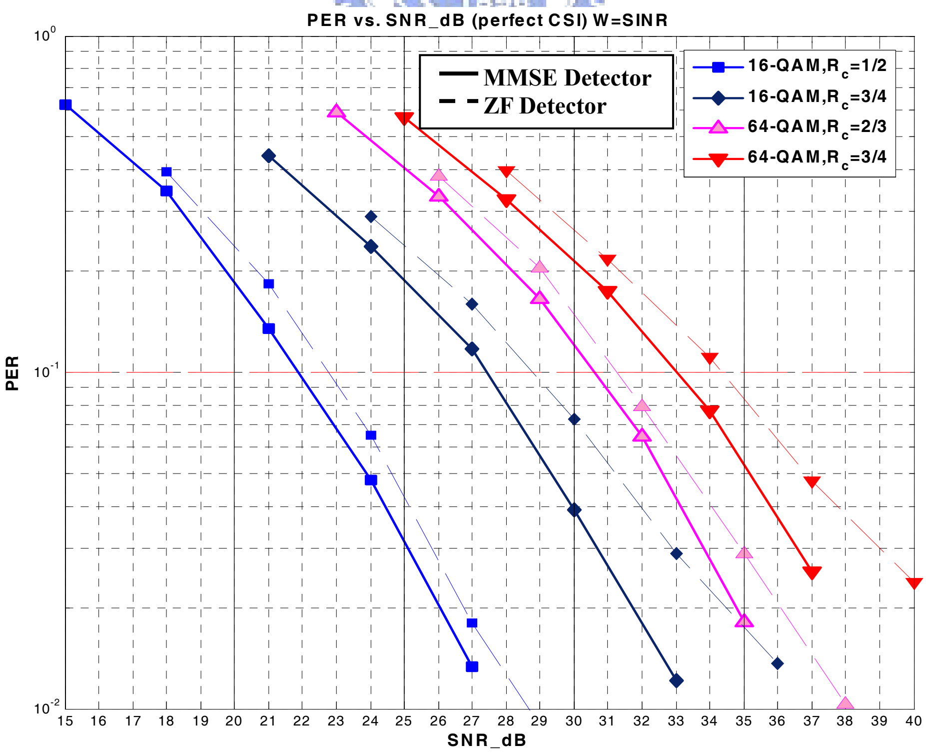

Fig. 3-21: PER of bit metrics calculation with weighted coefficients by MMSE detector and ZF detector for 16-QAM and 64-QAM in channel B, 2x2

3.4 Conclusions

In this chapter, we derived the approximation of bit metric for MMSE detector and ZF detector, respectively. We analyze the performance of bit metric calculation with equal and weighted coefficients for the MMSE detector and the ZF detector There are about 3~4dB improvement by using weighted coefficients compared to equal coefficients. But in the lower modulation scheme, the Gaussian approximation of the interference would be loose. Hence, the improvement for BPSK and QPSK is only about 1dB in the MMSE detector. By the way, the ZF detector has noise enhancement so the performance of MMSE detector is better than those of ZF detector about 1~4dB, especially at lower SNR. At high SNR, the performance of the ZF detector is close to those of the MMSE detector.

Chapter 4:

Low-Complexity Iterative Detection

Under the condition that the transmitter architecture is of no change and the receiver only uses available received signals, this chapter utilizes an iterative method to improve the performance of MIMO BICM systems. The receiver joints signal detection and soft decoding with turbo principles to suppress the strong co-antenna interference in MIMO systems. The receiver returns soft information of the MAP decoder back to the multistage detector to enhance the ability of detecting signals. The subchannel, i.e. subcarrier, of MIMO-OFDM system has constant channel gain on the multipath Rayleigh fading channel. The MIMO-OFDM receiver detects signals per subcarrier. It is similar to the receiver of MIMO Single-Carrier system on the flat fading channel. Here, our proposed algorithm can be used for general MIMO systems. It is more convenient to me to depict our proposed algorithm for MIMO BICM systems. The block diagram of MIMO transmitter structure is shown in Fig. 4-1.

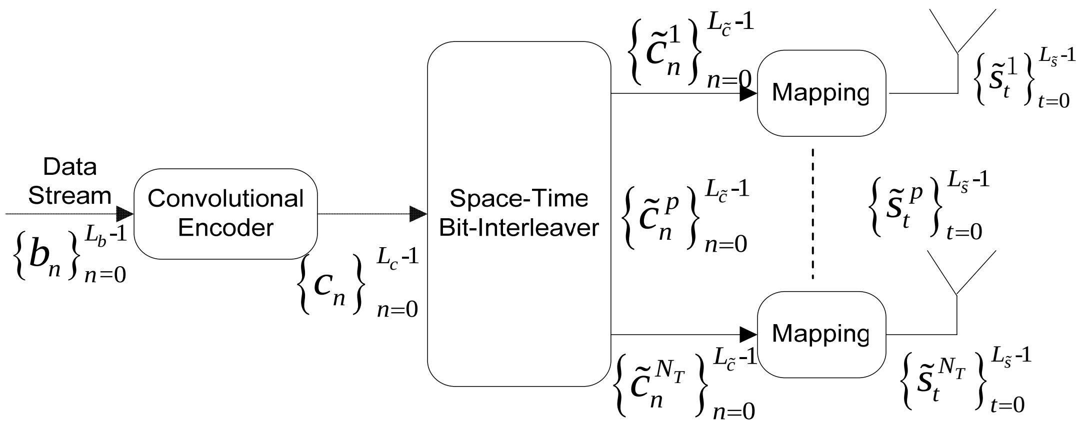

Fig. 4-1: A MIMO transmitter

where

- $p \in \{1, \cdots, N_T\}$ transmitter antenna index
- n : bit sequence index
- t : symbol sequence (time) index
- N_T: the number of transmitter antennas
- L_b : the number of information bits b_n
- $L_c = L_b / \mathrm{R_c}$: the number of coded bits c_n, where $\mathrm{R_c} = \frac{k_0}{n_0}$ is code rate
- $L_{\tilde{c}} = \left\lceil \frac{L_c}{N_T} \right\rceil$: the number of interleaved bits $\tilde{c}_n^p$ per tx antenna
- $L_{\tilde{s}} = \left\lceil \frac{L_{\tilde{c}}}{log_2 M} \right\rceil$: the number of symbols $\tilde{s}_t^p$ per tx antenna for M-QAM

The MIMO channel is shown in Fig. 4-2.

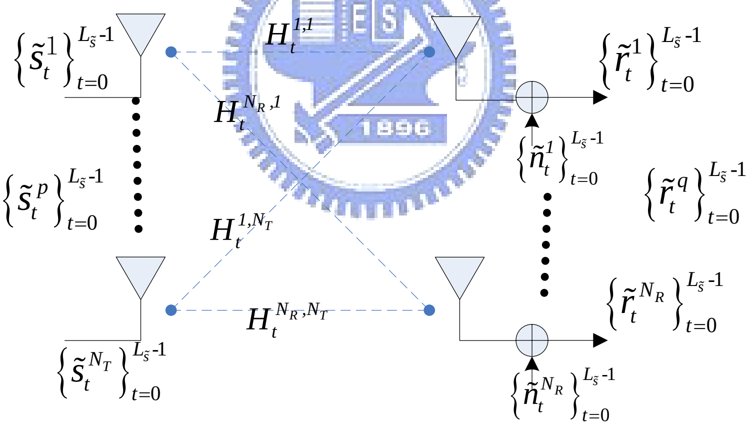

Fig. 4-2: The MIMO channel

The received signal is

$$\tilde{r}_t^q = \sum_{p=0}^{N_T-1} H_t^{q,p} \cdot \tilde{s}_t^p + \tilde{n}_t^p \quad \Rightarrow \quad \tilde{\mathbf{r}}_t = \mathbf{H}_t \tilde{\mathbf{s}}_t + \tilde{\mathbf{n}}_t \tag{3.45}$$

where

- assume $\mathbf{H}_t = \begin{bmatrix} H_t^{1,1} & \cdots & H_t^{1,N_T} \\ \vdots & \vdots & \vdots \\ H_t^{N_R,1} & \cdots & H_t^{N_R,N_T} \end{bmatrix} \in \mathbb{C}^{N_R \times N_T}$ is a flat Rayleigh fading channel

The block diagram of MIMO iterative receiver architecture is shown in Fig. 4-3.

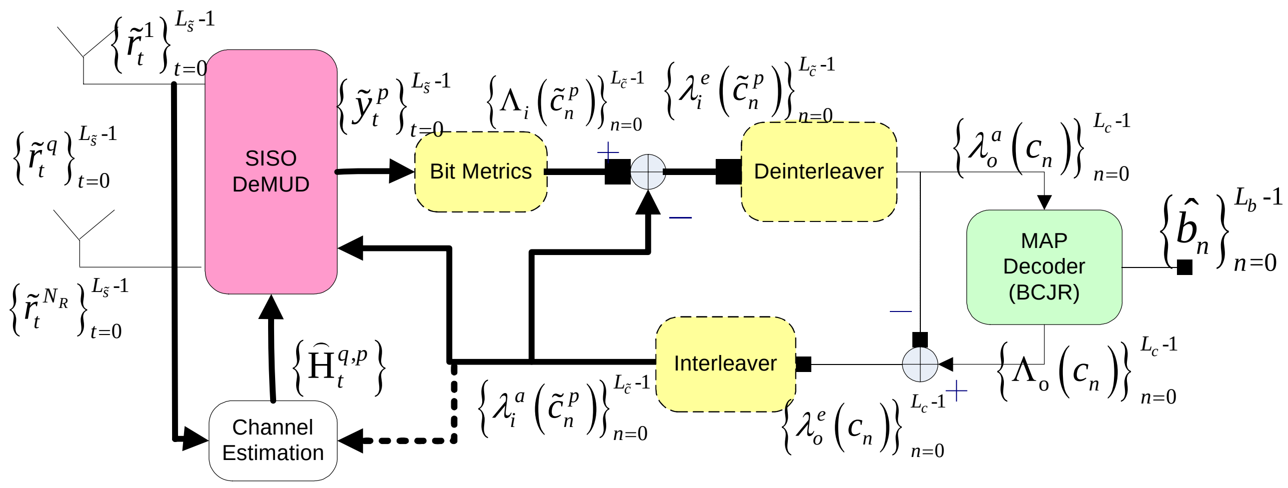

Fig. 4-3: A MIMO iterative receiver

where

- $\Lambda_i\left(\tilde{c}_n^p\right), \Lambda_o\left(c_n\right)$: a posteriori log likelihood ratio
- $\lambda_i^a\left(\tilde{c}_n^p\right), \lambda_i^e\left(\tilde{c}_n^p\right), \lambda_o^a\left(c_n\right), \lambda_o^e\left(c_n\right)$: log likelihood ratio
- $\lambda_i^a\left(\tilde{c}_n^p\right)=\pi\left(\lambda_o^e\left(c_n\right)\right)$ and $\lambda_o^a\left(c_n\right)=\pi\left(\lambda_i^e\left(\tilde{c}_n^p\right)\right)$

The index i and o denote the log likelihood ratio (LLR) associated with the inner detector and outer decoder, respectively. And the superscripts a and e denote a priori (intrinsic) information and extrinsic information, respectively. $\pi(\bullet)$ is an interleaver function.

This chapter is organized as follows: In the section 4.1, to describe the optimal detector based on MAP algorithm and MAP (BCJR) decoder. In the section 4.2, to provide the suboptimal low-complexity linear detector based on MMSE algorithm, and we propose four approximations to reduce the computation complexity of iterative MMSE receiver. Finally, in the section 4.3, the performances of various iterative MMSE receiver schemes proposed in this chapter are examined.

Equation Section 4

4.1 Optimal Receiver Based on MAP Algorithm

Assume MIMO channel is an flat quasi-static Rayleigh fading channel matrix **H**.

The received signal $\tilde{r}_t^q$ at the q^{th} receiver antenna at time t is

$$\tilde{r}_t^q = \sum_{p=0}^{N_T-1} H_t^{q,p} \cdot \tilde{s}_t^p + \tilde{n}_t^p \tag{4.1}$$

Then the received signal vector $\mathbf{r}_t$ is defined as

$$\tilde{\mathbf{r}}_t = \mathbf{H}_t \tilde{\mathbf{s}}_t + \tilde{\mathbf{n}}_t \quad \in \mathbb{C}^{N_T \times 1} \tag{4.2}$$

where $\tilde{\mathbf{r}}_t = \begin{bmatrix} \tilde{r}_t^1 \\ \vdots \\ \tilde{r}_t^{N_R} \end{bmatrix}$, $\tilde{\mathbf{s}}_t = \begin{bmatrix} \tilde{s}_t^1 \\ \vdots \\ \tilde{s}_t^{N_T} \end{bmatrix}$, $\tilde{\mathbf{n}}_t = \begin{bmatrix} \tilde{n}_t^1 \\ \vdots \\ \tilde{n}_t^{N_T} \end{bmatrix}$ and $\mathbf{H}_t = \begin{bmatrix} H_t^{1,1} & \cdots & H_t^{1,N_T} \\ \vdots & \vdots & \vdots \\ H_t^{N_R,1} & \cdots & H_t^{N_R,N_T} \end{bmatrix} \in \mathbb{C}^{N_R \times N_T}$

How to design an optimal receiver for MIMO system is to maximize a posteriori probability of information bit b_n with all received signal vectors.

$$\hat{b}_n = \arg \max_{b_n \in (0,1)} \left\{ p\left[b_n \middle| \left\{ \tilde{\mathbf{r}}_t \right\}_{t=0}^{L_{\tilde{s}}-1} \right] \right\} \tag{4.3}$$

Define a posteriori log likelihood ratio of b_n as

$$\text{a posterior LLR: } \Lambda_{\text{optimal}}\left(b_n\right) \triangleq ln\left(\frac{p\left[b_n = 1 \middle| \left\{ \tilde{\mathbf{r}}_t \right\}_{t=0}^{L_{\tilde{s}}-1} \right]}{p\left[b_n = 0 \middle| \left\{ \tilde{\mathbf{r}}_t \right\}_{t=0}^{L_{\tilde{s}}-1} \right]} \right) \tag{4.4}$$

Detect information bit b_n ,

$$\begin{cases} b_n = 1 \text{ , if } \Lambda_{\text{optimal}}\left(b_n\right) \geq 0 \\ b_n = 0 \text{ , if } \Lambda_{\text{optimal}}\left(b_n\right) < 0 \end{cases} \tag{4.5}$$

By the total probability theorem, the a posteriori probability of b_n can be shown as

$$p\left[b_n \middle| \left\{ \tilde{\mathbf{r}}_t \right\}_{t=0}^{L_{\tilde{s}}-1} \right] = \sum_{\left\{ \hat{\mathbf{s}}_t \right\}_{t=0}^{L_{\tilde{s}}-1}} p\left[b_n \middle| \left\{ \tilde{\mathbf{r}}_t \right\}_{t=0}^{L_{\tilde{s}}-1}, \left\{ \hat{\mathbf{s}}_t \right\}_{t=0}^{L_{\tilde{s}}-1} \right] \cdot p\left[\left\{ \hat{\mathbf{s}}_t \right\}_{t=0}^{L_{\tilde{s}}-1} \middle| \left\{ \tilde{\mathbf{r}}_t \right\}_{t=0}^{L_{\tilde{s}}-1} \right] \tag{4.6}$$

Due to information bit b_n depending on detected signal vector sequences $\{\hat{\mathbf{s}}_t\}_{t=0}^{L_{\hat{s}}-1}$, then

$$p\left[b_n \left| \{\tilde{\mathbf{r}}_t\}_{t=0}^{L_{\hat{s}}-1}, \{\hat{\mathbf{s}}_t\}_{t=0}^{L_{\hat{s}}-1} \right.\right] = p\left[b_n \left| \{\hat{\mathbf{s}}_t\}_{t=0}^{L_{\hat{s}}-1} \right.\right] \tag{4.7}$$

The channel is a flat fading and discrete memoryless channel so the detected signal vector $\hat{\mathbf{s}}_t$ at time t only depends on the received signal vector $\tilde{\mathbf{r}}_t$ at time t. Then,

$$p\left[\{\hat{\mathbf{s}}_t\}_{t=0}^{L_{\hat{s}}-1} \left| \{\tilde{\mathbf{r}}_t\}_{t=0}^{L_{\hat{s}}-1} \right.\right] = \prod_{t=0}^{L_{\hat{s}}-1} p\left[\hat{\mathbf{s}}_t \middle| \tilde{\mathbf{r}}_t\right] \tag{4.8}$$

Finally, the optimal receiver is able to calculate a posteriori LLR of information bit b_n.

$$\Lambda(b_n) = ln\left(\frac{p\left[b_n = 1 \left| \{\tilde{\mathbf{r}}_t\}_{t=0}^{L_{\hat{s}}-1} \right.\right]}{p\left[b_n = 0 \left| \{\tilde{\mathbf{r}}_t\}_{t=0}^{L_{\hat{s}}-1} \right.\right]} \right) = ln\left(\frac{\sum_{\{\hat{\mathbf{s}}_t\}_{t=0}^{L_{\hat{s}}-1}} \left(p\left[b_n = 1 \left| \{\hat{\mathbf{s}}_t\}_{t=0}^{L_{\hat{s}}-1} \right.\right] \cdot \prod_{t=0}^{L_{\hat{s}}-1} p\left[\hat{\mathbf{s}}_t \middle| \tilde{\mathbf{r}}_t\right] \right)}{\sum_{\{\hat{\mathbf{s}}_t\}_{t=0}^{L_{\hat{s}}-1}} \left(p\left[b_n = 0 \left| \{\hat{\mathbf{s}}_t\}_{t=0}^{L_{\hat{s}}-1} \right.\right] \cdot \prod_{t=0}^{L_{\hat{s}}-1} p\left[\hat{\mathbf{s}}_t \middle| \tilde{\mathbf{r}}_t\right] \right)} \right) \tag{4.9}$$

But the computation complexity of the optimal receiver is too high. It is impossible to realize an optimal receiver. In order to reduce the computation complexity, we divide the receiver into two parts: inner detector and outer decoder, as Fig. 4-4 .

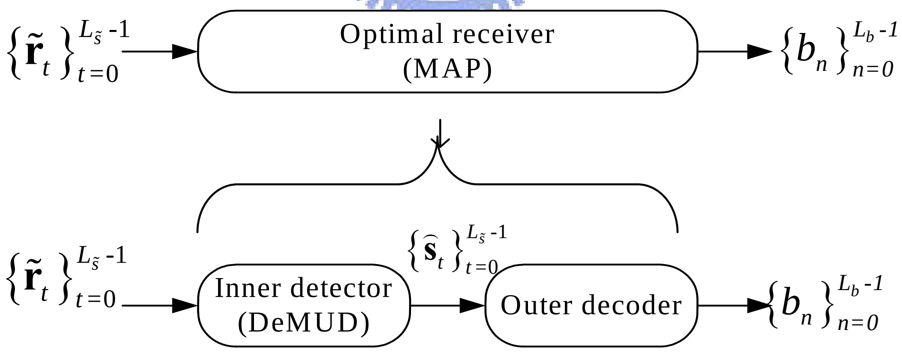

Fig. 4-4: A inner detector and a outer decoder

4.1.1 MAP Detector

The optimal detector for iterative receiver is an a posteriori probability (APP) detector.

$$\hat{\mathbf{s}}_t = \arg\max_{\tilde{\mathbf{s}}_t \in \Psi} \left\{ p\left[\tilde{\mathbf{s}}_t \middle| \tilde{\mathbf{r}}_t \right] \right\} \tag{4.10}$$

By the Bayes rule,

$$p\left[\tilde{\mathbf{s}}_t \middle| \tilde{\mathbf{r}}_t \right] = \frac{p\left[\tilde{\mathbf{r}}_t \middle| \tilde{\mathbf{s}}_t \right] \cdot p\left[\tilde{\mathbf{s}}_t \right]}{p\left[\tilde{\mathbf{r}}_t \right]} \propto p\left[\tilde{\mathbf{r}}_t \middle| \tilde{\mathbf{s}}_t \right] \cdot p\left[\tilde{\mathbf{s}}_t \right] \tag{4.11}$$

At the first iteration, there is no soft information about transmitted signal vector $\tilde{\mathbf{s}}_t$. It means that $p\left[\tilde{\mathbf{s}}_t \right]$ are equal. Then, the MAP detector is a maximum-likelihood (ML) detector.

$$\hat{\mathbf{s}}_t = \arg\max_{\mathbf{s}_t \in \Psi} \left\{ p\left[\mathbf{s}_t \middle| \mathbf{r}_t \right] \right\} = \arg\max_{\mathbf{s}_t \in \Psi} \left\{ p\left[\mathbf{r}_t \middle| \mathbf{s}_t \right] \right\} \tag{4.12}$$

The computation complexity of MAP detector (ML detector) is order of M^{N_T}. MAP detector is not feasible for larger number of transmit antennas or higher modulation schemes. The suboptimal detector is a linear detector based on MMSE criterion.

4.1.2 MAP (BCJR) Decoder

In this section, we describe how to use a MAP decoder as an optimal decoder and how to calculate the soft information pass to inner detector. Because the transmitter uses a bit interleaver after a convolutional encoder to overcome Rayleigh fading channel, the receiver needs to calculate the bit metrics before a bit de-interleaver for soft Viterbi decoding or MAP decoding. The de-interleaved codeword is denoted by $\mathbf{c}_n$. It is an encoder output tuple by encoding information bit b_n. Assume the code rate of a convolutional encoder is $R_c = 1/2$.

$$\mathbf{c}_n = \left(c_{n,0}, c_{n,1} \right) \tag{4.13}$$

$$b_n \rightarrow \boxed{\text{encoder}} \rightarrow \mathbf{c}_n$$

The a posteriori log likelihood ratio of $c_{n,j}$ for MAP decoder is denoted as

$$\Lambda_o\left(c_{n,j}\right) \triangleq ln\left(\frac{p\left[c_{n,j}=1\left|\left\{\lambda_o^a\left(\mathbf{c}_i\right)\right\}_{i=0}^{L_b-1}\right.;\text{ decoding}\right]}{p\left[c_{n,j}=0\left|\left\{\lambda_o^a\left(\mathbf{c}_i\right)\right\}_{i=0}^{L_b-1}\right.;\text{ decoding}\right]}\right) \tag{4.14}$$

where

- $\lambda_o^a\left(\mathbf{c}_n\right)=\left\{\lambda_o^a\left(c_{n,0}\right),\lambda_o^a\left(c_{n,1}\right)\right\}$
- $\lambda_o^a\left(c_{n,j}\right)$: a priori log likelihood ratio (soft information)

The a posteriori probability can be written as

$$p\left[c_{n,j}=k\left|\left\{\lambda_o^a\left(\mathbf{c}_i\right)\right\}_{i=0}^{L_b-1}\right.;\text{ decoding}\right]=\frac{\sum_{\mathrm{S}_j^{(k)}} p\left[S_{n-1}=\mathrm{S'},\,S_n=\mathrm{S},\ \left\{\lambda_o^a\left(\mathbf{c}_i\right)\right\}_{i=0}^{L_b-1}\right]}{p\left[\left\{\lambda_o^a\left(\mathbf{c}_i\right)\right\}_{i=0}^{L_b-1}\right]} \tag{4.15}$$

where

- S_n:the state of information bit at time n
- $\mathrm{S}_j^{(k)}$: the set of state transition from S' to S and the j^{th} bit of output tuple $\mathbf{c}_n$ is $k\in(0,1)$

Define the forward metrics denoted by $\alpha_n\left(\mathrm{S}\right)$ is

$$\alpha_n\left(\mathrm{S}\right)\triangleq p\left[S_n=\mathrm{S},\ \left\{\lambda_o^a\left(\mathbf{c}_i\right)\right\}_{i=0}^{i=n}\right] \tag{4.16}$$

Define the backward metrics denoted by $\alpha_n\left(\mathrm{S}\right)$ is

$$\beta_n\left(\mathrm{S}\right)\triangleq p\left[S_n=\mathrm{S},\ \left\{\lambda_o^a\left(\mathbf{c}_i\right)\right\}_{i=n+1}^{L_b-1}\right] \tag{4.17}$$

And define the branch metrics $\gamma_n\left(\mathrm{S',S}\right)$ from the state S' to the state S is

$$\gamma_n\left(\mathrm{S',S}\right)\triangleq p\left[S_n=\mathrm{S},\ \lambda_o^a\left(\mathbf{c}_n\right)\right|\ \mathrm{S}_{n-1}=\mathrm{S'}\right] \tag{4.18}$$

By [19], the authors tell us,

$$\alpha_n(\mathrm{S}) = \sum_{\mathbf{S}'} \alpha_{n\text{-}1}(\mathrm{S}')\gamma_n(\mathrm{S}',\mathrm{S}) \tag{4.19}$$

and

$$\beta_{n\text{-}1}(\mathrm{S}) = \sum_{\mathbf{S}'} \beta_n(\mathrm{S}')\gamma_n(\mathrm{S}',\mathrm{S}) \tag{4.20}$$

Calculate the branch metrics $\gamma_n(\mathrm{S}',\mathrm{S})$ by a priori information $\lambda_o^a(c_{n,0})$ and $\lambda_o^a(c_{n,1})$,

$$\begin{aligned}\gamma_n(\mathrm{S}',\mathrm{S}) &= p\left[\lambda_o^a(\mathbf{c}_n)\middle|S_n=\mathrm{S},\, S_{n\text{-}1}=\mathrm{S}'\right]p\left[S_n=\mathrm{S}\middle|S_{n\text{-}1}=\mathrm{S}'\right]\\ &= p\left[\mathrm{S}\middle|\mathrm{S}'\right]\prod_{j=0}^{j=1} p\left[c_{n,j}(\mathrm{S}',\mathrm{S})\right]\end{aligned} \tag{4.21}$$

where

- $p\left[c_{n,j}=1\right]=\exp\left(\lambda_o^a(c_{n,j})\right)\Big/\left\{1+\exp\left(\lambda_o^a(c_{n,j})\right)\right\}$
- $p\left[c_{n,j}=0\right]=\exp\left(-\lambda_o^a(c_{n,j})\right)\Big/\left\{1+\exp\left(\lambda_o^a(c_{n,j})\right)\right\}$

By the equations(4.14) and(4.15), the a posteriori LLR is

$$\Lambda_o(c_{n,j}) \triangleq ln\left(\frac{\sum_{\mathrm{S}_j^{(1)}} p\left[S_{n\text{-}1}=\mathrm{S}',\, S_n=\mathrm{S},\, \left\{\lambda_o^a(\mathbf{c}_i)\right\}_{i=0}^{L_b\text{-}1}\right]}{\sum_{\mathrm{S}_j^{(0)}} p\left[S_{n\text{-}1}=\mathrm{S}',\, S_n=\mathrm{S},\, \left\{\lambda_o^a(\mathbf{c}_i)\right\}_{i=0}^{L_b\text{-}1}\right]}\right) \tag{4.22}$$

Because,

$$\begin{aligned}&p\left[S_{n\text{-}1}=\mathrm{S}',\, S_n=\mathrm{S},\left\{\lambda_o^a(\mathbf{c}_i)\right\}_{i=0}^{L_b\text{-}1}\right]\\ &= p\left[S_{n\text{-}1}=\mathrm{S},\left\{\lambda_o^a(\mathbf{c}_i)\right\}_{i=0}^{i=n\text{-}1}\right]p\left[S_n=\mathrm{S},\, \lambda_o^a(\mathbf{c}_n)\middle|\, \mathrm{S}_{n\text{-}1}=\mathrm{S}'\right]p\left[S_n=\mathrm{S},\left\{\lambda_o^a(\mathbf{c}_i)\right\}_{i=n+1}^{L_b\text{-}1}\right]\\ &= \alpha_{n\text{-}1}(\mathrm{S}')\beta_n(\mathrm{S})\cdot\gamma_n(\mathrm{S}',\mathrm{S})\end{aligned} \tag{4.23}$$

then

$$\Lambda_o(c_{n,j}) = ln\left(\frac{\sum_{\mathrm{S}_j^{(1)}} \alpha_{n\text{-}1}(\mathrm{S}')\beta_n(\mathrm{S})\cdot\gamma_n(\mathrm{S}',\mathrm{S})}{\sum_{\mathrm{S}_j^{(0)}} \alpha_{n\text{-}1}(\mathrm{S}')\beta_n(\mathrm{S})\cdot\gamma_n(\mathrm{S}',\mathrm{S})}\right) \tag{4.24}$$

And

$$ln\left(\frac{\sum_{S_j^{(1)}} \alpha_{n\text{-}1}(S')\beta_n(S)\cdot\gamma_n(S',S)}{\sum_{S_j^{(0)}} \alpha_{n\text{-}1}(S')\beta_n(S)\cdot\gamma_n(S',S)}\right)$$

$$= ln\left(\frac{\sum_{S_j^{(1)}} \alpha_{n\text{-}1}(S')\beta_n(S)\cdot p\left[S|S'\right]\prod_{i=0}^{1} p\left[c_n^i(S',S)\right]}{\sum_{S_j^{(0)}} \alpha_{n\text{-}1}(S')\beta_n(S)\cdot p\left[S|S'\right]\prod_{i=0}^{1} p\left[c_n^i(S',S)\right]}\right)$$

$$= ln\left(\frac{\sum_{S_j^{(1)}} \alpha_{n\text{-}1}(S')\beta_n(S)\cdot p\left[S|S'\right]\prod_{i\neq j} p\left[c_n^i(S',S)\right]}{\sum_{S_j^{(0)}} \alpha_{n\text{-}1}(S')\beta_n(S)\cdot p\left[S|S'\right]\prod_{i\neq j} p\left[c_n^i(S',S)\right]}\right)+ln\left(\frac{p\left[c_n^j(S',S)=1\right]}{p\left[c_n^j(S',S)=0\right]}\right)$$

Finally, the a posteriori LLR can be shown as

$$\Lambda_o\left(c_{n,j}\right)=\lambda_o^e\left(c_{n,j}\right)+\lambda_o^a\left(c_{n,j}\right) \tag{4.25}$$

where

$$\lambda_o^e\left(c_{n,j}\right)= ln\left(\frac{\sum_{S_j^{(1)}} \alpha_{n\text{-}1}(S')\beta_n(S)\, p\left[S|S'\right]\prod_{i\neq j} p\left[c_n^i(S',S)\right]}{\sum_{S_j^{(0)}} \alpha_{n\text{-}1}(S')\beta_n(S) p\left[S|S'\right]\prod_{i\neq j} p\left[c_n^i(S',S)\right]}\right) \text{ extrinsic information} \tag{4.26}$$

and

$$\lambda_o^a\left(c_{n,j}\right)=ln\left(\frac{p\left[c_n^j(S',S)=1\right]}{p\left[c_n^j(S',S)=0\right]}\right) \text{ a priori (intrinsic) information} \tag{4.27}$$

To estimate information bit $\hat{b}_n$,

$$\begin{cases}\hat{b}_n=1 & \text{if } \Lambda\left(b_n\right)\geq 0\\ \hat{b}_n=0 & \text{if } \Lambda\left(b_n\right)<0\end{cases} \tag{4.28}$$

A posteriori LLR $\Lambda\left(b_n\right)$ of information bit b_n is

$$\Lambda\left(b_n\right)=ln\left(\frac{\sum_{B^{(1)}} \alpha_{n\text{-}1}(S')\beta_n(S)\cdot p\left[S|S'\right]\prod_{i=0}^{1} p\left[c_n^i(S',S)\right]}{\sum_{B^{(0)}} \alpha_{n\text{-}1}(S')\beta_n(S)\cdot p\left[S|S'\right]\prod_{i=0}^{1} p\left[c_n^i(S',S)\right]}\right) \tag{4.29}$$

where

- $B^{(1)}$: the set of state transition from S' to S and information bit $b_n=1$
- $B^{(0)}$: the set of state transition from S' to S and information bit $b_n=0$

If want to reduce the computation complexity of a decoder, you can use a suboptimal decoder, SOVA decoder.

4.2 Iterative MMSE Detector

The optimal detector of the iterative receiver, MAP detector, causes a large computational complexity. A suboptimal and low complex detector is using adaptive linear filter techniques. A linear minimum mean squared error (MMSE) detector is a simplified approach compared with an MAP detector. An MMSE detector has higher performance than other linear detector.

The received signal vector $\mathbf{r}_t$ as (4.2), can be decomposed three part: desired signal, co-antenna interferences and noise, see (4.30).

$$\tilde{\mathbf{r}}_t = \mathbf{H}_t \tilde{\mathbf{s}}_t + \tilde{\mathbf{n}}_t = \underbrace{\mathbf{h}_t^p \tilde{s}_t^p}_{\text{desired signal}} + \underbrace{\mathbf{H}_t^p \tilde{\mathbf{s}}_t^p}_{\text{interference}} + \underbrace{\tilde{\mathbf{n}}_t}_{\text{noise}} \tag{4.30}$$

where $\mathbf{h}_t^p = \begin{bmatrix} H_t^{1,p} \\ \vdots \\ H_t^{N_R,p} \end{bmatrix}$, $\mathbf{H}_t^p = \left[\mathbf{h}_t^1, \cdots, \mathbf{h}_t^{p\text{-}1}, \mathbf{h}_t^{p+1}, \cdots, \mathbf{h}_t^{N_T}\right]$ and $\tilde{\mathbf{s}}_t^p = \left[\tilde{s}_t^1, \cdots, \tilde{s}_t^{p\text{-}1}, \tilde{s}_t^{p+1}, \cdots, \tilde{s}_t^{N_T}\right]$

First step, to estimate the co-antenna interference $\boldsymbol{\mu}_t^p$ based on soft information $\lambda_i^a\left(\tilde{c}_n^j\right)$, see(4.31). Assume the channel estimation is perfect.

$$\boldsymbol{\mu}_t^p = \mathbf{H}_t^p \overline{\mathbf{s}}_t^{p(\mathrm{i})} \tag{4.31}$$

where $\overline{\mathbf{s}}_t^{p(\mathrm{i})} = [\overline{s}_t^{1(\mathrm{i})}, \cdots, \overline{s}_t^{p\text{-}1(\mathrm{i})}, \overline{s}_t^{p+1(\mathrm{i})}, \cdots, \overline{s}_t^{N_T(\mathrm{i})}]^{\mathrm{T}}$ and $\overline{s}_t^{j\,(\mathrm{i})} = \mathrm{E}\left\{\tilde{s}_t^j\right\}$ at i^{th} iteration.

The modulator maps the coded bits to complex symbol $\tilde{s}_t^j$.

$$\tilde{s}_t^j = \mathrm{map}\left(\tilde{c}_{t,0}^j, \cdots, \tilde{c}_{t,\log_2 M\text{-}1}^j\right) \tag{4.32}$$

Calculate $\bar{s}_t^{j(\mathrm{i})}=\mathrm{E}\left\{\tilde{s}_t^{j}\right\}$ based on a priori information $\left\{\lambda_i^{a}\left(\tilde{c}_{t,m}^{j}\right)\right\}_{\mathrm{m=0}}^{\log_2 M\text{-}1}$ from a MAP decoder.

Then, to remove the co-antenna interference

$$\tilde{\mathbf{x}}_t^{p}=\tilde{\mathbf{r}}_t-\boldsymbol{\mu}_t^{p}=\mathbf{h}_t^{p}\tilde{s}_t^{p}+\mathbf{H}_t^{p}\left(\mathbf{s}_t^{p}-\bar{\mathbf{s}}_t^{p(\mathrm{i})}\right)+\tilde{\mathbf{n}}_t \tag{4.33}$$

Output signal of adaptive linear detector $\tilde{y}_t^{p}$ is

$$\tilde{y}_t^{p}=\left(\hat{\mathbf{g}}_t^{p}\right)^{\mathrm{H}}\tilde{\mathbf{x}}_t^{p} \tag{4.34}$$

To calculate the coefficients of adaptive linear detector based on MMSE Criterion,

$$\left(\hat{\mathbf{g}}_t^{p}\right)^{\mathrm{H}}=\arg\underbrace{\min}_{\left(\hat{\mathbf{g}}_t^{p}\right)^{\mathrm{H}}}\left\{\mathrm{E}\left\{\left|\tilde{y}_t^{p}-\tilde{s}_t^{p}\right|^{2}\right\}\right\}=\arg\underbrace{\min}_{\left(\hat{\mathbf{g}}_t^{p}\right)^{\mathrm{H}}}\left\{\mathrm{E}\left\{\left|\left(\hat{\mathbf{g}}_t^{p}\right)^{\mathrm{H}}\tilde{\mathbf{x}}_t^{p}-\tilde{s}_t^{p}\right|^{2}\right\}\right\} \tag{4.35}$$

See.Appendix B.

$$\left(\hat{\mathbf{g}}_t^{p}\right)^{\mathrm{H}}=\mathrm{E}\left\{\tilde{s}_t^{p}\left(\tilde{\mathbf{r}}_t-\mathbf{H}_t^{p}\bar{\mathbf{s}}_t^{p(\mathrm{i})}\right)^{\mathrm{H}}\right\}\cdot\left[\mathrm{E}\left\{\left(\tilde{\mathbf{r}}_t-\mathbf{H}_t^{p}\bar{\mathbf{s}}_t^{p(\mathrm{i})}\right)\left(\tilde{\mathbf{r}}_t-\mathbf{H}_t^{p}\bar{\mathbf{s}}_t^{p(\mathrm{i})}\right)^{\mathrm{H}}\right\}\right]^{-1} \tag{4.36}$$

where

$$\mathrm{E}\left\{\tilde{s}_t^{p}\left(\tilde{\mathbf{r}}_t-\mathbf{H}_t^{p}\bar{\mathbf{s}}_t^{p(\mathrm{i})}\right)^{\mathrm{H}}\right\}=\mathrm{E}\left\{\tilde{s}_t^{p}\left(\tilde{s}_t^{p}\right)^{*}\right\}\left(\mathbf{h}_t^{p}\right)^{\mathrm{H}} \tag{4.37}$$

and

$$\mathrm{E}\left\{\left(\tilde{\mathbf{r}}_t-\mathbf{H}_t^{p}\bar{\mathbf{s}}_t^{p(\mathrm{i})}\right)\left(\tilde{\mathbf{r}}_t-\mathbf{H}_t^{p}\bar{\mathbf{s}}_t^{p(\mathrm{i})}\right)^{\mathrm{H}}\right\}=\mathbf{h}_t^{p}\mathrm{E}\left\{\tilde{s}_t^{p}\left(\tilde{s}_t^{p}\right)^{*}\right\}\left(\mathbf{h}_t^{p}\right)^{\mathrm{H}}+\mathbf{H}_t^{p}\tilde{\mathbf{V}}_t^{p}\left(\mathbf{H}_t^{p}\right)^{\mathrm{H}}+\sigma_{\tilde{n}}^{2}\mathbf{I}_{N_R} \tag{4.38}$$

$$\text{where } \tilde{v}_t^{j}=\mathrm{E}\left\{\tilde{s}_t^{j}\left(\tilde{s}_t^{j}\right)^{*}\right\}-\mathrm{E}\left\{\tilde{s}_t^{j}\right\}\mathrm{E}\left\{\left(\tilde{s}_t^{j}\right)^{*}\right\}=\mathrm{E}\left\{\tilde{s}_t^{j}\left(\tilde{s}_t^{j}\right)^{*}\right\}-\bar{s}_t^{j(\mathrm{i})}\left(\bar{s}_t^{j(\mathrm{i})}\right)^{*}$$

$$\text{and } \tilde{\mathbf{V}}_t^{p}=\mathrm{diag}\left(\tilde{v}_t^{1},\cdots,\tilde{v}_t^{p\text{-}1},\tilde{v}_t^{p+1},\cdots,\tilde{v}_t^{N_T}\right)$$

The coefficients of adaptive linear detector $\left(\hat{\mathbf{g}}_t^{p}\right)^{\mathrm{H}}$ is

$$\left(\hat{\mathbf{g}}_t^{p}\right)^{\mathrm{H}}=\mathrm{E}\left\{\tilde{s}_t^{p}\left(\tilde{s}_t^{p}\right)^{*}\right\}\left(\mathbf{h}_t^{p}\right)^{\mathrm{H}}\left[\mathbf{h}_t^{p}\mathrm{E}\left\{\tilde{s}_t^{p}\left(\tilde{s}_t^{p}\right)^{*}\right\}\left(\mathbf{h}_t^{p}\right)^{\mathrm{H}}+\mathbf{H}_t^{p}\tilde{\mathbf{V}}_t^{p}\left(\mathbf{H}_t^{p}\right)^{\mathrm{H}}+\sigma_{\tilde{n}}^{2}\mathbf{I}_{N_R}\right]^{-1} \tag{4.39}$$

Before bit de-interleaving and MAP decoding, we need to calculate bit metrics with output signal of adaptive linear detector $\tilde{y}_t^{p}$.

We redefine coded and interleaved bit $\tilde{c}_n^p$ to be $\tilde{c}_{t,m}^p$, as Fig. 4-5,

$$\tilde{c}_{t,m}^p = \tilde{c}_n^p , \tag{4.40}$$

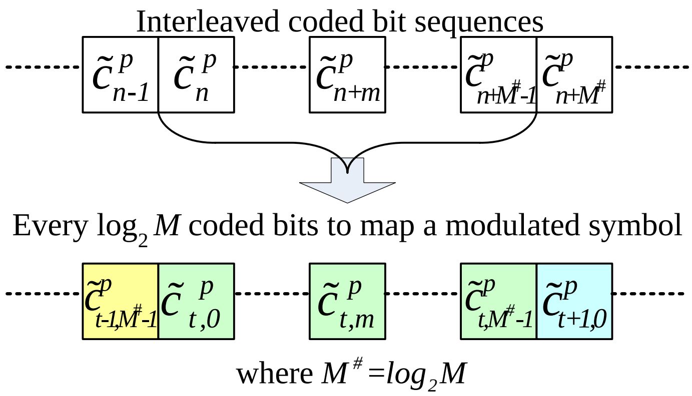

Fig. 4-5: To group $log_2 M$ interleaved-coded bits to map a modulated symbol for MIMO systems

where

- $n = t \cdot log_2 M + m$
- $m \in (0, \cdots, log_2 M - 1)$, the bit index of constellation
- $t \in (0, \cdots, L_{\tilde{s}} - 1)$, the symbol (time) index

$\tilde{c}_{t,m}^p$ is the coded bit in the m^{th} bit mapped onto a M-QAM symbol ψ at the t^{th} symbol, and at the p^{th} sub-stream. By the simplified computation of bit metrics of coded bit $\tilde{c}_{t,m}^p$, it is can be presented as

$$\Lambda_i(\tilde{c}_{t,m}^p) = ln\left(\frac{p\left[\tilde{c}_{t,m}^p = 1 \middle| \tilde{y}_t^p\right]}{p\left[\tilde{c}_{t,m}^p = 0 \middle| \tilde{y}_t^p\right]}\right) = ln\left(\frac{p\left[\tilde{y}_t^p \middle| \tilde{c}_{t,m}^p = 1\right]}{p\left[\tilde{y}_t^p \middle| \tilde{c}_{t,m}^p = 0\right]}\right) + ln\left(\frac{p\left[\tilde{c}_{t,m}^p = 1\right]}{p\left[\tilde{c}_{t,m}^p = 0\right]}\right) \tag{4.41}$$

And

$$ln\left(\frac{p\left[\tilde{c}_{t,m}^{p}=1\middle|y_t^p\right]}{p\left[\tilde{c}_{t,m}^{p}=0\middle|y_t^p\right]}\right) = ln\left(\frac{\sum_{\psi\in\Psi_m^{(1)}} p\left[\tilde{s}_t^p=\psi\middle|\tilde{y}_t^p\right]}{\sum_{\psi\in\Psi_m^{(0)}} p\left[\tilde{s}_t^p=\psi\middle|\tilde{y}_t^p\right]}\right)$$

$$= ln\left(\frac{\sum_{\psi\in\Psi_m^{(1)}} p\left[\tilde{y}_t^p\middle|\tilde{s}_t^p=\psi\right]p\left[\tilde{s}_t^p=\psi\right]}{\sum_{\psi\in\Psi_m^{(0)}} p\left[\tilde{y}_t^p\middle|\tilde{s}_t^p=\psi\right]p\left[\tilde{s}_t^p=\psi\right]}\right) \tag{4.42}$$

$$=ln\left(\frac{\sum_{\psi\in\Psi_m^{(1)}} p\left[\tilde{y}_t^p\middle|\tilde{s}_t^p=\psi\right]\prod_{j=0}^{log_2M-1} p\left[\tilde{c}_{t,j}^p\right]}{\sum_{\psi\in\Psi_m^{(0)}} p\left[\tilde{y}_t^p\middle|\tilde{s}_t^p=\psi\right]\prod_{j=0}^{log_2M-1} p\left[\tilde{c}_{t,j}^p\right]}\right)$$

$$= ln\left(\frac{\sum_{\psi\in\Psi_m^{(1)}} p\left[\tilde{y}_t^p\middle|\tilde{s}_t^p=\psi\right]\prod_{\substack{j=0\\ j\neq m}}^{log_2M-1} p\left[\tilde{c}_{t,j}^p\right]}{\sum_{\psi\in\Psi_m^{(0)}} p\left[\tilde{y}_t^p\middle|\tilde{s}_t^p=\psi\right]\prod_{j=0}^{log_2M-1} p\left[\tilde{c}_{t,j}^p\right]}\right)+ln\left(\frac{p\left[\tilde{c}_{t,m}^p=1\right]}{p\left[\tilde{c}_{t,m}^p=0\right]}\right)$$

where

- $p\left[\tilde{s}_t^p=\psi\right]=\prod_{m=0}^{(log_2M)-1} p\left[\tilde{c}_{t,m}^p\right]$, because $\tilde{c}_{t,0}^p,\cdots,\tilde{c}_{t,log_2M-1}^p$ are independent
- $\Psi_m^{(1)}$: the subset of all symbols with $\tilde{c}_{t,m}^p=1$
- $\Psi_m^{(0)}$: the subset of all symbols with $\tilde{c}_{t,m}^p=0$

Then, by (4.41) and (4.42), the bit metrics is

$$\Lambda_i\left(\tilde{c}_{t,m}^p\right)= ln\left(\frac{\sum_{\psi\in\Psi_m^{(1)}} p\left[\tilde{y}_t^p\middle|\tilde{s}_t^p=\psi\right]\prod_{\substack{j=0\\ j\neq m}}^{log_2M-1} p\left[\tilde{c}_{t,j}^p\right]}{\sum_{\psi\in\Psi_m^{(0)}} p\left[\tilde{y}_t^p\middle|\tilde{s}_t^p=\psi\right]\prod_{j=0}^{log_2M-1} p\left[\tilde{c}_{t,j}^p\right]}\right)+ln\left(\frac{p\left[\tilde{c}_{t,m}^p=1\right]}{p\left[\tilde{c}_{t,m}^p=0\right]}\right) \tag{4.43}$$

The extrinsic information is defined as

$$\lambda_i^e\left(\tilde{c}_{t,m}^p\right)\triangleq\ ln\left(\frac{\sum_{\psi\in\Psi_m^{(1)}} p\left[\tilde{y}_t^p\middle|\tilde{s}_t^p=\psi\right]\prod_{\substack{j=0\\ j\neq m}}^{log_2M-1} p\left[\tilde{c}_{t,j}^p\right]}{\sum_{\psi\in\Psi_m^{(0)}} p\left[\tilde{y}_t^p\middle|\tilde{s}_t^p=\psi\right]\prod_{j=0}^{log_2M-1} p\left[\tilde{c}_{t,j}^p\right]}\right) \tag{4.44}$$

And the a priori (intrinsic) information is defined as

$$\lambda_i^a\left(\tilde{c}_{t,m}^p\right) \triangleq ln\left(\frac{p\left[\tilde{c}_{t,m}^p=1\right]}{p\left[\tilde{c}_{t,m}^p=0\right]}\right) \tag{4.45}$$

By the turbo principle, the inner detector forwards the extrinsic information $\lambda_i^e\left(\tilde{c}_{t,m}^p\right)$ to the MAP decoder. We need to ensure that the equation (4.44) being **PURE** extrinsic information. It means that the conditional probability $p\left[\tilde{y}_t^p \middle| \tilde{s}_t^p=\psi\right]$ should not depend on its a priori information $\lambda_i^a\left(\tilde{c}_{t,m}^p\right)$. Therefore, we detect signal $\tilde{y}_t^p$ **WITHOUT** a priori information $\lambda_i^a\left(\tilde{c}_{t,m}^p\right)$. For this reason, computing $\left(\hat{\mathbf{g}}_{t,m}^p\right)^{\mathrm{H}}$ is shown in Fig. 4-6.

$$\left(\hat{\mathbf{g}}_{t,m}^p\right)^{\mathrm{H}}=\mathrm{E}\left\{\tilde{s}_t^p\left(\tilde{s}_t^p\right)^*\right\}\left(\mathbf{h}_t^p\right)^{\mathrm{H}}\left[\mathbf{h}_t^p\mathrm{E}\left\{\tilde{s}_t^p\left(\tilde{s}_t^p\right)^*\right\}\left(\mathbf{h}_t^p\right)^{\mathrm{H}}+\mathbf{H}_t^p\tilde{\mathbf{V}}_t^p\left(\mathbf{H}_t^p\right)^{\mathrm{H}}+\sigma_{\tilde{n}}^2\,\mathbf{I}_{N_R}\right]^{-1} \tag{4.46}$$

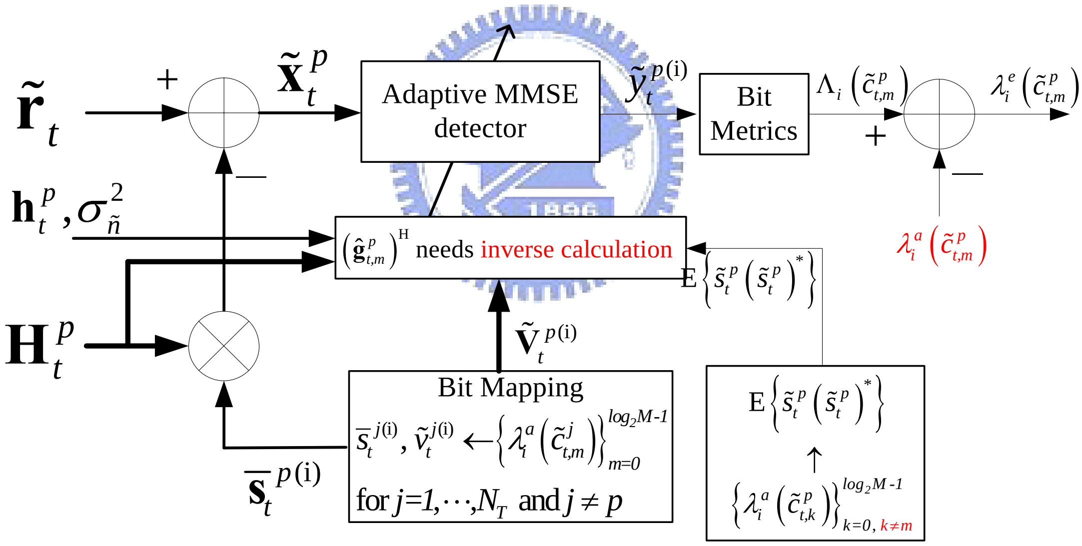

Fig. 4-6 : The block diagram of the proposed iterative MMSE receiver

The computation complexity of this iterative MMSE detector is proportional to $N_T \cdot L_{\tilde{s}} \cdot N_{iteration} \cdot log_2M$, where $N_{iterative}$ is the number of iterations.

4.2.1 Approximation I of the proposed iterative MMSE detector

The computation complexity of the proposed iterative MMSE detector is very high. It needs to compute $N_T \cdot L_{\tilde{s}} \cdot N_{iteration} \cdot log_2 M$ times the coefficients of iterative MMSE detector (pseudo inverse operations). In order to reduce the computation complexity, let $\mathrm{E}\left\{\tilde{s}_t^p\right\}=0$ and $\mathrm{E}\left\{\tilde{s}_t^p\left(\tilde{s}_t^p\right)^*\right\}=1$ when the receiver detects the p^{th} spatial stream signal at time t. Then, the coefficients of adaptive linear detector $\left(\hat{\mathbf{g}}_t^p\right)^{\mathrm{H}}$ is simplified to

$$\left(\hat{\mathbf{g}}_{\mathrm{apI}}^p\right)^{\mathrm{H}} = \left(\mathbf{h}_t^p\right)^{\mathrm{H}}\left[\mathbf{h}_t^p\left(\mathbf{h}_t^p\right)^{\mathrm{H}} + \mathbf{H}_t^p\tilde{\mathbf{V}}_t^p\left(\mathbf{H}_t^p\right)^{\mathrm{H}} + \sigma_{\tilde{n}}^2\,\mathbf{I}_{N_R}\right]^{-1} \qquad (4.47)$$

is shown in Fig. 4-7. The subscript of $\left(\hat{\mathbf{g}}_{\mathrm{apI}}^p\right)^{\mathrm{H}}$, "*apI* ", means approximation I of the proposed iterative MMSE detector.

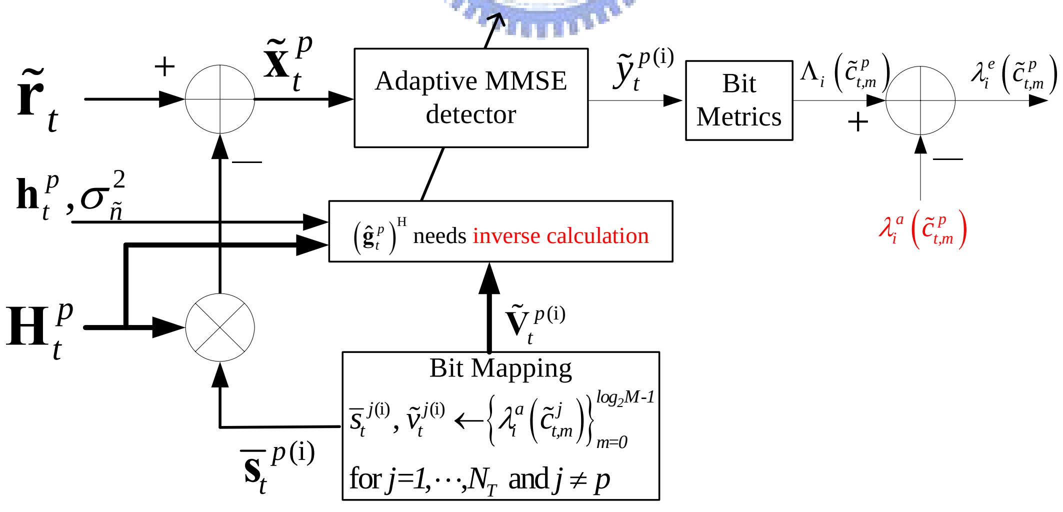

Fig. 4-7: The block diagram of the approximation I of the proposed iterative MMSE receiver

The computation of $\left(\hat{\mathbf{g}}_{\mathrm{apI}}^p\right)^{\mathrm{H}}$ is $N_T \cdot L_{\tilde{s}} \cdot N_{iterative}$ pseudo inverse operations. It does not need to calculate $\left(\widehat{\mathbf{g}}_{\mathrm{apI}}^{p}\right)^{\mathrm{H}}$ per modulated bit.

The output of inner detector $\tilde{y}_t^p$ can be shown as

$$\tilde{y}_t^p = \left(\widehat{\mathbf{g}}_{\mathrm{apI}}^{p}\right)^{\mathrm{H}} \mathbf{h}_t^p \tilde{s}_t^p + \left(\widehat{\mathbf{g}}_{\mathrm{apI}}^{p}\right)^{\mathrm{H}} \mathbf{H}_t^p \left(\mathbf{s}_t^p - \overline{\mathbf{s}}_t^{p(\mathrm{i})}\right) + \left(\widehat{\mathbf{g}}_{\mathrm{apI}}^{p}\right)^{\mathrm{H}} \tilde{\mathbf{n}}_t \tag{4.48}$$

Using Gaussian approximation to calculate the weight of bit metrics (chapter 3),

$$W_{\mathrm{apI}}^{p} \propto \frac{\mathrm{E}\left\{\left|\left(\widehat{\mathbf{g}}_{\mathrm{apI}}^{p}\right)^{\mathrm{H}} \mathbf{h}_t^p \tilde{s}_t^p\right|^2\right\}}{\mathrm{E}\left\{\left|\left(\widehat{\mathbf{g}}_{\mathrm{apI}}^{p}\right)^{\mathrm{H}} \mathbf{H}_t^p \left(\mathbf{s}_t^p - \overline{\mathbf{s}}_t^{p(\mathrm{i})}\right) + \left(\widehat{\mathbf{g}}_{\mathrm{apI}}^{p}\right)^{\mathrm{H}} \tilde{\mathbf{n}}_t\right|^2\right\}} \tag{4.49}$$

Where

$$\mathrm{E}\left\{\left|\left(\widehat{\mathbf{g}}_{\mathrm{apI}}^{p}\right)^{\mathrm{H}} \mathbf{h}_t^p \tilde{s}_t^p\right|^2\right\} = \left|\left(\widehat{\mathbf{g}}_{\mathrm{apI}}^{p}\right)^{\mathrm{H}} \mathbf{h}_t^p \left(\mathbf{h}_t^p\right)^{\mathrm{H}} \widehat{\mathbf{g}}_t^p\right| \sigma_{\tilde{s}}^2 \text{ , assume } \mathrm{E}\left\{\left|\tilde{s}_t^p\right|^2\right\} = \sigma_{\tilde{s}}^2 \tag{4.50}$$

and

$$\mathrm{E}\left\{\left|\left(\widehat{\mathbf{g}}_{\mathrm{apI}}^{p}\right)^{\mathrm{H}} \mathbf{H}_t^p \left(\tilde{\mathbf{s}}_t^p - \overline{\mathbf{s}}_t^{p(\mathrm{i})}\right) + \left(\widehat{\mathbf{g}}_t^p\right)^{\mathrm{H}} \tilde{\mathbf{n}}_t\right|^2\right\} = \mathrm{E}\left\{\left|\left(\widehat{\mathbf{g}}_{\mathrm{apI}}^{p}\right)^{\mathrm{H}} \mathbf{H}_t^p \left(\tilde{\mathbf{s}}_t^p - \overline{\mathbf{s}}_t^{p(\mathrm{i})}\right)\right|^2\right\} + \mathrm{E}\left\{\left|\left(\widehat{\mathbf{g}}_{\mathrm{apI}}^{p}\right)^{\mathrm{H}} \tilde{\mathbf{n}}_t\right|^2\right\} \tag{4.51}$$

$$\mathrm{E}\left\{\left|\left(\widehat{\mathbf{g}}_{\mathrm{apI}}^{p}\right)^{\mathrm{H}} \mathbf{H}_t^p \left(\tilde{\mathbf{s}}_t^p - \overline{\mathbf{s}}_t^{p(\mathrm{i})}\right)\right|^2\right\} = \left|\left(\widehat{\mathbf{g}}_{\mathrm{apI}}^{p}\right)^{\mathrm{H}} \mathbf{H}_t^p \tilde{\mathbf{V}}_t^p \left(\mathbf{H}_t^p\right)^{\mathrm{H}} \widehat{\mathbf{g}}_{\mathrm{apI}}^{p}\right| \tag{4.52}$$

$$\mathrm{E}\left\{\left|\left(\widehat{\mathbf{g}}_{\mathrm{apI}}^{p}\right)^{\mathrm{H}} \tilde{\mathbf{n}}_t\right|^2\right\} = \sigma_{\tilde{n}}^2 \cdot \left|\left(\widehat{\mathbf{g}}_{\mathrm{apI}}^{p}\right)^{\mathrm{H}} \widehat{\mathbf{g}}_{\mathrm{apI}}^{p}\right| \tag{4.53}$$

So,

$$W_{\mathrm{apI}}^{p} = \frac{\left|\left(\widehat{\mathbf{g}}_{\mathrm{apI}}^{p}\right)^{\mathrm{H}} \mathbf{h}_t^p \left(\mathbf{h}_t^p\right)^{\mathrm{H}} \widehat{\mathbf{g}}_{\mathrm{apI}}^{p}\right|}{\left|\left(\widehat{\mathbf{g}}_{\mathrm{apI}}^{p}\right)^{\mathrm{H}} \mathbf{H}_t^p \tilde{\mathbf{V}}_t^p \left(\mathbf{H}_t^p\right)^{\mathrm{H}} \widehat{\mathbf{g}}_{\mathrm{apI}}^{p}\right| + \sigma_{\tilde{n}}^2 \cdot \left|\left(\widehat{\mathbf{g}}_{\mathrm{apI}}^{p}\right)^{\mathrm{H}} \widehat{\mathbf{g}}_{\mathrm{apI}}^{p}\right|} \tag{4.54}$$

The weight of bit metrics W_{apI}^{p} is similar as signal-to-interference-and-noise ratio.

4.2.2 Approximation II of the proposed iterative MMSE detector

From the equation (4.47), the coefficients of adaptive linear detector $\left(\widehat{\mathbf{g}}_{\mathrm{apI}}^{p}\right)^{\mathrm{H}}$ is depends on the variance of interference $\tilde{v}_t^1,\cdots,\tilde{v}_t^{p\text{-}1},\tilde{v}_t^{p+1},\cdots,\tilde{v}_t^{N_T}$. The iterative receiver needs to compute $\left(\widehat{\mathbf{g}}_{\mathrm{apI}}^{p}\right)^{\mathrm{H}}$ at each time per transmitter antenna per iteration. The computation of the coefficients of adaptive linear detector is $N_T \cdot L_{\tilde{s}} \cdot N_{iterative}$. Because it needs to compute pseudo inverse, the computation complexity is still higher. As the variances of signal within each layer to be similar, $\tilde{v}_t^j$ can be approximated by its average.

We use approximation to calculate $\left(\widehat{\mathbf{g}}_{\mathrm{apI}}^{p}\right)^{\mathrm{H}}$ by averaging the variance of interference, as (4.55)

$$\bar{v}^j = \frac{1}{L_{\tilde{s}}}\sum_{t=0}^{L_{\tilde{s}}\text{-}1}\tilde{v}_t^j \quad \text{, where } L_{\tilde{s}} \text{ is the number of symbols} \tag{4.55}$$

Average the variance of the signal from j^{th} transmitter antenna over the transmitted symbols.

And

$$\bar{\mathbf{V}}^p = \mathrm{diag}\left(\bar{v}^1,\cdots,\bar{v}^{p\text{-}1},\bar{v}^{p+1},\cdots,\bar{v}^{N_T}\right) \tag{4.56}$$

Then, assume in quai-static Rayleigh fading channel

$$\left(\widehat{\mathbf{g}}_{\mathrm{apII}}^{p}\right)^{\mathrm{H}} = \left(\mathbf{h}^p\right)^{\mathrm{H}}\left[\mathbf{h}^p\left(\mathbf{h}^p\right)^{\mathrm{H}} + \mathbf{H}^p\bar{\mathbf{V}}^p\left(\mathbf{H}^p\right)^{\mathrm{H}} + \sigma_{\tilde{n}}^2\,\mathbf{I}_{N_R}\right]^{-1} \tag{4.57}$$

The block diagram of $\left(\widehat{\mathbf{g}}_{\mathrm{apII}}^{p}\right)^{\mathrm{H}}$ computation is shown in Fig. 4-8.

Using Gaussian approximation to calculate the weight of bit metrics,

$$W_{\mathrm{apII}}^{p} = \frac{\left|\left(\hat{\mathbf{g}}_{\mathrm{apII}}^{p}\right)^{\mathrm{H}}\mathbf{h}^p\left(\mathbf{h}^p\right)^{\mathrm{H}}\hat{\mathbf{g}}_{\mathrm{apII}}^{p}\right|}{\left|\left(\hat{\mathbf{g}}_{\mathrm{apII}}^{p}\right)^{\mathrm{H}}\mathbf{H}^p\bar{\mathbf{V}}^p\left(\mathbf{H}^p\right)^{\mathrm{H}}\hat{\mathbf{g}}_{\mathrm{apII}}^{p}\right| + \sigma_{\tilde{n}}^2 \cdot \left|\left(\hat{\mathbf{g}}_{\mathrm{apII}}^{p}\right)^{\mathrm{H}}\hat{\mathbf{g}}_{\mathrm{apII}}^{p}\right|} \tag{4.58}$$

The weight of bit metrics W_{apII}^{p} is similar as signal-to-interference-and-noise ratio.

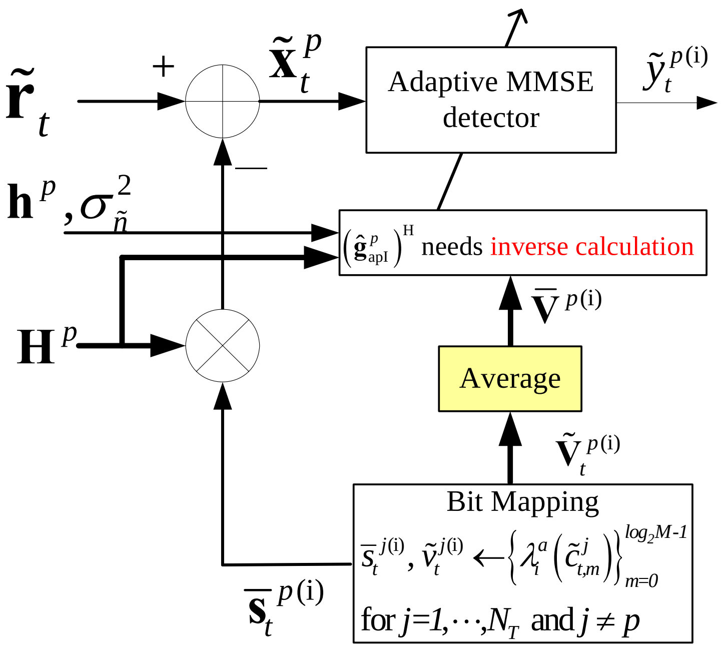

Fig. 4-8: The block diagram of the approximation II of the proposed iterative MMSE receiver

We only need to compute $\left(\hat{\mathbf{g}}_{\mathrm{apII}}^{p}\right)^{\mathrm{H}}$ and W_{apII}^{p} per transmitter antenna per iteration. The $\left(\hat{\mathbf{g}}_{\mathrm{apII}}^{p}\right)^{\mathrm{H}}$ is the same value over all the time. This approximation to reduce $\left(\hat{\mathbf{g}}_{\mathrm{apII}}^{p}\right)^{\mathrm{H}}$ computations from $N_T \cdot L_{\tilde{s}} \cdot N_{iterative}$ to $N_T \cdot N_{iterative}$.

4.2.3 Approximation III of the proposed iterative MMSE detector

The complex symbol $\tilde{s}_t^j$ is mapped from $\tilde{c}_{t,0}^j, \cdots, \tilde{c}_{t,\log_2 M-1}^j$, see (4.32).

If the absolute value of a priori information $\lambda_i^a\left(\tilde{c}_{t,m}^j\right)$ is very large, the variance of interference is close to zero.

$$\left|\lambda_i^a\left(\tilde{c}_{t,m}^j\right)\right|_{m=0}^{M-1} >> 0 \;\Rightarrow\; \mathrm{E}\left\{\tilde{s}_t^j\left(\tilde{s}_t^j\right)^*\right\} \to \mathrm{E}\left\{\tilde{s}_t^j\right\}\mathrm{E}\left\{\left(\tilde{s}_t^j\right)^*\right\} \text{ and } \tilde{v}_t^j \approx 0 \qquad (4.59)$$

Then we can ignore the term $\mathbf{H}^p \tilde{\mathbf{V}}_t^p \left(\mathbf{H}^p\right)^{\mathrm{H}}$

Finally, the $\left(\widehat{\mathbf{g}}_t^p\right)^{\mathrm{H}}$ can be approximated to

$$\left(\widehat{\mathbf{g}}_{\mathrm{apIII}}^p\right)^{\mathrm{H}} = \left(\mathbf{h}^p\right)^{\mathrm{H}}\left[\mathbf{h}^p\left(\mathbf{h}^p\right)^{\mathrm{H}} + \sigma_{\tilde{n}}^2 \mathbf{I}_{N_R}\right]^{-1} \tag{4.60}$$

The block diagram of $\left(\widehat{\mathbf{g}}_{\mathrm{apIII}}^p\right)^{\mathrm{H}}$ computation is shown in Fig. 4-9.

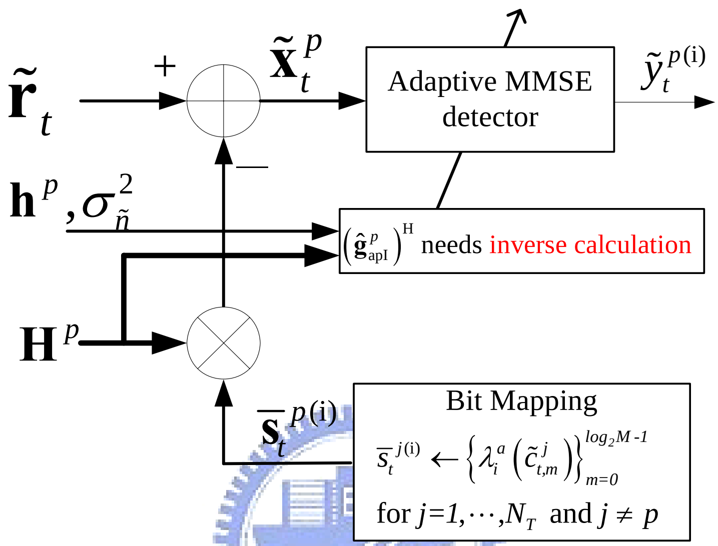

Fig. 4-9: The block diagram of the approximation III of the proposed iterative MMSE receiver

Using Gaussian approximation to calculate the weight of bit metrics,

$$W_{\mathrm{apIII}}^p = \frac{\left|\left(\widehat{\mathbf{g}}_{\mathrm{apIII}}^p\right)^{\mathrm{H}} \mathbf{h}^p \left(\mathbf{h}^p\right)^{\mathrm{H}} \widehat{\mathbf{g}}_{\mathrm{apIII}}^p\right|}{\sigma_{\tilde{n}}^2 \cdot \left|\left(\widehat{\mathbf{g}}_{\mathrm{apIII}}^p\right)^{\mathrm{H}} \widehat{\mathbf{g}}_{\mathrm{apIII}}^p\right|} \tag{4.61}$$

The weight of bit metrics W_{apIII}^p is similar as signal-to-noise ratio.

We only need to compute $\left(\widehat{\mathbf{g}}_{\mathrm{apIII}}^p\right)^{\mathrm{H}}$ and W_{apIII}^p per transmitter antenna at the first iteration. The $\left(\widehat{\mathbf{g}}_{\mathrm{apIII}}^p\right)^{\mathrm{H}}$ is the same value over all the time and at all iterations. This approximation to reduce $\left(\widehat{\mathbf{g}}_{\mathrm{apIII}}^p\right)^{\mathrm{H}}$ computations to N_T .

4.2.4 Approximation IV of the proposed iterative MMSE detector

Compare to the first term of inverse of $\left(\hat{\mathbf{g}}^{p}_{\mathrm{apII}}\right)^{\mathrm{H}}, \mathbf{h}^{p}\left(\mathbf{h}^{p}\right)^{\mathrm{H}}$, the term $\sigma_{\tilde{n}}^{2}\mathbf{I}_{N_R}$ is very small at high SNR. Therefore, we can ignore the term $\sigma_{\mathrm{n}}^{2}\mathbf{I}_{\mathrm{N_R}}$ at high SNR or no information about SNR in the receiver.

Then,

$$\left(\hat{\mathbf{g}}^{p}_{\mathrm{apIV}}\right)^{\mathrm{H}} = \left(\mathbf{h}^{p}\right)^{\mathrm{H}}\left[\mathbf{h}^{p}\left(\mathbf{h}^{p}\right)^{\mathrm{H}}\right]^{-1} = \mathrm{pinv}\left(\mathbf{h}^{p}\right) \tag{4.62}$$

where $\mathrm{pinv}(\bullet)$ is a pseudo inverse function

It is similar as to Maximum Ration Combining (MRC) with normalization.

The computation of $\left(\hat{\mathbf{g}}^{p}_{\mathrm{apIV}}\right)^{\mathrm{H}}$ is N_T. We need to compute $\left(\hat{\mathbf{g}}^{p}_{\mathrm{apIV}}\right)^{\mathrm{H}}$ per transmitter antenna at the first iteration. The $\left(\hat{\mathbf{g}}^{p}_{\mathrm{apIV}}\right)^{\mathrm{H}}$ is the same value over all the time and at any iteration. And this approximation is suitable to no information about SNR or at high SNR condition.

4.3 Simulation Results

Our simulation platform is based on the proposal of TGn Sync. The signal bandwidth (BW) is 20MHz. The transmitter and receiver use 128-points IFFT and FFT, respectively. The antenna spacing in the transmitter and receiver are equal to 0.5 wavelength. The decoder uses MAP algorithm (BCJR) to decide information bits with trace back length of 42. Assume there are perfect synchronization in the receiver, i.e. without frequency offset, clock offset, and phase rotation. The channel is well-kwon in the receiver. And the channel model is IEEE802.11n Channel Model B. There are at least 200 packet errors down to 1% packet error rate (PER) or a total of 3,000 packets in our simulation. The iterative detector design in this section is based on the MMSE criterion. Compare the performance of iterative MMSE detector with proposed algorithm and four approximations. The SNR is defined in chapter 2.

Case1: Observe the performance of proposed iterative MMSE detector

$$\left(\hat{\mathbf{g}}_{t,m}^{p}\right)^{\mathrm{H}}=\mathrm{E}\left\{\tilde{s}_{t}^{p}\left(\tilde{s}_{t}^{p}\right)^{*}\right\}\left(\mathbf{h}_{t}^{p}\right)^{\mathrm{H}}\left[\mathbf{h}_{t}^{p}\mathrm{E}\left\{\tilde{s}_{t}^{p}\left(\tilde{s}_{t}^{p}\right)^{*}\right\}\left(\mathbf{h}_{t}^{p}\right)^{\mathrm{H}}+\mathbf{H}_{t}^{p}\tilde{\mathbf{V}}_{t}^{p}\left(\mathbf{H}_{t}^{p}\right)^{\mathrm{H}}+\sigma_{\tilde{n}}^{2}\mathbf{I}_{N_R}\right]^{-1}$$

From the simulation result Fig. 4-11, we find that there is 1dB enhancement at first iteration and about 2dB enhancement at more iteration.

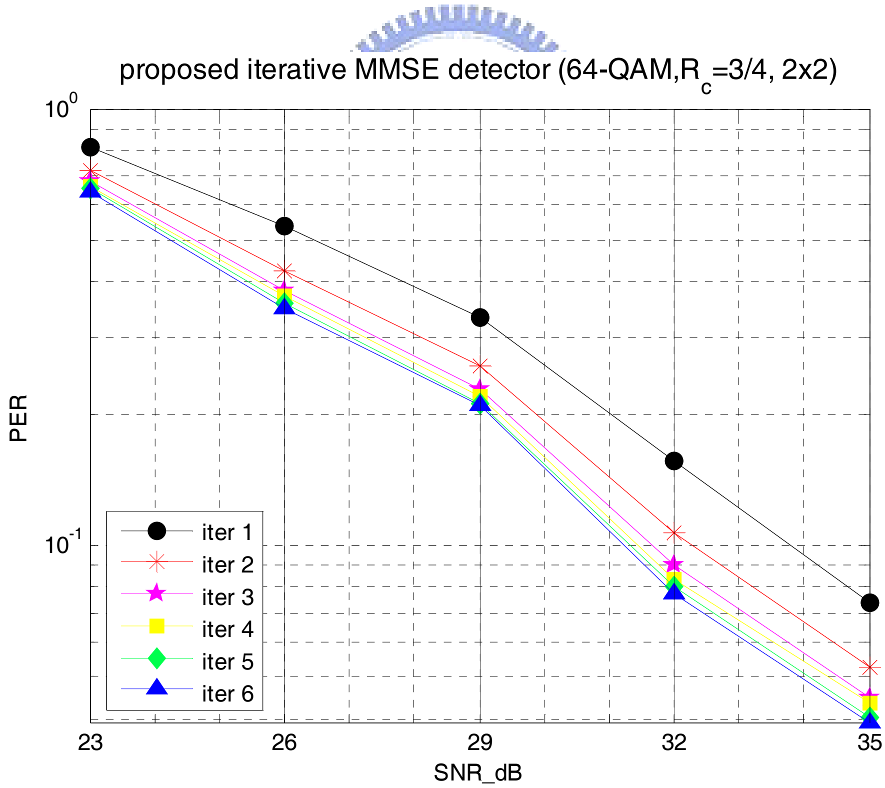

Fig. 4-10: Performance of the proposed iterative MMSE detector (64QAM, R_c=3/4, 2x2)

Case2: Observe the performance of proposed iterative MMSE detector with approximation I, shown in Fig. 4-11, Fig. 4-12, and Fig. 4-13.

$$\left(\widehat{\mathbf{g}}_{\mathrm{apI}}^{p}\right)^{\mathrm{H}}=\left(\mathbf{h}_t^p\right)^{\mathrm{H}}\left[\mathbf{h}_t^p\left(\mathbf{h}_t^p\right)^{\mathrm{H}}+\mathbf{H}_t^p\tilde{\mathbf{V}}_t^p\left(\mathbf{H}_t^p\right)^{\mathrm{H}}+\sigma_{\tilde{n}}^2\,\mathbf{I}_{N_R}\right]^{-1}$$

From the simulation results Fig. 4-10 and Fig. 4-12, the performance of the proposed iterative MMSE detector with approximation I is very close to the performance of the proposed iterative MMSE detector.

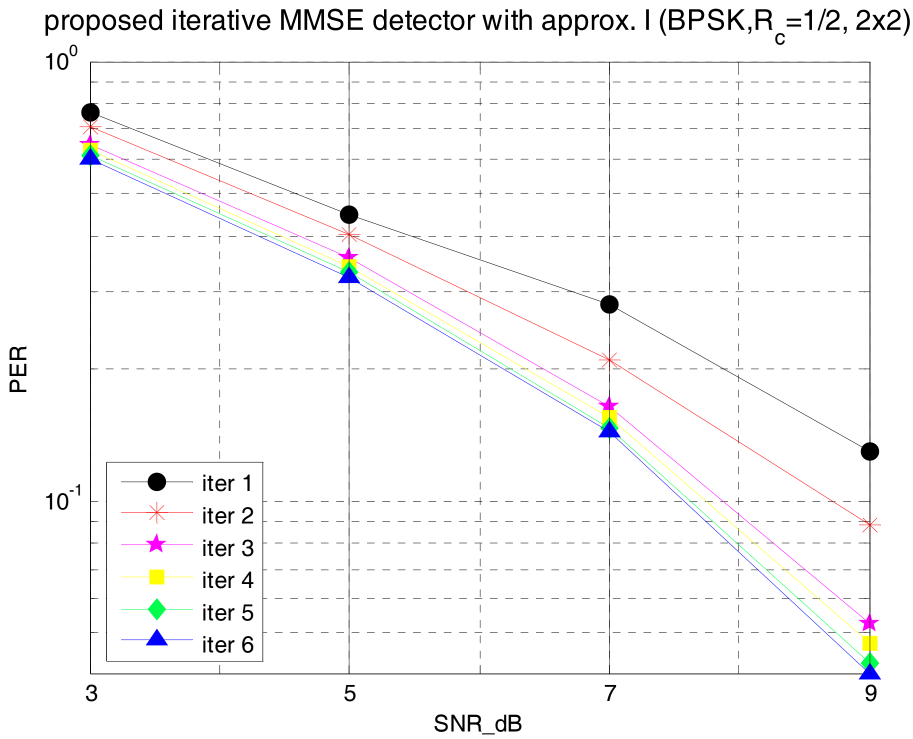

Fig. 4-11: Performance of proposed iterative MMSE detector with approximation I (BPSK, R_c=1/2, 2x2)

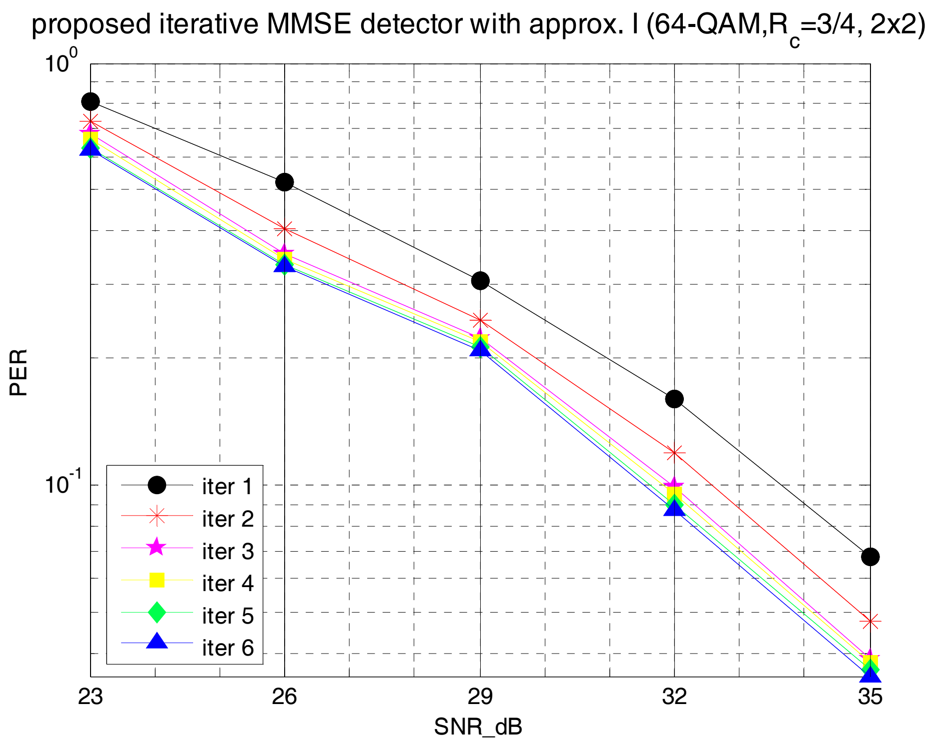

Fig. 4-12: Performance of proposed iterative MMSE detector with approximation I (64-QAM, R_c=3/4, 2x2)

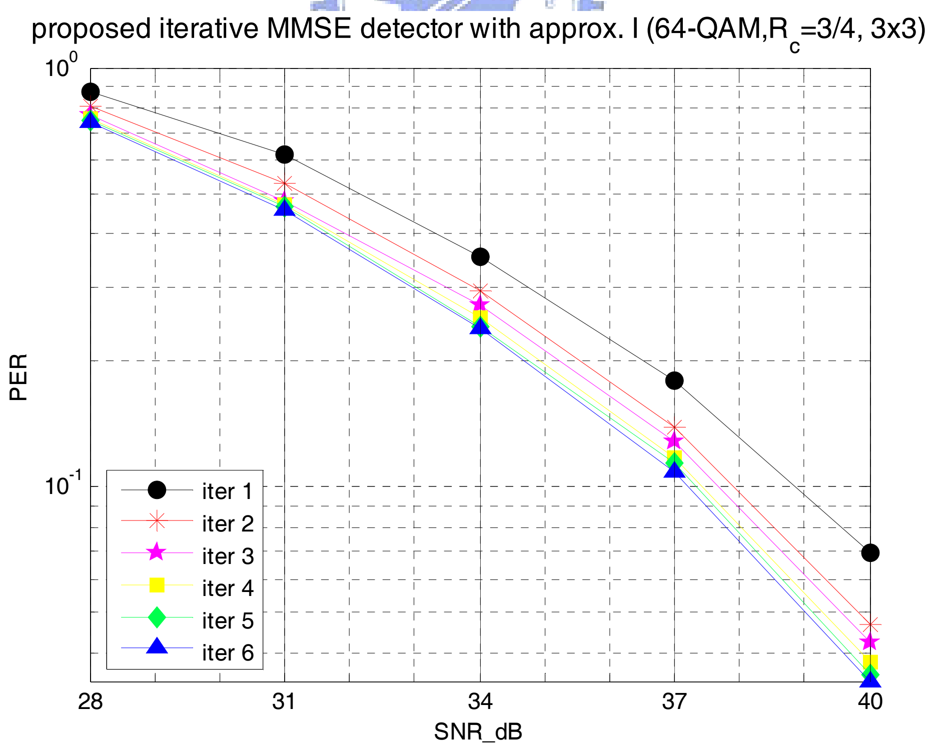

Fig. 4-13: Performance of proposed iterative MMSE detector with approximation I (64-QAM, R_c=3/4, 3x3)

Case3: Observe the performance of the proposed iterative MMSE detector with approximation II compared to the proposed iterative MMSE detector.

$$\left(\hat{\mathbf{g}}_{\mathrm{apII}}^{p}\right)^{\mathrm{H}} = \left(\mathbf{h}^{p}\right)^{\mathrm{H}} \left[\mathbf{h}^{p}\left(\mathbf{h}^{p}\right)^{\mathrm{H}} + \mathbf{H}^{p}\bar{\mathbf{V}}^{p}\left(\mathbf{H}^{p}\right)^{\mathrm{H}} + \sigma_{\tilde{n}}^{2}\,\mathbf{I}_{N_R}\right]^{-1}$$

From the simulation result Fig. 4-14, we can find that the performance of the proposed iterative MMSE detector with approximation II is very close to the performance of the proposed iterative MMSE detector.

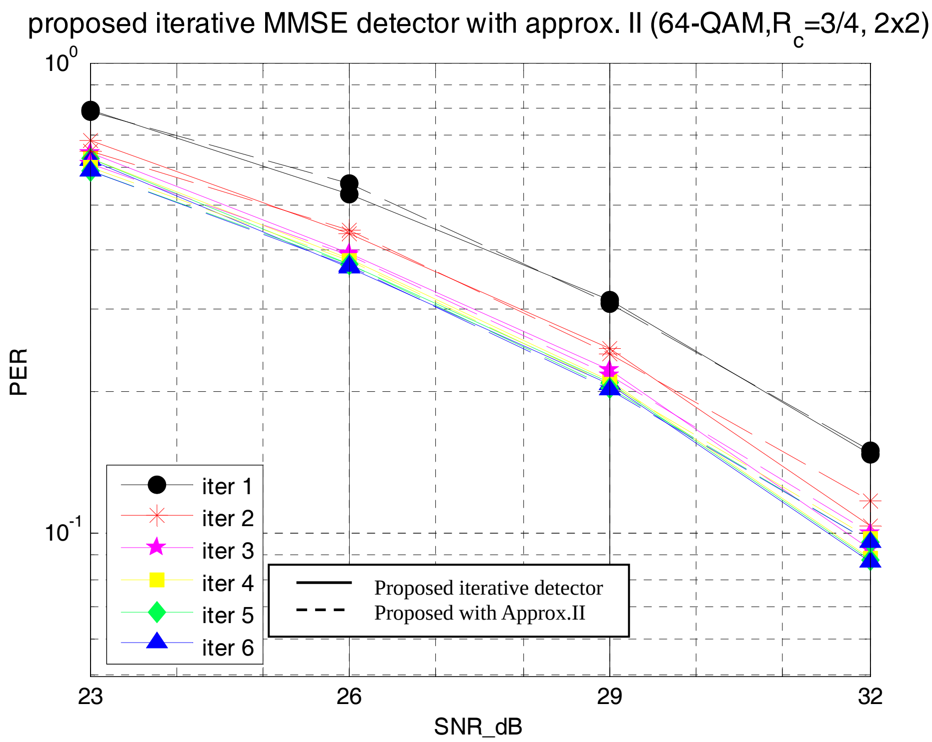

Fig. 4-14: Compare the performance of the proposed iterative MMSE detector with approximation II to the proposed iterative MMSE detector (64-QAM, R_c=3/4, 2x2)

Case4: Observe the performance of the proposed iterative MMSE detector with approximation III compared to the proposed iterative MMSE detector.

$$\left(\hat{\mathbf{g}}_{\text{apIII}}^{p}\right)^{\mathrm{H}}=\left(\mathbf{h}^{p}\right)^{\mathrm{H}}\left[\mathbf{h}^{p}\left(\mathbf{h}^{p}\right)^{\mathrm{H}}+\sigma_{\tilde{n}}^{2}\mathbf{I}_{N_R}\right]^{-1}$$

From simulation result Fig. 4-15, we can find that the performance of the proposed iterative MMSE detector with approximation III by ignoring interference term is very close to the performance of the proposed iterative MMSE detector.

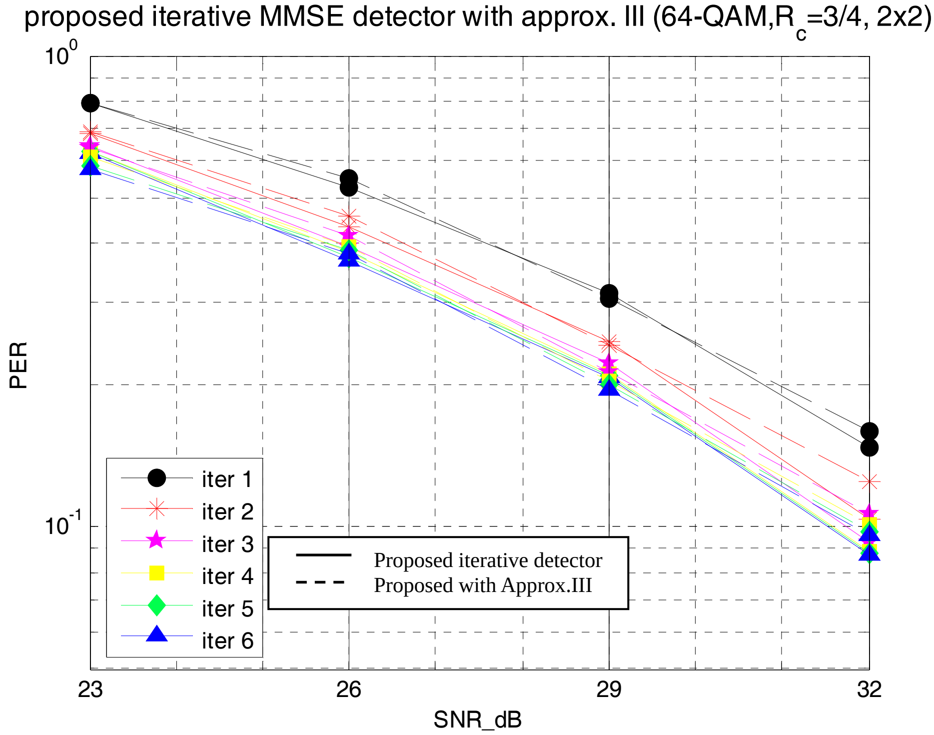

Fig. 4-15: Compare the performance of the proposed iterative MMSE detector with approximation III to the proposed iterative MMSE detector (64-QAM, Rc=3/4, 2x2)

Case5: Observe the performance of the proposed iterative MMSE detector with approximation IV compared to the proposed iterative MMSE detector.

$$\left(\hat{\mathbf{g}}_{\text{apIV}}^{p}\right)^{\text{H}}=\left(\mathbf{h}^{p}\right)^{\text{H}}\left[\mathbf{h}^{p}\left(\mathbf{h}^{p}\right)^{\text{H}}\right]^{-1}=\text{pinv}\left(\mathbf{h}^{p}\right)$$

From simulation result Fig. 4-16, we can find that the performance of the proposed iterative MMSE detector with approximation IV by ignoring interference and noise terms is very close to the performance of the proposed iterative MMSE detector.

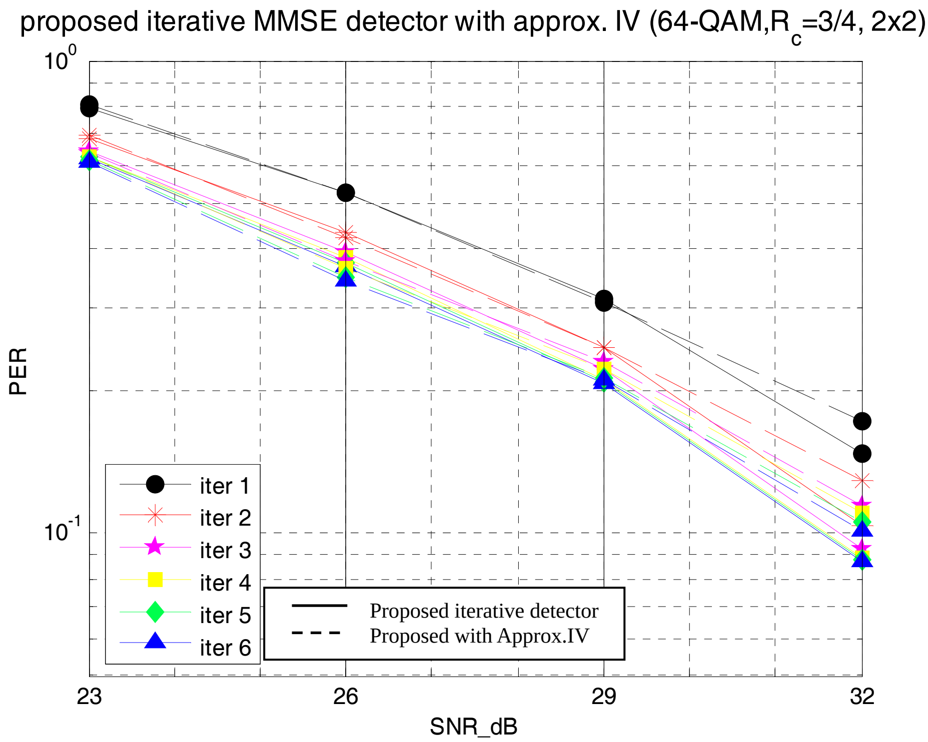

Fig. 4-16: Compare the performance of the proposed iterative MMSE detector with approximation IV to the proposed iterative MMSE detector (64-QAM, R_c=3/4, 2x2)

4.4 Conclusions

There is 1dB enhancement at first iteration and about 2dB enhancement at more iteration in iterative MMSE detector. The performances of three methods of approximation are similar to the performance of iterative MMSE detector without approximation. That is because that in the inverse of the equation (4.47), the interference and noise term are very small compared to the first term $\mathbf{h}_t^p\left(\mathbf{h}_t^p\right)^{\mathrm{H}}$. However, if we use those methods of approximation, we can reduce the times of inverse computation from $N_T \cdot L_{\tilde{s}} \cdot N_{iteration} \cdot log_2 M$ to N_T without degrading the performance.

Chapter 5:

Conclusions and Future Works

5.1 Conclusions

In this thesis, at first, we introduce to the system architectures of 802.11n proposal of TGn Sync and the channel models. Then, we derive the weight of bit metrics for MIMO BICM systems in the MMSE detector and the ZF detector. We analyze the performance of bit metric calculation with weighted gain and equal gain. If we can present exactly the pdf of the interference and noise, there is about 3~4dB enhancement of performance. At lower modulation scheme, there is only about 1dB enhancement with pdf of the interference and noise by Gaussian approximation. By the way, the ZF detector has noise enhancement so the performance of MMSE detector is better than those of ZF detector about 1~4dB, especially at lower SNR. At high SNR, the MMSE detector is similar as the ZF detector and makes more effort on interference suppression.

Besides, we design low complexity iterative MMSE detector with turbo principle and propose some methods of approximation to reduce computation complexity. From the simulation results, it proves that using weighted bit metrics can improve the performance. There is 1dB enhancement at first iteration and about 2dB enhancement at more iteration in iterative MMSE detector. Employing approximation of iterative MMSE detector can reduce the computation complexity without performance deterioration. That is because that in the inverse of the equation(4.47), the interference and noise term are very small compared to the first term $\mathbf{h}_t^p \left(\mathbf{h}_t^p\right)^{\mathrm{H}}$. However, if we use those methods of approximation, we can reduce the times of inverse computation from $N_T \cdot L_{\tilde{s}} \cdot N_{iteration} \cdot log_2 M$ to N_T without degrading the performance.

5.2 Future Works

We combine detection and decoding to design a lower-complexity and higher-performance iterative signal detector based on MMSE criterion and turbo principle for MIMO BICM systems. We may consider advanced codes, such as turbo code and LDPC, to improve performance. We may design a iterative signal detector based on LDPC principle. We can joint channel estimation and decoding or detection to improve the ability of estimating channels. We can use geometrical approaches, such as sphere decoding and lattice decoding, to approximate ML detection.

Appendix A:

Multistage Detection for A Linear MMSE Receiver

To calculate the coefficients of adaptive linear detector based on MMSE Criterion,

$$\mathbf{G}_k^{\mathrm{MMSE}} = \arg\min_{\mathbf{G}_k} \mathrm{E}\left\{\left|\tilde{\mathbf{y}}_{\ell.k} - \tilde{\mathbf{s}}_{\ell.k}\right|^2\right\} = \arg\min_{\mathbf{G}_k} \mathrm{E}\left\{\left|\mathbf{G}_k\tilde{\mathbf{r}}_{\ell.k} - \tilde{\mathbf{s}}_{\ell.k}\right|^2\right\} \tag{A.1}$$

Let the cost function

$$\begin{aligned} J &= \mathrm{E}\left\{\left|\mathbf{G}_k\tilde{\mathbf{r}}_{\ell.k} - \tilde{\mathbf{s}}_{\ell.k}\right|^2\right\} \\ &= \mathbf{G}_k\mathrm{E}\left\{\tilde{\mathbf{r}}_{\ell.k}\tilde{\mathbf{r}}_{\ell.k}^{\mathrm{H}}\right\}\left(\mathbf{G}_k\right)^{\mathrm{H}} - \mathbf{G}_k\mathrm{E}\left\{\tilde{\mathbf{r}}_{\ell.k}\tilde{\mathbf{s}}_{\ell.k}^{\mathrm{H}}\right\} - \mathrm{E}\left\{\tilde{\mathbf{s}}_{\ell.k}\tilde{\mathbf{r}}_{\ell.k}^{\mathrm{H}}\right\}\left(\mathbf{G}_k\right)^{\mathrm{H}} + \mathrm{E}\left\{\tilde{\mathbf{s}}_{\ell.k}\tilde{\mathbf{s}}_{\ell.k}^{\mathrm{H}}\right\} \end{aligned} \tag{A.2}$$

And $\tilde{\mathbf{r}}_{\ell.k} = \mathbf{H}_k\tilde{\mathbf{s}}_{\ell.k} + \tilde{\mathbf{n}}_{\ell.k}$

Find the minimum value of J,

$$\frac{\partial J}{\partial\left(\mathbf{G}_k\right)^{\mathrm{H}}} = \mathbf{G}_k\mathrm{E}\left\{\tilde{\mathbf{r}}_{\ell.k}\tilde{\mathbf{r}}_{\ell.k}^{\mathrm{H}}\right\} - \mathrm{E}\left\{\tilde{\mathbf{s}}_{\ell.k}\tilde{\mathbf{r}}_{\ell.k}^{\mathrm{H}}\right\} = 0 \tag{A.3}$$

Therefore,

$$\mathbf{G}_k^{\mathrm{MMSE}} = \mathrm{E}\left\{\tilde{\mathbf{s}}_{\ell.k}\tilde{\mathbf{r}}_{\ell.k}^{\mathrm{H}}\right\}\left[\mathrm{E}\left\{\tilde{\mathbf{r}}_{\ell.k}\tilde{\mathbf{r}}_{\ell.k}^{\mathrm{H}}\right\}\right]^{-1} \tag{A.4}$$

where

$$\begin{aligned} \mathrm{E}\left\{\tilde{\mathbf{s}}_{\ell.k}\tilde{\mathbf{r}}_{\ell.k}^{\mathrm{H}}\right\} &= \mathrm{E}\left\{\tilde{\mathbf{s}}_{\ell.k}\left(\mathbf{H}_k\tilde{\mathbf{s}}_{\ell.k} + \tilde{\mathbf{n}}_{\ell.k}\right)^{\mathrm{H}}\right\} \\ &= \mathrm{E}\left\{\tilde{\mathbf{s}}_{\ell.k}\tilde{\mathbf{s}}_{\ell.k}\right\}\left(\mathbf{H}_k\right)^{\mathrm{H}} + \mathrm{E}\left\{\tilde{\mathbf{s}}_{\ell.k}\tilde{\mathbf{n}}_{\ell.k}^{\mathrm{H}}\right\} \end{aligned} \tag{A.5}$$

and

$$\begin{aligned} \mathrm{E}\left\{\tilde{\mathbf{r}}_{\ell.k}\tilde{\mathbf{r}}_{\ell.k}^{\mathrm{H}}\right\} &= \mathrm{E}\left\{\left(\mathbf{H}_k\tilde{\mathbf{s}}_{\ell.k} + \tilde{\mathbf{n}}_{\ell.k}\right)\left(\mathbf{H}_k\tilde{\mathbf{s}}_{\ell.k} + \tilde{\mathbf{n}}_{\ell.k}\right)^{\mathrm{H}}\right\} \\ &= \mathbf{H}_k\mathrm{E}\left\{\tilde{\mathbf{s}}_{\ell.k}\tilde{\mathbf{s}}_{\ell.k}^{\mathrm{H}}\right\}\mathbf{H}_k^{\mathrm{H}} + \mathbf{H}_k\mathrm{E}\left\{\tilde{\mathbf{s}}_{\ell.k}\tilde{\mathbf{n}}_{\ell.k}^{\mathrm{H}}\right\} + \mathrm{E}\left\{\tilde{\mathbf{n}}_{\ell.k}\tilde{\mathbf{s}}_{\ell.k}^{\mathrm{H}}\right\}\mathbf{H}_k^{\mathrm{H}} + \mathrm{E}\left\{\tilde{\mathbf{n}}_{\ell.k}\tilde{\mathbf{n}}_{\ell.k}^{\mathrm{H}}\right\} \end{aligned} \tag{A.6}$$

Because $\tilde{s}_{\ell.k}^{1},\cdots,\tilde{s}_{\ell.k}^{N_T}$ and $\tilde{n}_{\ell.k}^{1},\cdots,\tilde{n}_{\ell.k}^{N_R}$ are statistically independent

$$\mathrm{E}\left\{\tilde{\mathbf{s}}_{\ell.k}\tilde{\mathbf{s}}_{\ell.k}^{\mathrm{H}}\right\} = \sigma_{\tilde{s}}^2\mathbf{I}_{N_T},\ \mathrm{E}\left\{\tilde{\mathbf{s}}_{\ell.k}\tilde{\mathbf{n}}_{\ell.k}^{\mathrm{H}}\right\} = \mathbf{0},\ \text{and } \mathrm{E}\left\{\tilde{\mathbf{n}}_{\ell.k}\tilde{\mathbf{n}}_{\ell.k}^{\mathrm{H}}\right\} = \sigma_{\tilde{n}}^2\mathbf{I}_{N_R} \tag{A,7}$$

Assume the energy of signal is equal to 1.

$$\mathrm{E}\left\{\tilde{s}_{\ell.k}^{p}\left(\tilde{s}_{\ell.k}^{p}\right)^{*}\right\}=\sigma_{\tilde{s}}^{2}=1$$

Then, the coefficient of linear MMSE detector is

$$\mathbf{G}_{k}^{\mathrm{MMSE}}=\left(\mathbf{H}_{k}\right)^{\mathrm{H}}\left[\mathbf{H}_{k}\left(\mathbf{H}_{k}\right)^{\mathrm{H}}+\sigma_{\tilde{n}}^{2}\mathbf{I}_{N_{R}}\right]^{-1} \tag{A.8}$$

Appendix B:

Multistage Detection for Iterative MMSE Receiver

To calculate the coefficients of adaptive linear iterative detector based on MMSE Criterion,

$$\left(\widehat{\mathbf{g}}_t^p\right)^{\mathrm{H}} = \arg \underbrace{\min}_{\left(\widehat{\mathbf{g}}_t^p\right)^{\mathrm{H}}} \left\{ \mathrm{E}\left\{ \left| \tilde{y}_t^p - \tilde{s}_t^p \right|^2 \right\} \right\} = \arg \underbrace{\min}_{\left(\widehat{\mathbf{g}}_t^p\right)^{\mathrm{H}}} \left\{ \mathrm{E}\left\{ \left| \left(\widehat{\mathbf{g}}_t^p\right)^{\mathrm{H}} \tilde{\mathbf{x}}_t^p - \tilde{s}_t^p \right|^2 \right\} \right\} \tag{B.1}$$

Let cost function $J = \mathrm{E}\left\{ \left| \left(\widehat{\mathbf{g}}_t^p\right)^{\mathrm{H}} \tilde{\mathbf{x}}_t^p - \tilde{s}_t^p \right|^2 \right\}$ and $\tilde{\mathbf{r}}_t = \mathbf{h}_t^p \tilde{s}_t^p + \mathbf{H}_t^p \tilde{\mathbf{s}}_t^p + \tilde{\mathbf{n}}_t$.

Then,

$$\begin{aligned} J &= \mathrm{E}\left\{ \left| \left(\widehat{\mathbf{g}}_t^p\right)^{\mathrm{H}} \left(\mathbf{h}_t^p \tilde{s}_t^p + \mathbf{H}_t^p \left(\tilde{\mathbf{s}}_t^p - \overline{\mathbf{s}}_t^{p(\mathrm{i})} \right) + \tilde{\mathbf{n}}_t \right) - \tilde{s}_t^p \right|^2 \right\} \\ &= \mathrm{E}\left\{ \begin{aligned} &\left(\widehat{\mathbf{g}}_t^p\right)^{\mathrm{H}} \left(\tilde{\mathbf{r}}_t - \mathbf{H}_t^p \overline{\mathbf{s}}_t^{p(\mathrm{i})} \right) \left(\tilde{\mathbf{r}}_t - \mathbf{H}_t^p \overline{\mathbf{s}}_t^{p(\mathrm{i})} \right)^{\mathrm{H}} \widehat{\mathbf{g}}_t^p - \mathbf{g}_p^{\mathrm{H}} \left(\tilde{\mathbf{r}}_t - \mathbf{H}_t^p \overline{\mathbf{s}}_t^{p(\mathrm{i})} \right) \left(\tilde{s}_t^p \right)^* \\ &- \tilde{s}_t^p \left(\tilde{\mathbf{r}}_t - \mathbf{H}_t^p \overline{\mathbf{s}}_t^{p(\mathrm{i})} \right)^{\mathrm{H}} \widehat{\mathbf{g}}_t^p + \tilde{s}_t^p \left(\tilde{s}_t^p \right)^* \end{aligned} \right\} \end{aligned} \tag{B.2}$$

Find the minimum value of J,

$$\frac{\partial J}{\partial \widehat{\mathbf{g}}_t^p} = \left(\widehat{\mathbf{g}}_t^p\right)^{\mathrm{H}} \cdot \mathrm{E}\left\{ \left(\tilde{\mathbf{r}}_t - \mathbf{H}_t^p \overline{\mathbf{s}}_t^{p(\mathrm{i})} \right) \left(\tilde{\mathbf{r}}_t - \mathbf{H}_t^p \overline{\mathbf{s}}_t^{p(\mathrm{i})} \right)^{\mathrm{H}} \right\} - \mathrm{E}\left\{ \tilde{s}_t^p \left(\tilde{\mathbf{r}}_t - \mathbf{H}_t^p \overline{\mathbf{s}}_t^{p(\mathrm{i})} \right)^{\mathrm{H}} \right\} = 0 \tag{B.3}$$

$$\Rightarrow \left(\widehat{\mathbf{g}}_t^p\right)^{\mathrm{H}} = \mathrm{E}\left\{ \tilde{s}_t^p \left(\tilde{\mathbf{r}}_t - \mathbf{H}_t^p \overline{\mathbf{s}}_t^{p(\mathrm{i})} \right)^{\mathrm{H}} \right\} \cdot \left[\mathrm{E}\left\{ \left(\tilde{\mathbf{r}}_t - \mathbf{H}_t^p \overline{\mathbf{s}}_t^{p(\mathrm{i})} \right) \left(\tilde{\mathbf{r}}_t - \mathbf{H}_t^p \overline{\mathbf{s}}_t^{p(\mathrm{i})} \right)^{\mathrm{H}} \right\} \right]^{-1} \tag{B.4}$$

where

$$\begin{aligned} \mathrm{E}\left\{ \tilde{s}_t^p \left(\tilde{\mathbf{r}}_t - \mathbf{H}_t^p \overline{\mathbf{s}}_t^{p(\mathrm{i})} \right)^{\mathrm{H}} \right\} &= \mathrm{E}\left\{ \tilde{s}_t^p \left(\mathbf{h}_t^p \tilde{s}_t^p + \mathbf{H}_t^p \tilde{\mathbf{s}}_t^p + \tilde{\mathbf{n}}_t - \mathbf{H}_t^p \overline{\mathbf{s}}_t^{p(\mathrm{i})} \right)^{\mathrm{H}} \right\} \\ &= \mathrm{E}\left\{ \tilde{s}_t^p \left(\tilde{s}_t^p \right)^* \right\} \left(\mathbf{h}_t^p \right)^{\mathrm{H}} + \mathrm{E}\left\{ \tilde{s}_t^p \left(\tilde{\mathbf{s}}_t^p \right)^{\mathrm{H}} \right\} \left(\mathbf{H}_t^p \right)^{\mathrm{H}} - \mathrm{E}\left\{ \tilde{s}_t^p \right\} \left(\overline{\mathbf{s}}_t^{p(\mathrm{i})} \right)^{\mathrm{H}} \left(\mathbf{H}_t^p \right)^{\mathrm{H}} \end{aligned} \tag{B.5}$$

and

$$
\begin{aligned}
&\mathrm{E}\left\{\left(\tilde{\mathbf{r}}_t-\mathbf{H}_t^p\bar{\mathbf{s}}_t^{p(\mathrm{i})}\right)\left(\tilde{\mathbf{r}}_t-\mathbf{H}_t^p\bar{\mathbf{s}}_t^{p(\mathrm{i})}\right)^{\mathrm{H}}\right\}\\
&=\mathrm{E}\left\{\left(\mathbf{h}_t^p\tilde{s}_t^p+\mathbf{H}_t^p\tilde{\mathbf{s}}_t^p+\tilde{\mathbf{n}}_t-\mathbf{H}_t^p\bar{\mathbf{s}}_t^{p(\mathrm{i})}\right)\left(\mathbf{h}_t^p\tilde{s}_t^p+\mathbf{H}_t^p\tilde{\mathbf{s}}_t^p+\tilde{\mathbf{n}}_t-\mathbf{H}_t^p\bar{\mathbf{s}}_t^{p(\mathrm{i})}\right)^{\mathrm{H}}\right\}\\
&=\mathbf{h}_t^p\mathrm{E}\left\{\tilde{s}_t^p\left(\tilde{s}_t^p\right)^*\right\}\left(\mathbf{h}_t^p\right)^{\mathrm{H}}+\mathbf{h}_t^p\mathrm{E}\left\{\tilde{s}_t^p\left(\tilde{\mathbf{s}}_t^p\right)^{\mathrm{H}}\right\}\left(\mathbf{H}_t^p\right)^{\mathrm{H}}-\mathbf{h}_t^p\mathrm{E}\left\{\tilde{s}_t^p\right\}\left(\bar{\mathbf{s}}_t^{p(\mathrm{i})}\right)^{\mathrm{H}}\left(\mathbf{H}_t^p\right)^{\mathrm{H}}\\
&\quad+\mathbf{H}_t^p\mathrm{E}\left\{\tilde{\mathbf{s}}_t^p\left(\tilde{s}_t^p\right)^*\right\}\left(\mathbf{h}_t^p\right)^{\mathrm{H}}+\mathrm{E}\left\{\tilde{\mathbf{n}}_t\tilde{\mathbf{n}}_t^{\mathrm{H}}\right\}-\mathbf{H}_t^p\bar{\mathbf{s}}_t^{p(\mathrm{i})}\mathrm{E}\left\{\left(\tilde{s}_t^p\right)^*\right\}\left(\mathbf{h}_t^p\right)^{\mathrm{H}}\\
&\quad+\mathbf{H}_t^p\left\{\mathrm{E}\left\{\tilde{\mathbf{s}}_t^p\left(\tilde{\mathbf{s}}_t^p\right)^{\mathrm{H}}\right\}-\mathrm{E}\left\{\tilde{\mathbf{s}}_t^p\right\}\left(\bar{\mathbf{s}}_t^{p(\mathrm{i})}\right)^{\mathrm{H}}-\bar{\mathbf{s}}_t^{p(\mathrm{i})}\mathrm{E}\left\{\left(\tilde{\mathbf{s}}_t^p\right)^{\mathrm{H}}\right\}+\bar{\mathbf{s}}_t^{p(\mathrm{i})}\left(\bar{\mathbf{s}}_t^{p(\mathrm{i})}\right)^{\mathrm{H}}\right\}\left(\mathbf{H}_t^p\right)^{\mathrm{H}}
\end{aligned}
\quad \text{(B.6)}
$$

Therefore,

$$\mathrm{E}\left\{\tilde{s}_t^p\left(\tilde{\mathbf{s}}_t^p\right)^{\mathrm{H}}\right\}=\mathrm{E}\left\{\tilde{s}_t^p\right\}\mathrm{E}\left\{\left(\tilde{\mathbf{s}}_t^p\right)^{\mathrm{H}}\right\} \text{ and } \bar{\mathbf{s}}_t^{p(\mathrm{i})}=\mathrm{E}\left\{\tilde{\mathbf{s}}_t^p\right\} \quad \text{(B.7)}$$

And assume noise is AWGN and $\tilde{n}_t^1,\cdots\tilde{n}_t^{N_T}$ are independent.

$$\mathrm{E}\left\{\tilde{\mathbf{n}}_t\tilde{\mathbf{n}}_t^{\mathrm{H}}\right\}=\sigma_{\tilde{n}}^2\mathbf{I}_{N_R} \quad \text{(B.8)}$$

Let

$$\tilde{v}_t^j=\mathrm{E}\left\{\tilde{s}_t^j\left(\tilde{s}_t^j\right)^*\right\}-\mathrm{E}\left\{\tilde{s}_t^j\right\}\mathrm{E}\left\{\left(\tilde{s}_t^j\right)^*\right\}=\mathrm{E}\left\{\tilde{s}_t^j\left(\tilde{s}_t^j\right)^*\right\}-\bar{\mathbf{s}}_t^{j(\mathrm{i})}\left(\bar{\mathbf{s}}_t^{j(\mathrm{i})}\right)^{\mathrm{H}} \quad \text{(B.9)}$$

and

$$\tilde{\mathbf{V}}_t^p=\mathrm{diag}\left(\tilde{v}_t^1,\cdots,\tilde{v}_t^{p-1},\tilde{v}_t^{p+1},\cdots,\tilde{v}_t^{N_T}\right) \quad \text{(B.10)}$$

Then,

$$\mathrm{E}\left\{\tilde{s}_t^p\left(\tilde{\mathbf{r}}_t-\mathbf{H}_t^p\bar{\mathbf{s}}_t^{p(\mathrm{i})}\right)^{\mathrm{H}}\right\}=\mathrm{E}\left\{\tilde{s}_t^p\left(\tilde{s}_t^p\right)^*\right\}\left(\mathbf{h}_t^p\right)^{\mathrm{H}} \quad \text{(B.11)}$$

and

$$\mathrm{E}\left\{\left(\tilde{\mathbf{r}}_t-\mathbf{H}_t^p\bar{\mathbf{s}}_t^{p(\mathrm{i})}\right)\left(\tilde{\mathbf{r}}_t-\mathbf{H}_t^p\bar{\mathbf{s}}_t^{p(\mathrm{i})}\right)^{\mathrm{H}}\right\}=\mathbf{h}_t^p\mathrm{E}\left\{\tilde{s}_t^p\left(\tilde{s}_t^p\right)^*\right\}\left(\mathbf{h}_t^p\right)^{\mathrm{H}}+\mathbf{H}_t^p\tilde{\mathbf{V}}_t^p\left(\mathbf{H}_t^p\right)^{\mathrm{H}}+\sigma_{\tilde{n}}^2\mathbf{I}_{N_R} \quad \text{(B.12)}$$

Replace (B.4) by (B.11) and (B.12),

$$\left(\hat{\mathbf{g}}_t^p\right)^{\mathrm{H}}=\mathrm{E}\left\{\tilde{s}_t^p\left(\tilde{s}_t^p\right)^*\right\}\left(\mathbf{h}_t^p\right)^{\mathrm{H}}\left[\mathbf{h}_t^p\mathrm{E}\left\{\tilde{s}_t^p\left(\tilde{s}_t^p\right)^*\right\}\left(\mathbf{h}_t^p\right)^{\mathrm{H}}+\mathbf{H}_t^p\tilde{\mathbf{V}}_t^p\left(\mathbf{H}_t^p\right)^{\mathrm{H}}+\sigma_{\tilde{n}}^2\mathbf{I}_{N_R}\right]^{-1} \quad \text{(B.13)}$$

Appendix C:

Modulation-Coding Scheme (MCS)

The TGn Sync proposal augments the 802.11a MCS set through the use of multiple spatial streams and bandwidth extension. The MCS filed defines the modulation and coding scheme, as indicated in Table C-1. The proposal recommends a mandatory data of 243Mbps using two spatial streams in regulatory domains that permit 40MHz operation. In the future, their proposal supports scalability to 4 spatial streams, offering data rates in excess of 600Mbps.

Bits 18-23 in HT-SIG1 (MCS index)	Number of spatial streams	Modulation	Coding rate	GI = 800ns		GI = 400ns	
				Rate in 20MHz	Rate in 40MHz	Rate in 20MHz	Rate in 40MHz
0	1	BPSK	1/2	6	13.5	6.67	15
1	1	QPSK	1/2	12	27	13.33	30
2	1	QPSK	3/4	18	40.5	20	45
3	1	16-QAM	1/2	24	54	26.67	60
4	1	16-QAM	3/4	36	81	40	90
5	1	64-QAM	2/3	48	108	53.33	120
6	1	64-QAM	3/4	54	121.5	60	135
7	1	64-QAM	7/8	63	141.75	70	157.5
8	2	BPSK	1/2	12	27	13.33	30
9	2	QPSK	1/2	24	54	26.67	60
10	2	QPSK	3/4	36	81	40	90
11	2	16-QAM	1/2	48	108	53.33	120
12	2	16-QAM	3/4	72	162	80	180
13	2	64-QAM	2/3	96	216	106.67	240
14	2	64-QAM	3/4	108	243	120	270
15	2	64-QAM	7/8	126	283.5	140	315
16	3	BPSK	1/2	18	40.5	20	45

17	3	QPSK	1/2	36	81	40	90
18	3	QPSK	3/4	54	121.5	60	135
19	3	16-QAM	1/2	72	162	80	180
20	3	16-QAM	3/4	108	243	120	270
21	3	64-QAM	2/3	144	324	160	360
22	3	64-QAM	3/4	162	364.5	180	405
23	3	64-QAM	7/8	189	425.25	210	472.5
24	4	BPSK	1/2	24	54	26.67	60
25	4	QPSK	1/2	48	108	53.33	120
26	4	QPSK	3/4	72	162	80	180
27	4	16-QAM	1/2	96	216	106.67	240
28	4	16-QAM	3/4	144	324	160	360
29	4	64-QAM	2/3	192	432	213.33	480
30	4	64-QAM	3/4	216	486	240	540
31	4	64-QAM	7/8	252	567	280	630
32	1	BPSK	1/2		6		6.67

Table C-1: Modulation-coding scheme

Appendix D:

IEEE 802.11n Channel Model B

	Tap index	1	2	3	4	5	6	7	8	9
	Excess delay [ns]	0	10	20	30	40	50	60	70	80
Cluster 1	Power [dB]	0	-5.4	-10.8	-16.2	-21.7				
AoA	AoA [°]	4.3	4.3	4.3	4.3	4.3				
AS (receiver)	AS [°]	14.4	14.4	14.4	14.4	14.4				
AoD	AoD [°]	225.1	225.1	225.1	225.1	225.1				
AS (transmitter)	AS [°]	14.4	14.4	14.4	14.4	14.4				
Cluster 2	Power [dB]			-3.2	-6.3	-9.4	-12.5	-15.6	-18.7	-21.8
AoA	AoA [°]			118.4	118.4	118.4	118.4	118.4	118.4	118.4
AS	AS [°]			25.2	25.2	25.2	25.2	25.2	25.2	25.2
AoD	AoD [°]			106.5	106.5	106.5	106.5	106.5	106.5	106.5
AS	AS [°]			25.4	25.4	25.4	25.4	25.4	25.4	25.4

References

[1]. J. G. Proakis, *Digital Communications*, 4^{th} edition, McGRAW-HILL, 2001.

[2]. T. S. Rappaport, *Wireless Communications: Principles and Practice*, Prentice Hall, 2^{nd} edition, 2002.

[3]. Branka Vucetic and Jinhong Yuan, *Turbo Codes: Principles and Applications*, Kluwer, 2000.

[4]. Branka Vucetic and Jinhong Yuan, *Space-Time Coding*, Willey 2003.

[5]. H.Vincent Poor, *An Introduction to Signal Detection and Estimation*, Springer, New York, 2^{nd} edition, 1994.

[6]. S.Verdu, *Multiuser Detection*, Cambridge University Press, 1998.

[7]. C. Berru, A. Glavieux, and P. Thitimajshima, "Near Shannon limit error-correcting coding and decoding: turbo codes," *International Conference Communications*, pp 1064-1070, 1993.

[8]. R. G. Gallager, *Low Density Parity Check Codes*, MIT Press, Cambridge, Massachusets, 1963.

[9]. C. E. Shannon, "A mathematical theory of communication," *Bell Syst. Tech. J.*, vol. 27, pp. 379-423 (Part one), pp.623-656 (Part two). Oct. 1948.

[10]. E. Telatar, "Capacity of multi-antenna Gaussian channels," *European Transactions on Telecommunications*, vol. 10, no. 6, pp. 585-595, Nov./Dec. 1999.

[11]. G. J. Foschini and M. J. Gans, "On the limits of wireless communications in a fading environment when using multiple antennas," *Wireless Personal Communications*, vol. 6, pp. 311-335, 1998

[12]. B. R. Salzberg, "Performance of an efficient parallel data transmission system," *IEEE Transactions on Communications*, vol.COM-15, pp. 805-811, Dec. 1967.

[13]. G. Caire, G. Taricco and E. Biglieri, "Bit-Interleaved Coded Modulation," *IEEE Communications Letters*, vol. 1, no. 6, pp. 169-171, Nov. 1997.

[14]. S. H. Muller-Weinfurtner, "Coding approaches from multiple antenna transmission in fast fading and OFDM," *IEEE Transactions on Signal Processing*, vol. 50, pp. 2442-2450, Oct. 2002.

[15]. M. R. G. Butler, I. B. Collings, "A zero-forcing approximate log-likelihood receiver for MIMO bit-interleaved coded modulation," *IEEE communications Letters*, vol. 8, no. 2, pp. 105-107, Feb. 2004.

[16]. D. Wubben, R. Bohnke, V. kuhn, and K-D. Kammeyer, "MMSE extension of V-BLAST based on sorted QR decomposition," *VTC-Fall2003*, vol. 1, pp. 508-512, 2003.

[17]. D. Wubben, R. Bohnke, V. kuhn, and K-D. Kammeyer, "Reduced complexity MMSE detection for BLAST architectures," *GLOBECOM2003*, vol. 4, pp. 2258-2262, 2003.

[18]. D. Wubben, R. Bohnke, V. kuhn, and K-D. Kammeyer, "Efficient algorithm for detecting layered space-time codes," *Electronics Letters*, vol. 37, no. 22, pp. 1348-1350, Oct. 2001.

[19]. L. R. Bahl, J. Cocke, F. Jelinek, and J. Raviv, "Optimal decoding of linear codes for minimizing symbol error rate," *IEEE Transactions on Information Theory*, vol. IT-20, pp. 284-287, Mar. 1974.

[20]. X. Wang and H.V. Poor, "Iterative (turbo) soft interference cancellation and decoding for coded CDMA," *IEEE Transactions on Communications*, vol. 47, no. 7, pp. 1046-1061, July 1999.

[21]. H.V. Poor and S.Verdu, "Probability of error in MMSE multiuser detection," *IEEE Transactions on Information Theory*, vol. 43, no. 3, pp. 858-871, May 1997.

[22]. M. Tuchler, A.C. Singer, and R. Koetter, "Minimum mean squared error equalization using a priori information," *IEEE Transactions on Signal Processing*, vol. 50, no 3, pp. 673-683, Mar. 2002.

[23]. E. Zehavi, "8-PSK trellis codes for a Rayleigh Channel," *IEEE Transactions on Communications*, vol. 40, pp. 837-884, May 1992.

[24]. F. Tosato and P. Bisaglia, "Simplified soft-output demapper for binary interleaved COFDM with application to HIPERLAN/2," *IEEE International Conference on Communications*, vol. 2, pp. 664-668, May 2002

[25]. M. Sellathurai and S. Haykin, "Turbo-BLAST: performance evaluation in correlated Rayleigh-fading envirnoment," *IEEE Journal on Selected Areas in Communications*, vol. 21, no. 3, pp.340-349, April. 2003.

[26]. M. Sellathurai and S. Haykin, "Turbo-BLAST for wireless communications: theory and experiments," *IEEE Transactions on Signal Processing*, vol. 50, no. 10, pp.2538-2546, Oct. 2002.

[27]. M. Sellathurai and S. Haykin, "Turbo-BLAST for high speed wireless communications," *Wireless Communications and Networking Conference*, vol. 1, pp. 315-320, Sept. 2000.

[28]. IEEE Std 802.11a-1999, *Part II: Wireless LAN Medium Access Control (MAC) and Physical Layer (PHY) Specifications: High-Speed Physical Layer in the 5 GHz Band*, Sept. 1999.

[29]. V. Erceg et al., IEEE 802.11 document 03/940r4 "TGn Channel Models," May 2004. Available at

[30]. S. A. Mujtaba, IEEE 802.11 document 04/889r3 "TGn Sync Proposal Technical Specification," Jan. 2005. Available at ftp://ieee:wireless@ftp.802wirelessworld.com/11/04/11-04-0889-03-000n-tgnsync-proposal-technical-specification.doc